Luca Giovanella
Giorgio Treglia
Roberto Valcavi *Editors*

Atlas of Head and Neck Endocrine Disorders

Special Focus on Imaging and Imaging-Guided Procedures

Springer

Atlas of Head and Neck Endocrine Disorders

Luca Giovanella • Giorgio Treglia
Roberto Valcavi
Editors

Atlas of Head and Neck Endocrine Disorders

Special Focus on Imaging and Imaging-Guided Procedures

Springer

Editors
Luca Giovanella
Department of Nuclear Medicine
and Thyroid Center
Oncology Institute of Southern
Switzerland
Bellinzona and Lugano
Switzerland

Giorgio Treglia
Department of Nuclear Medicine
and Thyroid Center
Oncology Institute of Southern
Switzerland
Bellinzona and Lugano
Switzerland

Roberto Valcavi
Endocrinologia
Centro Palmer
Reggio Emilia
Italy

ISBN 978-3-319-22275-2 ISBN 978-3-319-22276-9 (eBook)
DOI 10.1007/978-3-319-22276-9

Library of Congress Control Number: 2015952689

Springer Cham Heidelberg New York Dordrecht London

Printed on acid-free paper

Springer International Publishing AG Switzerland is part of Springer Science+Business Media (www.springer.com)

To our patients and their families for giving meaning to our work
To all our staff who supported us throughout this project

Luca Giovanella
Giorgio Treglia
Roberto Valcavi

Preface

Head and neck endocrine disorders include several diseases involving different organs and with variable outcome and prognosis.

A crucial step for the correct management of these disorders is the early diagnosis, the proper differential diagnosis, and, when appropriate, an accurate disease staging. Beyond clinical and laboratory data, different imaging modalities are now available to evaluate head and neck endocrine disorders. These imaging modalities include both morphological and functional imaging methods, sometimes combined by using hybrid devices.

The aim of this atlas is to provide a comprehensive overview on endocrine disorders of the head and neck region, with particular emphasis on the role of imaging and image-guided procedures.

We strongly believe that a multidisciplinary approach is needed for the proper diagnosis and management of head and neck endocrine disorders in the current clinical practice. Accordingly, several international experts in endocrine disorders, including endocrinologists, pathologists, radiologists, nuclear medicine physicians, and surgeons were involved as authors of chapters in this atlas in order to provide a multidisciplinary approach.

The first section discusses the basic characteristics of the imaging methods and other techniques used for evaluation and diagnosis, including ultrasonography, nuclear medicine techniques, computed tomography, and magnetic resonance imaging. Furthermore, a summary of pathology findings in head and neck endocrine disorders is provided.

The remainder of this book focuses on the application of imaging methods in thyroid, parathyroid, and other endocrine disorders of the head and neck region. The coverage is wide ranging, encompassing Graves' disease, toxic multinodular goiter, toxic adenoma, thyroiditis, nontoxic goiter, benign thyroid nodules, and the different forms of thyroid carcinoma, as well as primary hyperparathyroidism, paragangliomas, and other neuroendocrine tumors of the head and neck region.

We hope that the high-quality images provided in this atlas could assist the clinicians in their diagnostic approach to these disorders.

Bellinzona, Switzerland — Prof. Dr. med. Luca Giovanella, MD, PhD
Bellinzona, Switzerland — Giorgio Treglia, MD, MSc
Reggio Emilia, Italy — Roberto Valcavi, MD, FACE

Contents

Contributors

Massimiliano Andrioli, MD EndocrinologiaOggi, Rome, Italy

Massimo Bongiovanni, MD Department of Laboratory, Institute of Pathology, University Hospital of Lausanne, Lausanne, Switzerland

Luca Ceriani, MD Department of Nuclear Medicine, PET/CT and Thyroid Centre, Oncology Institute of Southern Switzerland, Bellinzona and Lugano, Switzerland

Luca Giovanella, MD, PhD Department of Nuclear Medicine, PET/CT and Thyroid Centre, Oncology Institute of Southern Switzerland, Bellinzona and Lugano, Switzerland

Alexander Stephan Kroiss, MD Department of Nuclear Medicine, Innsbruck Medical University, Innsbruck, Austria

Antoine Nobile, MD Department of Laboratory, Institute of Pathology, University of Lausanne, Lausanne, Switzerland

Mariana Raditchkova, MD Department of Nuclear Medicine, PET/CT and Thyroid Centre, Oncology Institute of Southern Switzerland, Bellinzona and Lugano, Switzerland

Camilla Schalin-Jäntti, MD, PhD Division of Endocrinology, Department of Medicine, Abdominal Center, University of Helsinki and Helsinki University Hospital, Helsinki, Finland

Jukka Schildt, MD Department of Clinical Physiology and Nuclear Medicine, University of Helsinki and Helsinki University Hospital, Helsinki, Finland

Marko Seppänen, MD Department of Clinical Physiology and Nuclear Medicine and PET Centre, University of Turku and Turku University Hospital, Turku, Finland

Giorgio Treglia, MD, MSc Department of Nuclear Medicine, PET/CT and Thyroid Centre, Oncology Institute of Southern Switzerland, Bellinzona and Lugano, Switzerland

Pierpaolo Trimboli, MD Section of Endocrinology and Diabetology, Ospedale Israelitico of Rome, Rome, Italy

Department of Nuclear Medicine and Thyroid Centre, Oncology Institute of Southern Switzerland, Bellinzona and Lugano, Switzerland

Virpi Tunninen, MD Department of Nuclear Medicine, Satakunta Central Hospital, Pori, Finland

Roberto Valcavi, MD Endocrinologia, Centro Palmer, Reggio Emilia, Italy

Irene Johanna Virgolini, MD Department of Nuclear Medicine, Innsbruck Medical University, Innsbruck, Austria

Part I

Basic Characteristics of Imaging Methods and Other Techniques for Evaluation of Neck Endocrine Diseases

Ultrasonography

1

Pierpaolo Trimboli

Abstract

The aim of this chapter is to discuss the general aspects of ultrasonography (US) for the evaluation of head and neck endocrine diseases. The normal US presentation of the thyroid gland is discussed and US evaluation of thyroid diseases is summarized. Furthermore some paragraphs are dedicated to elucidate the significance of incidental lesions detected by US, the role of this method in the follow-up of thyroid cancer patients, and the use of US to guide fine-needle aspiration cytology (FNAC) or core needle biopsy (CNB). Lastly, the role of US in evaluating hyperfunctioning parathyroid glands is briefly described.

Keywords

Ultrasonography • Ultrasound • Thyroid nodule • Thyroid cancer • Parathyroid • Neck

P. Trimboli, MD
Section of Endocrinology and Diabetology,
Ospedale Israelitico di Roma, Via Fulda 14, 00148
Rome, Italy

Department of Nuclear Medicine and Thyroid Centre,
Oncology Institute of Southern Switzerland,
Bellinzona, Switzerland
e-mail: pierpaolo.trimboli@gmail.com

L. Giovanella et al. (eds.), *Atlas of Head and Neck Endocrine Disorders: Special Focus on Imaging and Imaging-Guided Procedures*, DOI 10.1007/978-3-319-22276-9_1

1.1 Thyroid Ultrasonography

1.1.1 General Aspects

In the last decades ultrasonography (US) has become the most common imaging tool for the thyroid gland. In fact, US allows to accurately evaluate thyroid size, morphology, and structure [1, 2]. Furthermore, the main strength of thyroid US is the detection of those lesions that are not evident at palpation or using other imaging instruments [1, 2]. The procedure is safe, takes about ten minutes, and is relatively cheap. The test does not require discontinuation of any medication or preparation of the patient. Due to these reasons US has begun the optimal in-office instrument for thyroidologists.

The most diffuse application of thyroid US is to detect thyroid nodules and select suspicious ones for cytology examination. Overall, based on the US risk stratification, up to 80 % of thyroid cancers are correctly identified [1, 2]. However, specificity of US in this context was reported as low. Then, the high reliability in detecting non-palpable nodules combined with poor specificity for cancer led to a worldwide clinical and socio-economical problem [1, 2].

Main reliability of thyroid US is in the:

- Detection of non-palpable thyroid lesions
- Stratification of risk for malignancy of nodules, regardless of their size
- Diagnosis of autoimmune thyroid diseases
- Detection of suspicious neck lymph nodes
- Identification of neck recurrence/persistence of thyroid cancers

Thyroid US examination is also frequently used to:

- Verify the presence of thyroid lesions after suspicious palpation
- Assist nodule's fine-needle aspiration cytology (FNAC) or core needle biopsy (CNB)
- Assess thyroid and neck lymph nodes before surgery, when indicated
- Verify thyroid remnants after total thyroidectomy (limited sensitivity)
- Follow up patients previously treated for thyroid cancer

1.1.2 Normal Ultrasound Presentation of Thyroid Gland

The thyroid gland is more echo-dense than the adjacent structures and appears as homogenous. As a main rule, normal cells/colloid ratio gives homogeneous and normoechoic thyroid presentation at US, while hypoechogenicity of the thyroid gland is due to higher cells/colloid ratio. The size of the normal thyroid can be estimated by ellipsoid volume formula applied to each lobe. The normal dimension of one lobe is up to 5 cm in longitudinal axis, 2 cm in anterior-posterior axis, and 2 cm in transverse axis. The isthmus (generally not included in the size formula) has a depth of 3 mm. Normal references of adult thyroid size range from 7 to 18 ml [3–8]. Normal thyroid appearance at US correlates with normal thyroid function and negative thyroid antibodies measurement [9, 10]. On the contrary, hypoechoic and inhomogeneous thyroid gland is highly suspicious for autoimmune thyroid diseases (i.e., autoimmune thyroiditis, Graves' disease) [11, 12].

1.1.3 Ultrasound Evaluation of Thyroid Lesions

Thyroid nodules are a very common entity (prevalence up to 70 %) and US can detect a lot of clinically nonrelevant nodules. As a consequence, performing US in patients with no clear risk factors (i.e., previous neck irradiation) or clinical indications is strongly discouraged (see below). When nodules are detected at clinical examination, and vice versa, US is very useful to stratify the risk of malignancy. The following nodule's features must be evaluated to discriminate nodules at risk of malignancy from lesions probably benign [1, 2]:

A. Relevant features:
   - Echogenicity: thyroid cancers are often solid hypoechoic because of their high cells/colloid ratio. Some particular cancers (i.e., medullary type) may manifest by other fashions (such as mixed or spongiform). Rarely, papillary cancers have cystic presentation.

- Microcalcifications: these are the most specific features; however, microcalcifications may be detected in up to 20 % of thyroid cancers. Macrocalcifications do not raise the risk for cancer.
- Perilesional hypoechoic halo: it represents the most accurate feature to identify a benign nodule. Rarely, papillary cancers have a halo.

B. Ancillary features:
- Shape: nodules that are taller than wide should be viewed as at enhanced risk for malignancy. Nevertheless, new studies are needed to confirm this information.
- Vascularization: regardless of the enthusiastic studies of 1990s, the intranodular vascular signal should not be considered as a single diagnostic factor for thyroid cancer. A few cancers have intranodular vascularization, but this aspect is low accurate.
- Elastography: the recently introduced elastographic examination should increase the sensitivity of thyroid cancer detection by US. However, different color scales and elastographic methods have been reported and future studies have to be performed before to routinely introduce thyroid elastography.
- Margins: up to 30 % of thyroid cancers appear with irregular, spiculated, or blurred borders. However, to detect these characteristics needs an expert US examiner.

Table 1.1 Diagnostic accuracy of main ultrasound features of thyroid nodule in detecting cancers

More sensitive features	
Hypoechogenicity	Sensitivity 85 %
Hardness at elastography	Sensitivity 85 %
Taller shape	Sensitivity 85 %
More specific features	
Presence of microcalcifications	Specificity 90 %
Absence of halo	Specificity 85 %
Intranodular vascularization	Specificity 80 %
Irregular or blurred margins	Specificity 85 %

Overall, none of the above features alone is accurate to discriminate thyroid cancers from benign nodules, while the combination of all features achieves relevance to identify malignant nodules. Table 1.1 illustrates the diagnostic accuracy of main US single characters in detecting thyroid cancer.

1.1.4 The Dilemma of Small Non-palpable Thyroid Nodules Incidentally Discovered by US

Micronodules are often detected by thyroid US. Because the large majority of these subclinical diseases are discovered during US of other neck structures (i.e., carotid, jugular veins, etc.), their actual clinical significance is questionable [13]. Rarely, one micronodule is a cancer (generally papillary carcinoma), but the clinical relevance of detecting these cancers at a preclinical stage is highly debatable. In addition, US has lower accuracy in lesions with size <1 cm, and the abovementioned US risk factors are difficult to assess due to the small size of the nodule. Also, fine-needle aspiration cytology (FNAC) is not simple to be performed, and cytologic sample is often unsatisfactory due to the poor cellular amount. Only micronodules with high clinical/echographic/laboratory risk for malignancy should be submitted to FNAC or, alternatively, strictly monitored by serial US examinations [1, 2].

1.1.5 Neck Ultrasonography in the Follow-Up of Thyroid Cancer Patients

After surgery and iodine-131 ablation, persistent or recurrent disease is diagnosed in about 20 % of cases during follow-up over time. In the large majority of cases, the relapse of disease occurs in the neck, being frequently discovered in cervical lymph nodes or more rarely in the thyroid bed. Distant extracervical metastases are more rare [1, 2]. Ultrasonography is highly reliable in detecting thyroid cancer persistence and recurrence

when they are localized in the neck, with the exception of the central compartment more difficult to be examined by US. Thus, US has become the most diffused and useful imaging procedure in patients followed up for these cancers.

In 2013 the European Thyroid Association (ETA) task force on US in thyroid cancer follow-up has assessed a sort of guidelines on this topic. There, sensitivity and specificity of several US signs are reported. Of very high utility in clinical practice, the authors describe the rate of normal (i.e., nonmetastatic) lymph nodes with specific US signs; microcalcifications and cystic changes are never recordable in normal nodes, and round shape, peripheral vascularization, and hyperechogenicity are rarely present in these nodes. Thus, these have to be considered as major risk factors [14].

Finally, US should be useful in the operating room during surgery. This intraoperative US examination can improve the localization of metastases to be excised. In this view, the preoperative US in patients with thyroid cancer has to be routinely performed to reduce the need of reoperation for recurrent/persistent disease.

1.1.6 Use of Ultrasound to Guide Fine-Needle Aspiration Cytology (FNAC) or Core Needle Biopsy (CNB)

1.1.6.1 Fine-Needle Aspiration Cytology (FNAC)

Cytologic evaluation of thyroid nodule aspirates represents a pivotal tool to assess patients with discovered thyroid lesion(s). Usually, cytologic samples are satisfactory and permit to be classified as diagnostic. In fact, false-negative and false-positive FNAC reports are very rare (i.e., <2 %) [1]. However, a non-negligible rate (up to 15–25 %) of thyroid cytology is inconclusive due to inadequate material (Thy 1, Category I) or indeterminate diagnosis (Thy 3, Category III or IV). Nodules with Thy 1 or Category I need to undergo new FNAC, and those lesions with repeated inadequate sample should be addressed to diagnostic surgery or CNB (see below) [2]. A large amount of articles published in the last decade focused on the use of several potential markers to diagnose thyroid nodules with indeterminate FNAC report. However, no laboratory, US, scintigraphic, molecular, or clinical feature can be used alone to exclude thyroid malignancy. In these cases the diagnostic surgery remains mandatory.

Until the 1990s FNAC was performed without US guidance, and the rate of inadequate samples was high; also, the overall accuracy of the technique was reported as suboptimal. In the last years US-guided FNAC has been worldwide diffused. So, the accuracy of cytologic reports has been significantly improved. Real-time US guidance improves accuracy in positioning the needle into the nodule. Moreover, complications are very rare and FNAC can be performed in ambulatory office [1, 2].

Generally, a 23–27 gauge needle attached to a syringe is used. Several fashions can be adopted for thyroid FNAC. Free-hand mode is one of those more diffuse. On the other hand, the use of a device is frequently adopted. In these methods the needle is inserted parallel to the probe or at an angle of that. The parallel approach is more comfortable for the operator because the needle may be viewed as it traverses the nodule. A perpendicular approach is largely used due to its simplicity for less experienced operators. Complications are reduced by the latter. Regardless of fashion to perform the aspiration, US is highly useful to guide the procedure.

Once obtained the cytologic sample, the specimen is traditionally prepared on slides (in a number of 4 to 6, the majority of which are fixed for Papanicolaou stain). Recently, the thin-layer preparation is diffusing; the needle is washed into a syringe of solution and the sample is prepared for cell block. In specific conditions, such as nodules with prior indeterminate FNAC report, ancillary studies (i.e., immunocytochemistry for galectin-3) may be applied to cell blocks. As an extension of cytologic examination, the measurement of calcitonin in the washout fluids of the needle achieves high interest in those patients with suspicious medullary thyroid cancer; this approach significantly improves the detection of this cancer [15, 16].

As mentioned above, US is an accurate method for identifying suspected recurrence of thyroid cancer in enlarged lymph nodes; then,

neck lymph nodes suspicious for metastases from thyroid cancers can be aspirated. The procedure, generally, is easy. However, the cytologic sample may not be adequate for diagnosis. The measurement of thyroglobulin in the washout of the needle is necessary; high levels of thyroglobulin can detect a metastasis from differentiated thyroid cancer [17]. Furthermore, high calcitonin value in a cervical lymph node identifies a metastasis from medullary cancer [16].

1.1.6.2 Core Needle Biopsy (CNB)

Similarly to FNAC, US is highly useful also for guidance of CNB. In the last decade, several papers described the use of CNB as a second-line approach to assess those thyroid nodules with prior indeterminate (i.e., Thy 3/Category III–IV) or inadequate (i.e., Thy 1/Category I) FNAC report [18]. Data from these papers are so interesting that this biopsy has been included in AACE/AME/ETA guidelines.

1.1.7 Thyroid Ultrasound Reports

The thyroid US report must answer the question that has been posed by the clinician and not be just a routine recitation. Then it has to be performed by well-trained physicians and should be brief and concise. The examiner should interpret the images based on the above criteria and the specific question posed by the attending physician. Some examples of US findings are reported in Figs. 1.1, 1.2, 1.3, 1.4, 1.5, 1.6, 1.7, and 1.8.

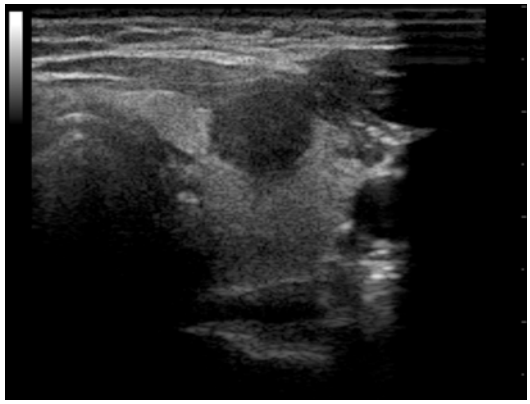

Fig. 1.1 Hypoechoic and solid thyroid nodule in the left lobe. Margins are not defined and the invasion of gland's capsule is evident. The histological examination after surgery demonstrates papillary cancer (pT3)

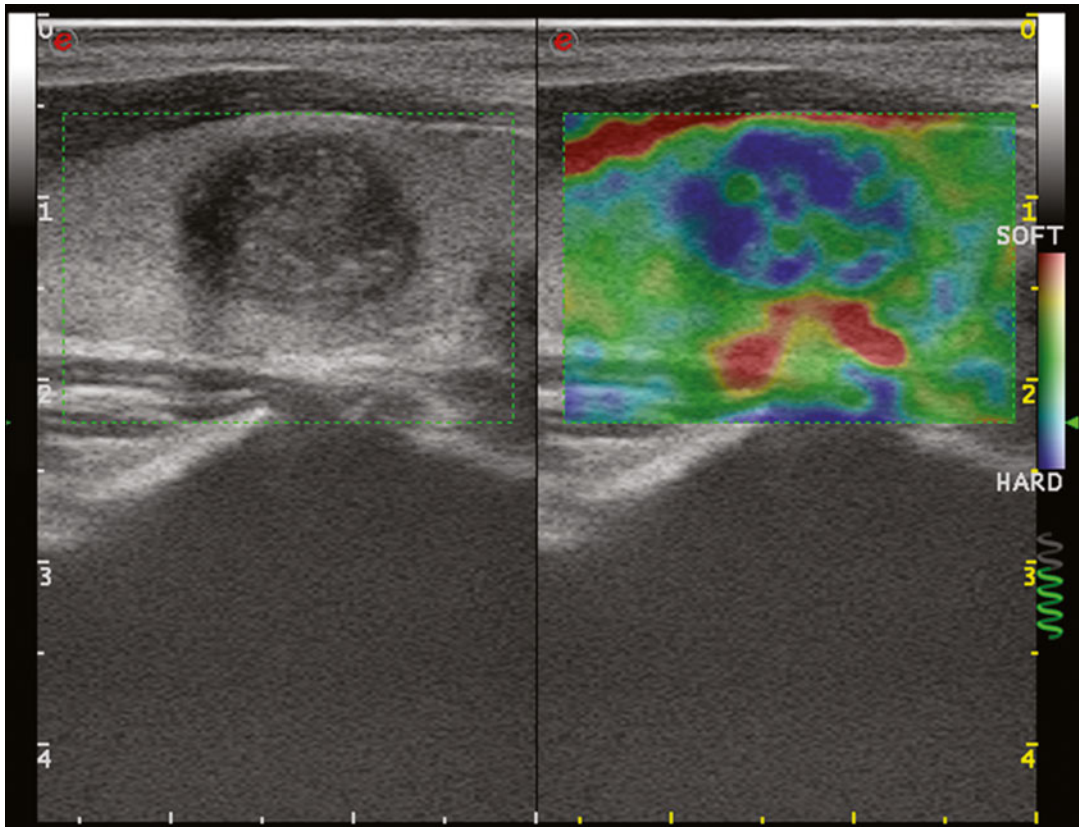

Fig. 1.2 Hypoechoic and solid thyroid nodule. Elastographic examination shows a hard structure. Papillary cancer (T1b) is demonstrated at histology

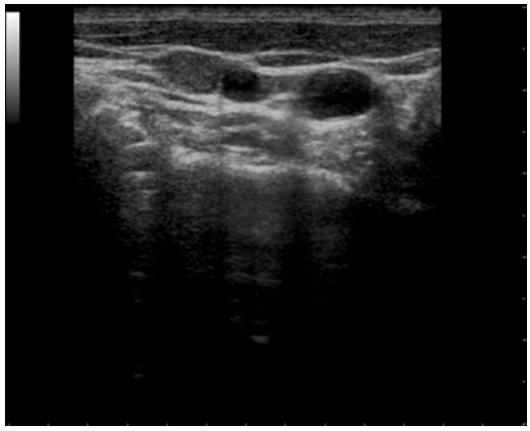

Fig. 1.3 Metastasis from papillary carcinoma (5 mm) at right neck level III

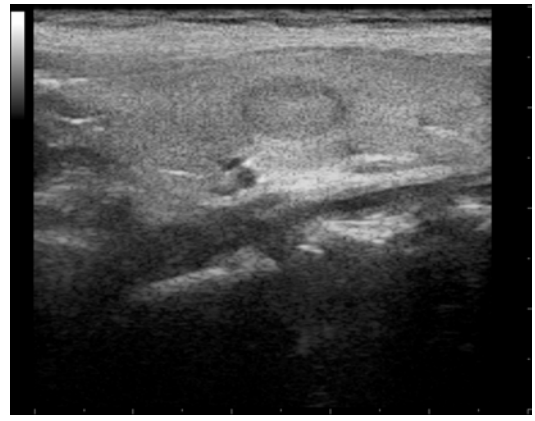

Fig. 1.4 Isoechoic nodule with hypoechoic halo. Cytology was benign (Thy 2)

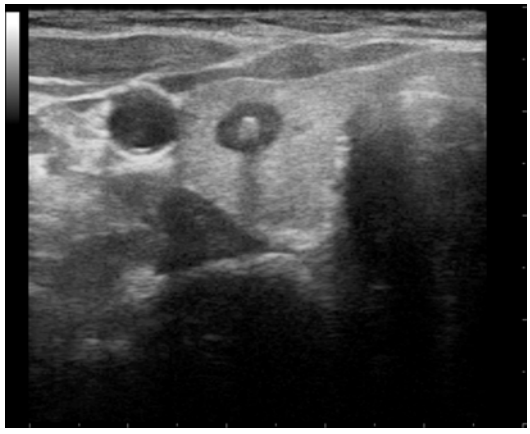

Fig. 1.5 Small (4 mm) solid hypoechoic nodule with calcification (medullary carcinoma at histology)

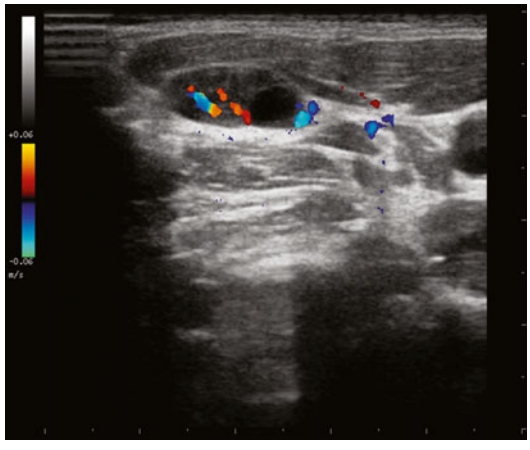

Fig. 1.6 Neck metastasis from papillary cancer at right level III. Lymph node appears mixed with cystic changes and spots of vascularization

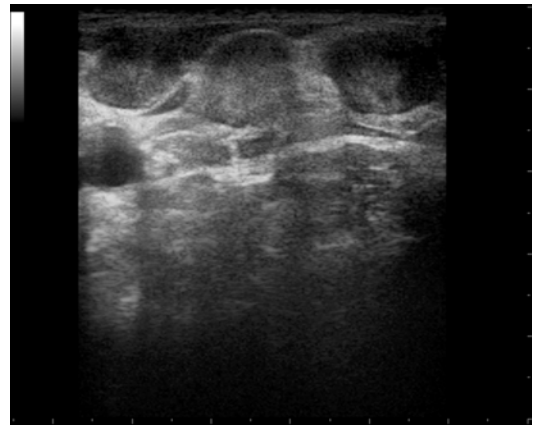

Fig. 1.7 Multiple neck metastases from medullary cancer in the left cervical level IV

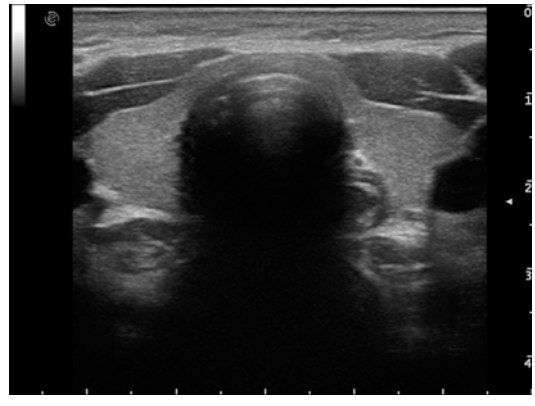

Fig. 1.8 Normal echographic appearance of thyroid

1.2 Ultrasonography of Parathyroid Glands

Generally, parathyroid glands are not detectable by US (similarly to the other image techniques). Parathyroids may be observed only when they are enlarged. They are less ultrasonographically dense (hypoechoic) than thyroid tissue. For these reasons a specific US examination of the parathyroid gland should be performed only in case of true hyperparathyroidism to localize the hyperplastic lesion or adenoma producing parathyroid hormone (PTH).

A parathyroid lesion producing PTH is often solid and hypoechoic, with regular margins and with 1–3 cm in size. At echo-color-Doppler examination, a main vascular septum is present. Remarkably, specificity of US in localized enlarged parathyroids is low, and scintigraphy is mandatory. Then, surgeons should consider that US cannot exclude multiple parathyroid diseases.

References

1. Cooper DS, Doherty GM, Haugen BR et al (2009) Revised American Thyroid Association management guidelines for patients with thyroid nodules and differentiated thyroid cancer. Thyroid 19:1167–1214
2. Gharib H, Papini E, Paschke R et al (2010) American Association of Clinical Endocrinologists, Associazione Medici Endocrinologi, and European Thyroid Association medical guidelines for clinical practice for the diagnosis and management of thyroid nodules. J Endocrinol Invest 33:1–50
3. Rago T, Bencivelli W, Scutari M et al (2006) The newly developed three-dimensional (3D) and two-dimensional (2D) thyroid ultrasound are strongly correlated, but 2D overestimates thyroid volume in the presence of nodules. J Endocrinol Invest 29:423–426
4. Shapiro RS (2003) Panoramic ultrasound of the thyroid. Thyroid 13:177–181
5. Lyshchik A, Drozd V, Reiners C (2004) Accuracy of three-dimensional ultrasound for thyroid volume measurement in children and adolescents. Thyroid 14:113–120
6. Deveci MS, Deveci G, LiVolsi VA et al (2007) Concordance between thyroid nodule sizes measured by ultrasound and gross pathology examination: effect on patient management. Diagn Cytopathol 35:579–583
7. Vejbjerg P, Knudsen N, Perrild H et al (2006) The association between hypoechogenicity or irregular echo pattern at thyroid ultrasonography and thyroid function in the general population. Eur J Endocrinol 155:547–552
8. Trimboli P, Ruggieri M, Fumarola A et al (2008) A mathematical formula to estimate in vivo thyroid volume from two-dimensional ultrasonography. Thyroid 18:879–882
9. Trimboli P, Rossi F, Condorelli E et al (2010) Does normal thyroid gland by ultrasonography match with normal serum thyroid hormones and negative thyroid antibodies? Exp Clin Endocrinol Diabetes 118:630–632
10. Trimboli P, Rossi F, Thorel F et al (2012) One in five subjects with normal thyroid ultrasonography has altered thyroid tests. Endocr J 59:137–143
11. Marcocci C, Vitti P, Cetani F et al (1991) Thyroid ultrasonography helps to identify patients with diffuse lymphocytic thyroiditis who are prone to develop hypothyroidism. J Clin Endocrinol Metab 72:209–213
12. Rago T, Chiovato L, Grasso L et al (2001) Thyroid ultrasonography as a tool for detecting thyroid autoimmune diseases and predicting thyroid dysfunction in apparently healthy subjects. J Endocrinol Invest 24:763–769
13. Tan GH, Gharib H (1997) Thyroid incidentalomas: management approaches to nonpalpable nodules discovered incidentally on thyroid imaging. Ann Intern Med 126:226–231

14. Leenhardt L, Erdogan MF, Hegedus L et al (2013) European thyroid association guidelines for cervical ultrasound scan and ultrasound-guided techniques in the postoperative management of patients with thyroid cancer. Eur Thyroid J 2:147–159
15. Trimboli P, Treglia G, Guidobaldi L et al (2015) Detection rate of FNA cytology in medullary thyroid carcinoma: a meta-analysis. Clin Endocrinol 82:280–285
16. Trimboli P, Cremonini N, Ceriani L et al (2014) Calcitonin measurement in aspiration needle washout fluids has higher sensitivity than cytology in detecting medullary thyroid cancer: a retrospective multicentre study. Clin Endocrinol 80:135–140
17. Giovanella L, Bongiovanni M, Trimboli P (2013) Diagnostic value of thyroglobulin assay in cervical lymph node fine-needle aspirations for metastatic differentiated thyroid cancer. Curr Opin Oncol 25:6–13
18. Trimboli P, Crescenzi A (2015) Thyroid core needle biopsy: taking stock of the situation. Endocrine 48:779–785

Nuclear Medicine Techniques

2

Luca Ceriani, Giorgio Treglia, and Luca Giovanella

Abstract

This chapter provides an introduction to nuclear medicine technique useful for evaluating head and neck endocrine diseases. Different radiotracers can be used for thyroid imaging and they can be classified in two groups: a) radiotracers describing the function of follicular cells and b) radiotracers mapping the proliferative activity of follicular cells. The first group includes technetium-99m-pertechnetate (^{99m}TcO4–) and radioiodine; the second group includes Tc99m-methoxyisobutylisonitrile (^{99m}Tc-MIBI) and fluorodeoxyglucose (^{18}F-FDG).

About parathyroid nuclear imaging, ^{99m}Tc-MIBI is the most used tracer in clinical practice, usually combined with a thyroid tracer. Planar and tomographic images can be used for detecting hyperfunctioning parathyroid glands. The role of PET tracers seems promising.

Lastly, several tracers evaluating different metabolic pathways can be used to detect neuroendocrine tumors of head and neck region.

Keywords

Thyroid • Parathyroid • Neuroendocrine • Scintigraphy • SPECT • PET

2.1 Introduction

Nuclear medicine techniques were first employed for the diagnosis and therapy of thyroid diseases in the 1950s. Despite the subsequent development of thyroid ultrasound and fine-needle aspiration (FNA), thyroid scintigraphy with either iodine or iodine-analogue isotopes remains the

L. Ceriani, MD (✉) • G. Treglia, MD, MSc
Prof. Dr. med. L. Giovanella, MD, PhD
Department of Nuclear Medicine and PET/CT Center, Oncology Institute of Southern Switzerland, Via Ospedale 12, CH-6500 Bellinzona and Lugano, Switzerland
e-mail: luca.ceriani@eoc.ch; giorgio.treglia@eoc.ch; luca.giovanella@eoc.ch

L. Giovanella et al. (eds.), *Atlas of Head and Neck Endocrine Disorders: Special Focus on Imaging and Imaging-Guided Procedures*, DOI 10.1007/978-3-319-22276-9_2

only method able to characterize functionally the thyroid tissue and especially to demonstrate the presence of autonomously functioning nodules [1]. An increased tracer uptake within a nodule excludes malignancy with high accuracy and, additionally, allows a timely and appropriate treatment. More recently, different tracers have become available to evaluate the proliferation rate of the thyroid cells and, due to their very high negative predictive values, have proved to be useful for reducing the number of unnecessary thyroidectomies [2, 3]. Finally, novel imaging technologies such as single-photon emission computed tomography (SPECT) and positron emission tomography (PET) are now available and consistently increase the quality of nuclear medicine images and allow sophisticated quantification procedures [3]. These technological developments associated to the introduction of new tracers allowed more recently to extend the diagnostic role of nuclear medicine imaging toward patients with parathyroid diseases and neuroendocrine tumors of head and neck region.

2.2 Thyroid Diseases: Radioactive Tracers and Nuclear Medicine Methods

Thyroid radiotracers can be classified in two groups: (a) radiotracers describing the function of follicular cells and (b) radiotracers mapping the proliferative activity of follicular cells.

2.2.1 Radiotracers Describing the Function of Follicular Cells

Normal thyroid tissue is characterized by the unique capability of its follicular cells to trap and to process stable iodine (I) which is subsequently incorporated in thyroglobulin (Tg) in order to form thyroid hormones. The I uptake into the follicular cells is regulated by the sodium-iodide symporter (NIS), a transmembrane protein that carries sodium and iodine from the blood into the follicular cells [4, 5]. The NIS allows the thyroid trapping of different radioactive thyroid tracers. Iodine-123 (^{123}I) is an ideal thyroid radiopharmaceutical due to low radiation burden and optimal imaging quality, as opposed to the use of iodine-131 (^{131}I), which is strongly discouraged for routine diagnostic use because of its much higher radiation burden to the thyroid. Finally, iodine-124 (^{124}I) is a positron-emitting isotope that allows high-quality imaging of the thyroid. Currently, however, its use is restricted to clinical trials involving patients with differentiated thyroid cancer while it is not indicated for the diagnostic workup of patients with thyroid nodules. The thyroid uptake of a different tracer, ^{99m}Tc-pertechnetate, is also related to NIS expression. Importantly, it is not a substrate for any metabolic pathways and a complete washout from thyroid cells occurs in about 30 min. However, although the thyroid does not organify ^{99m}Tc-pertechnetate, in the majority of cases the uptake and imaging data provide all the information needed for accurate diagnosis [1, 5]. ^{99m}Tc-pertechnetate has a shorter half-life and a preferred energy for scintigraphic imaging compared to ^{123}I. Additionally, it is cheaper and readily available in nuclear medicine departments. As a consequence, it has generally been adopted as the primarily used thyroid tracer in clinical practice [1, 5].

2.2.2 Radiotracers Mapping Cellular Proliferative Activity

The thyroid cells may be stimulated to proliferate by controlled growth mechanisms leading to benign diseases (i.e., benign goiters) or lose their differentiation following uncontrolled growth mechanisms leading to malignant diseases (i.e., thyroid cancer). The more the follicular cells become undifferentiated, the more they lose NIS expression [5]. The loss of NIS expression reduces the ability of the thyroid cells to trap and concentrate iodine. Recently, oncotropic radiotracers, mapping cell density and cellular metabolism and viability, have been developed. The ^{99m}Tc-MIBI is a lipophilic cation that crosses the cell membrane and penetrates reversibly into the cytoplasm via thermodynamic driving forces and

then irreversibly passes the mitochondrial membrane using a different electrical gradient regulated by a high negative inner membrane potential [6]. The cancer cells, with their greater metabolic turnover, are characterized by a higher electrical gradient of mitochondrial membrane, thus determining an increased accumulation of ^{99m}Tc-MIBI compared to normal cells. Recent studies demonstrate that dedifferentiating follicular thyroid cells reduce the expression of the NIS while they increase glucose metabolism [7–9]. Interestingly, the glucose metabolism can be tracked by a radioactive glucose analogue, fluorodeoxyglucose (^{18}F-FDG). As glucose, it is transported into the blood flow and can diffuse into the cells through selective and specific transporters. The best known glucose transporter is an insulin-independent transmembrane protein, the glucose transporter 1 (GLUT 1). Once entering the cells, ^{18}F-FDG is phosphorylated to glucose-6-phosphate and trapped in the cells [10]. A positive relationship between GLUT 1 overexpression and aggressive biology of thyroid tumors has been shown [11]. In addition, overexpression of hexokinase I has also been demonstrated in thyroid cancer cells as reflected by an increased ^{18}F-FDG uptake [12].

The characteristics of various nuclides used for the visualization of the thyroid gland are shown in Fig. 2.1 and Table 2.1.

2.2.3 Thyroid Diseases: Nuclear Medicine Imaging Methods

Thyroid scans with either ^{99m}Tc-pertechnetate, ^{123}I, or ^{99m}Tc-MIBI are obtained by a gamma-camera equipped with a parallel-hole collimator. Sometimes dedicated "pinhole" collimators are employed to increase focal resolution, in particular to increase the detection rate of little nodular lesions. Nevertheless, a significant geometric distortion should be taken into account. Planar images, acquired in the anterior view for some minutes, provide a reliable map of thyroid function and metabolism (Fig. 2.2). Additional views may be useful when searching for ectopic tissue. Tomographic techniques, such as SPECT and SPECT/CT, may be very useful to better localize in the body the pathological findings, particularly in case of ectopic tissue or intrathoracic goiter. To be noted, as the diagnostic specificity is decreased in lesions that are below the resolution threshold of gamma-cameras, thyroid scans are not indi-

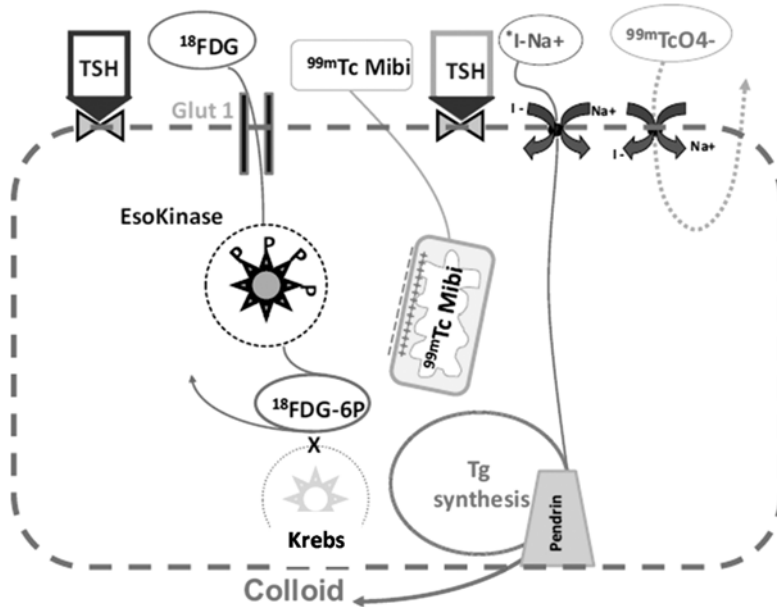

Fig. 2.1 Molecular basis of nuclear imaging of follicular thyroid cell. *^{18}F-FDG* fluorodeoxyglucose, *^{18}F-FDG-6P* fluorodeoxyglucose-6-phosphate, **I-Na* radioiodine, *^{99m}Tc-MIBI* Tc99m-methoxyisobutylisonitrile, *^{99m}TcO4$^-$* Tc99m-pertechnetate, *TSH* thyroid stimulating hormone, *Tg* thyroglobulin (Figure modified from Ref. [5])

Table 2.1 Thyroid scintigraphy: tracers and technical procedures

	$^{99m}TcO_4$–	^{123}I	^{99m}Tc-MIBI	^{18}F-FDG
Administration	i.v.	o.a.	i.v.	i.v.
Activity (adults)	74–111 MBq	7.4–14.8 MBq	185–370 MBq	200–370 MBq
Technique	Planar	Planar	Planar (ev. SPET or SPET/CT)	PET or PET/CT
Acquisition start	15 min p.i	4 and 24 h p.o.	30–45 min p.i.	60 min. p.i.
Acquisition time	5 min	10 min	10 min	12 min (whole body)
Effective dose (mSv/MBq)	0.013	0.20	0.009	0.02 (PET) 0.04 (PET/CT)

Adapted at Department of Nuclear Medicine and PET/CT Centre – Oncology Institute of Southern Switzerland
Abbreviations: *CT* computed tomography, *i.v.* intravenous, *mSv* millisievert, *MBq* megabecquerel, *o.a.* oral administration, *PET* positron emission tomography, *p.i.* post injection, *p.o.* post oral administration, *SPET* single-photon emission computed tomography, *$^{99m}TcO_4$–* ^{99m}Tc-pertechnetate

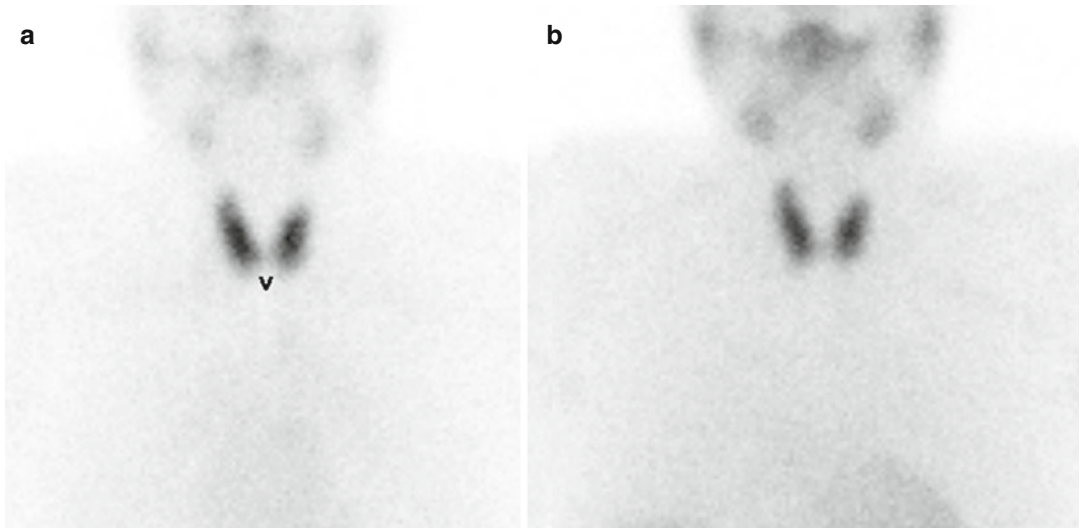

Fig. 2.2 Normal technetium-99m pertechnetate [$^{99m}TcO4^-$] (**a**) and technetium-99m methoxyisobutylisonitrile [^{99m}Tc-MIBI] (**b**) scintigraphy

cated in patients with subcentimetric nodules [5]. For oncologic indications a planar whole body imaging in both anterior and posterior views is the technique of choice for the assessment of metastatic spread of the disease. The recent introduction in the current practice of the SPET/CT derived hybrid imaging improved the interpretation of abnormal uptakes, particularly in studies with radioiodine, providing integrated anatomical and metabolic images suitable also to plan the further therapeutic strategies [3]. Finally, the use of positron-emitting tracers, such as ^{18}F-FDG and ^{124}I, requires dedicated PET scanners or, preferably, hybrid PET/CT scanners that provide whole body integrated morphologic-metabolic images [13].

2.3 Parathyroid Nuclear Medicine Imaging

The peculiarity of the parathyroid scintigraphy derives from the fact that a specific tracer able to characterize selectively the parathyroid tissue and to map the function of the parathyroid cells does not exist. Consequently, it is not possible to visualize normal parathyroid glands or use the uptake of tracers to grade/measure the parathyroid function.

In routine parathyroid nuclear medicine imaging, oncotropic radiotracers mapping cell density and cellular metabolism and viability are employed. These tracers are taken up not only by

the hyperfunctioning parathyroid glands but also by other tissues. The detection of the hyperfunctioning lesions is, therefore, due to the contrast between the increased metabolism of the parathyroid glands and that of the surrounding normal tissues [14, 15].

^{99m}Tc-MIBI is the most used tracer for parathyroid scintigraphy. The well-known high uptake of the thyroid parenchyma makes necessary, in particular to detect hyperfunctioning parathyroid glands localized within the thyroid parenchyma, a comparison with a second tracer, which is taken up by the thyroid gland only, such as ^{99m}Tc-pertechnetate ($^{99m}TcO4^-$) or ^{123}I. The distributions of the two tracers can be compared and, afterward, the thyroid scan can be digitally subtracted from the parathyroid scan to remove the thyroid activity and enhance the visualization of parathyroid tissue. This technique of images is defined as "dual-tracer scintigraphy" [14, 15].

^{99m}Tc-MIBI usually washes out from normal and possibly abnormal thyroid tissue more rapidly than from abnormal parathyroid tissue. A "dual-phase" imaging with early and delayed images, generally obtained 20 min and 2 h after ^{99m}Tc-MIBI injection, has been proposed to maximize this characteristic and it is used in many centers to increase the detection rate of parathyroid lesions [14, 15].

^{99m}Tc-tetrofosmin can be used alternatively to ^{99m}Tc-MIBI using the dual-tracer subtraction procedure. ^{99m}Tc-tetrofosmin localizes in both parathyroid tissue and functioning thyroid tissue, but in contrast to ^{99m}Tc-MIBI, there is no differential washout between thyroid and parathyroid tissues [16].

The standard protocols with planar images have been recently replaced by tomographic techniques. SPECT and SPECT/CT allow more precise anatomic localization, particularly for localizing ectopic lesions [17, 18]. The combination of anatomic and functional imaging, that is, SPECT/CT, provides the optimal localization for surgical planning and additional diagnostic information. Moreover the tomographic imaging can be associated with a "dual-phase" protocol and, today, a SPECT/ CT dual-phase ^{99m}Tc-MIBI scintigraphy, performed on an integrated SPECT/CT device, can be considered the optimal technical approach for parathyroid imaging [18].

Positron emission tomography (PET) tracers have met variable success in this field. ^{18}F-FDG is considered of limited usefulness for the identification of parathyroid adenomas. Recent studies seem to demonstrate that ^{11}C-methionine PET/CT may play a role in the localization of hyperfunctioning parathyroid glands, especially for the detection of the smaller lesions [19]. However, all the experiences agree to define ^{11}C-methionine PET/CT a useful complementary imaging technique to identify parathyroid adenoma or hyperplastic glands in ^{99m}Tc-MIBI SPECT/CT-negative patients with or without previous neck surgery [19].

Preliminary results demonstrate that radiolabeled choline PET/CT could be a promising tool for localization of hyperfunctioning parathyroid glands, providing clearer images than ^{99m}Tc-MIBI, equal or better accuracy, and quicker and easier acquisition [20].

2.4 Nuclear Medicine Imaging in Head and Neck Neuroendocrine Tumors

The majority of the head and neck neuroendocrine tumors are represented by paragangliomas (PGLs) derived from the cells of the parasympathetic paraganglia and the medullary thyroid carcinomas (MTC) derived from thyroid parafollicular cells, both developed from the neural crest cells.

For the imaging of these neuroendocrine tumors, several radiopharmaceuticals are available (Fig. 2.3) with variable affinity and diagnostic accuracy for the different subtypes [21–23]. In such complex anatomical district, the use of a tomographic imaging hybrid (PET/CT or SPET/CT) is fundamental to enhance sensitivity and specificity increasing diagnostic confidence in image interpretation by means of the proper location of lesions.

Based on the most recent studies, ^{18}F-DOPA PET/CT has been shown to be a useful addition to anatomical imaging in the preoperative localization and molecular assessment of head and neck PGLs. It is estimated that the frequency of metabolically active head and neck PGLs on

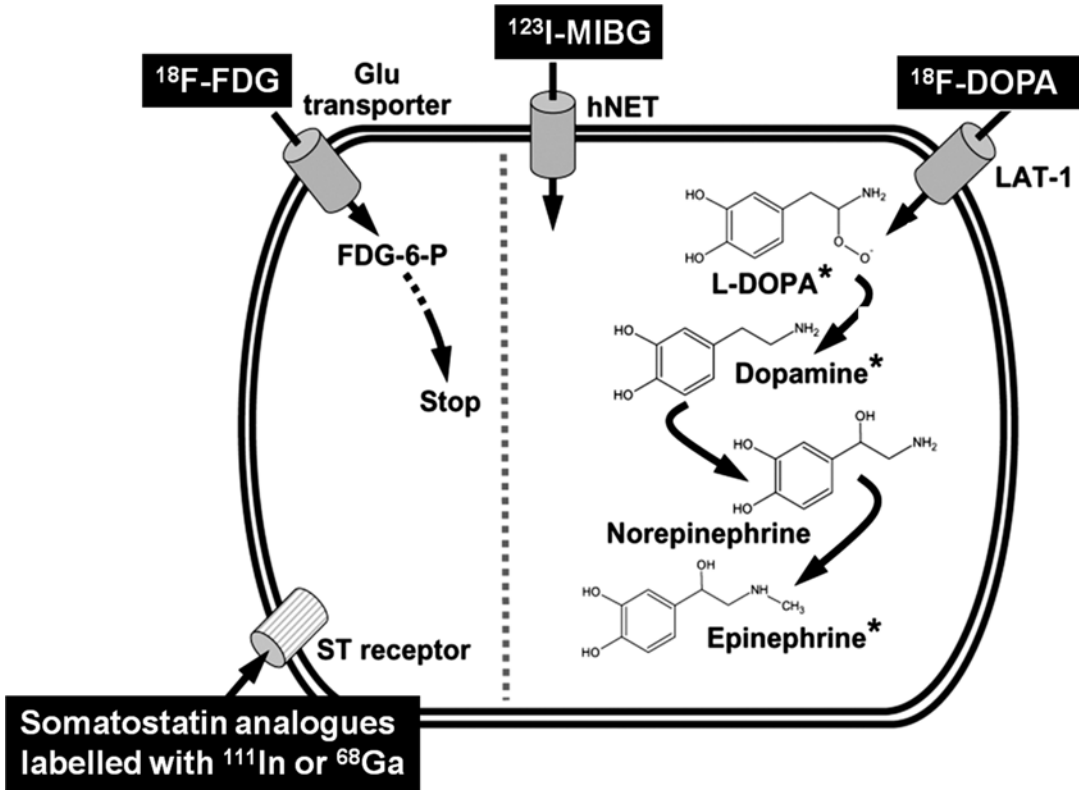

Fig. 2.3 Molecular basis of nuclear imaging of neuroendocrine tumor cell. *18F-FDG* fluorodeoxyglucose, *18F-FDG-6P* fluorodeoxyglucose-6-phosphate, *123I-MIBG* metaiodobenzylguanidine, *hNET* human norepinephrine transporter, *18F-DOPA* fluorodihydroxyphenylalanine, *LAT-1* large amino acid transporter, *ST receptor* somatostatin receptor, *asterisk* catecholamines and their precursors which can be radiolabelled (Figure modified from Ref. [22])

^{18}F-FDOPA PET/CT in this region is higher than 90 %. For patients with hereditary PGL syndromes, ^{18}F-FDG PET/CT should be reserved. Imaging of somatostatin receptors using ^{111}In-pentetreotide or ^{68}Ga-labeled somatostatin analogues plays an important role in selecting patients for targeted peptide radioreceptor therapy [21, 22].

In detecting MTC recurrence, ^{18}F-DOPA is the best radiopharmaceutical with significant diagnostic performance if calcitonin values are higher than 150 pg/mL; an early image acquisition starting during the first 15 min is advised. ^{18}F-FDG PET/CT could be particularly useful if calcitonin and CEA levels are rapidly rising. Somatostatin receptor imaging by SPECT or PET tracers could be performed when ^{18}F-DOPA or ^{18}F-FDG PET/CT are inconclusive [23].

References

1. Giovanella L (2009) Thyroid nodules: clinical management and differential diagnosis. Praxis 98:83–90
2. Treglia G, Caldarella C, Saggiorato E et al (2013) Diagnostic performance of 99mTc-MIBI scan in predicting the malignancy of thyroid nodules: a meta-analysis. Endocrine 44:70–78
3. Wonga KT, Choi FP, Lee YY et al (2008) Current role of radionuclide imaging in differentiated thyroid cancer. Cancer Imaging 8:159–162
4. Baker CH, Morris JC (2004) The sodium-iodide symporter. Curr Drug Targets Immune Endocr Metabol Disord 4:167–174
5. Giovanella L, Ceriani L, Treglia G (2014) Role of isotope scan, including positron emission tomography/computed tomography, in nodular goitre. Best Pract Res Clin Endocrinol Metab 28:507–518
6. Moretti JL, Hauet N, Caglar M et al (2005) To use MIBI or not to use MIBI? That is the question when assessing tumour cells. Eur J Nucl Med Mol Imaging 32:836–842

7. Feine U, Lietzenmayer R, Hanke JP et al (1995) 18FDG whole-body PET in differentiated thyroid carcinoma. Flipflop in uptake patterns of 18FDG and 131I. Nuklearmedizin 34:127–134
8. Grabellus F, Nagarajah L, Bockisch A et al (2012) Glucose transporter 1 expression, tumor proliferation, and iodine/glucose uptake in thyroid cancer with emphasis on poorly differentiated thyroid carcinoma. Clin Nucl Med 37:121–127
9. Treglia G, Annunziata S, Muoio B et al (2013) The role of fluorine-18-fluorodeoxyglucose positron emission tomography in aggressive histological subtypes of thyroid cancer: an overview. Int J Endocrinol 2013:856189
10. Thorens B (1993) Facilitated glucose transporters in epithelial cells. Annu Rev Physiol 55:591–608
11. Schönberger J, Rüschoff J, Grimm D et al (2002) Glucose transporter 1 gene expression is related to thyroid neoplasms with an unfavorable prognosis: an immunohistochemical study. Thyroid 12:747–754
12. Hooft L, van der Veldt AA, van Diest PJ et al (2001) [18F]fluorodeoxyglucose uptake in recurrent thyroid cancer is related to hexokinase I expression in the primary tumor. J Clin Endocrinol Metab 90:328–334
13. Treglia G, Muoio B, Giovanella L et al (2013) The role of positron emission tomography and positron emission tomography/computed tomography in thyroid tumours: an overview. Eur Arch Otorhinolaryngol 270:1783–1787
14. Hindiè E, Ugur O, Fuster D et al (2009) 2009 EANM parathyroid guidelines. Eur J Nucl Med Mol Imaging 36:1201–1216
15. Taieb D, Hindie E, Grassetto G et al (2012) Parathyroid scintigraphy: when, how, and why? A concise systematic review. Clin Nucl Med 37:568–574
16. Fröberg AC, Valkema R, Bonjer HJ et al (2003) 99mTc-tetrofosmin or 99mTc-sestamibi for double-phase parathyroid scintigraphy? Eur J Nucl Med Mol Imaging 30:193–196
17. Cheung K, Wang TS, Farrokhyar F et al (2012) A meta-analysis of preoperative localization techniques for patients with primary hyperparathyroidism. Ann Surg Oncol 19:577–583
18. Treglia G, Sadeghi R, Schalin-Jäntii C et al (2015) Detection rate of (99m) Tc-MIBI SPECT/CT in the preoperative planning of patients with primary hyperparathyroidism: a meta-analysis. Head Neck. doi:10.1002/hed.24027
19. Caldarella C, Treglia G, Isgrò MA et al (2013) Diagnostic performance of positron emission tomography using ^{11}C-methionine in patients with suspected parathyroid adenoma: a meta-analysis. Endocrine 43:78–83
20. Orevi M, Freedman N, Mishani E et al (2014) Localization of parathyroid adenoma by ^{11}C-choline PET/CT: preliminary results. Clin Nucl Med 39: 1033–1038
21. Taïeb D, Varoquaux A, Chen CC et al (2013) Current and future trends in the anatomical and functional imaging of head and neck paragangliomas. Semin Nucl Med 43:462–473
22. Shulkin BL, Ilias I, Sisson JC et al (2006) Current trends in functional imaging of pheochromocytomas and paragangliomas. Ann N Y Acad Sci 1073: 374–382
23. Slavikova K, Montravers F, Treglia G et al (2013) What is currently the best radiopharmaceutical for the hybrid PET/CT detection of recurrent medullary thyroid carcinoma? Curr Radiopharm 6:96–105

Computed Tomography and Magnetic Resonance Imaging

3

Mariana Raditchkova and Giorgio Treglia

Abstract

The aim of this chapter is to introduce the role of computed tomography (CT) and magnetic resonance imaging (MRI) in patients with endocrine diseases of the neck region.

The role of CT in thyroid disorders is mainly limited to presurgical evaluation to assess the extent of the disease, substernal components, or relationship with extrathyroidal structures. MRI is generally used for specific indications, including the evaluation of substernal goiters and their relation to other structures.

CT and MRI are usually less sensitive than ultrasonography and scintigraphy in detecting hyperfunctioning parathyroid glands. Hybrid tomographic SPECT/CT and four-dimensional CT could be useful alternatives in detecting hyperfunctioning parathyroid glands when previous imaging methods are inconclusive.

In head and neck paragangliomas, accurate diagnosis is usually made by clinical examination together with MRI and hybrid morphological and functional imaging studies, including PET/CT with different tracers.

Keywords

CT • MRI • SPECT/CT • PET/CT • Radiology • Endocrine

3.1 CT and MRI in Thyroid Diseases

Because of its high iodine content, the thyroid gland attenuates more than nearby soft tissues, appearing slightly hyperdense at CT imaging [1].

If possible, CT should be performed without contrast media in patients with thyroid disorders

M. Raditchkova, MD • G. Treglia, MD, MSc (✉)
Department of Nuclear Medicine,
Thyroid and PET/CT Center,
Oncology Institute of Southern Switzerland,
Via Ospedale 12, CH-6500 Bellinzona and Lugano,
Switzerland
e-mail: giorgio.treglia@eoc.ch

L. Giovanella et al. (eds.), *Atlas of Head and Neck Endocrine Disorders: Special Focus on Imaging and Imaging-Guided Procedures*, DOI 10.1007/978-3-319-22276-9_3

and when a scintigraphy for thyroid disease is planned because the iodine load received may delay treatment with radioiodine and may also lead to thyrotoxicosis (i.e., Jod-Basedow) [2].

The role of CT in thyroid disorders is mainly limited to presurgical evaluation to assess the extent of the disease, substernal components, or relationship with extrathyroidal structures, i.e., the trachea, esophagus, or vascular structures (Fig. 3.1) [1].

Furthermore CT scan can also be used to evaluate extrathyroidal manifestations of thyroid disorders. For example, in patients with Graves' orbitopathy, CT provides precise imaging of the osseous periorbital structures [3].

Overall CT is not as sensitive as ultrasonography or scintigraphy for the evaluation of intrathyroidal lesions, but it can show enlarged cervical lymph nodes, evaluate thyroid tumor extension in the surrounding tissues, and detect distant metastases (Fig. 3.1) [4].

Lastly hybrid tomographs such as single-photon computed emission tomography (SPECT)/CT and positron emission tomography/CT provide combined morphological and functional information in thyroid diseases. The CT portion provides the structural map to accurately localize the radiotracer uptake site [5, 6].

For MRI dedicated surface coil centered over the thyroid gland is needed and generally used for specific indications, including the evaluation of substernal goiters and their relation to other structures, assessment of the local extent, and localization of recurrent sites in thyroid tumors [1]. The normal thyroid gland has homogeneous signal intensity slightly greater than neck musculature in T1-weighted images. Normal thyroid glands appear as hyperintense in T2-weighted images. Thyroid carcinomas are isointense or slightly hypointense lesions on T1-weighted images and hyperintense lesions on T2-weighted images compared with normal thyroid tissue [1].

MRI has also been used for the investigation of congenital disorders of the thyroid gland and the evaluation of diffuse thyroid diseases, such as Graves' disease, Hashimoto and Riedel thyroiditis, and hemochromatosis [7].

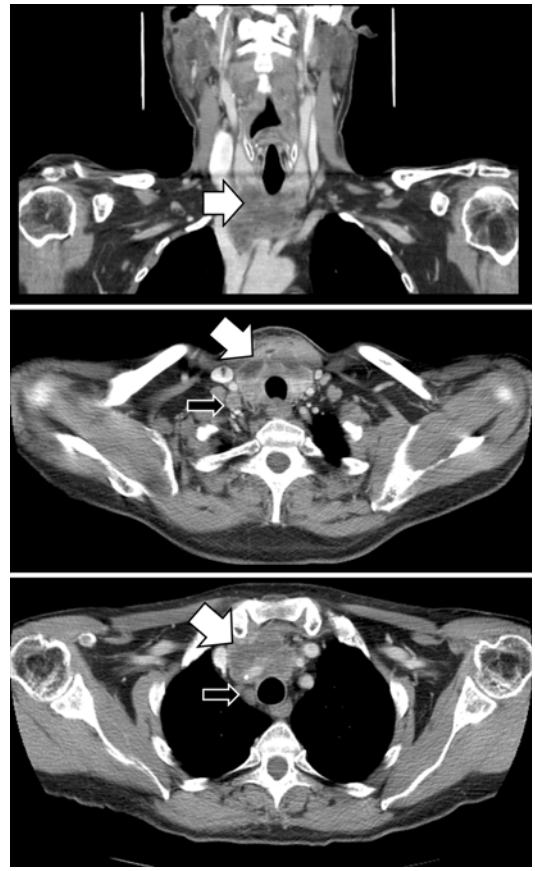

Fig. 3.1 Enlarged and inhomogeneous thyroid mass with extension to the mediastinal region imaged by contrast-enhanced computed tomography (*white arrows*). Enlarged cervical and mediastinal lymph nodes are also evident (*black arrows*)

3.2 CT and MRI in Parathyroid Diseases

Thin-cut, contrast-enhanced CT from the base of the skull to the mediastinum can be used to detect hypefunctioning parathyroid glands (Fig. 3.2). Parathyroid adenomas have low density on CT scans and show intense enhancement during the arterial phase [1, 8].

An emerging technique for the evaluation of initial, recurrent, persistent primary hyperparathyroidism and for preoperative localization of hyperfunctioning parathyroid glands is four-dimensional CT (4D CT) [9]. Although 4D CT may be comparable or even superior to other imaging techniques for the detection of abnormal parathyroid tissue, further cost analysis and large sample studies are needed to recommend it as the imaging modality of choice in the setting of primary hyperparathyroidism [9].

Hybrid tomographs such as SPECT/CT and PET/CT can be used to detect hyperfunctioning parathyroid glands. In particular ^{99m}Tc-MIBI SPECT/CT has high detection rate for hyperfunctioning parathyroid glands in patients with primary hyperparathyroidism [10], including ectopic glands. Moreover, the detection rate of ^{99m}Tc-MIBI SPECT/CT to identify solitary parathyroid adenomas can be increased with the addition of ultrasonography [10].

PET/CT with ^{11}C-methionine could be helpful in patients with diagnosis of primary hyperparathyroidism when conventional imaging techniques are negative or inconclusive in localizing parathyroid adenomas [11].

The role of MRI is limited to parathyroid localization in the setting of persistent disease or recurrence. The sensitivity in the reoperative setting was found to be comparable to that of ultrasonography and scintigraphy. The characteristic signals of hyperfunctioning parathyroid glands are low intensity on T1-weighted sequences and high intensity on T2-weighted sequences [1].

The lack of radiation exposure, the superior anatomic detail without need for contrast administration, and the minimal artifact effect on surrounding tissues make MRI superior to thin-cut CT [1].

3.3 CT and MRI in Head and Neck Paragangliomas

Head and neck paragangliomas (HNPGLs) are usually nonsecreting tumors and thus often discovered on imaging studies or revealed by the presence of cervical masses with or without compression or infiltration of adjacent structures. In nonsecreting cases, accurate diagnosis of HNPGLs is made by thorough clinical examination together with MRI and paraganglioma-specific functional imaging studies, including PET/CT with different tracers [12].

HNPGLs usually demonstrate marked enhancement following contrast administration on CT scan and, after gadolinium injection on MRI, low signal on T1-weighted images and an intermediate to high signal on T2-weighted MRI images (Fig. 3.3) [12].

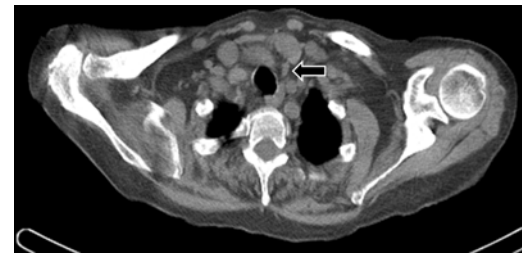

Fig. 3.2 Parathyroid adenoma imaged by computed tomography (*arrow*)

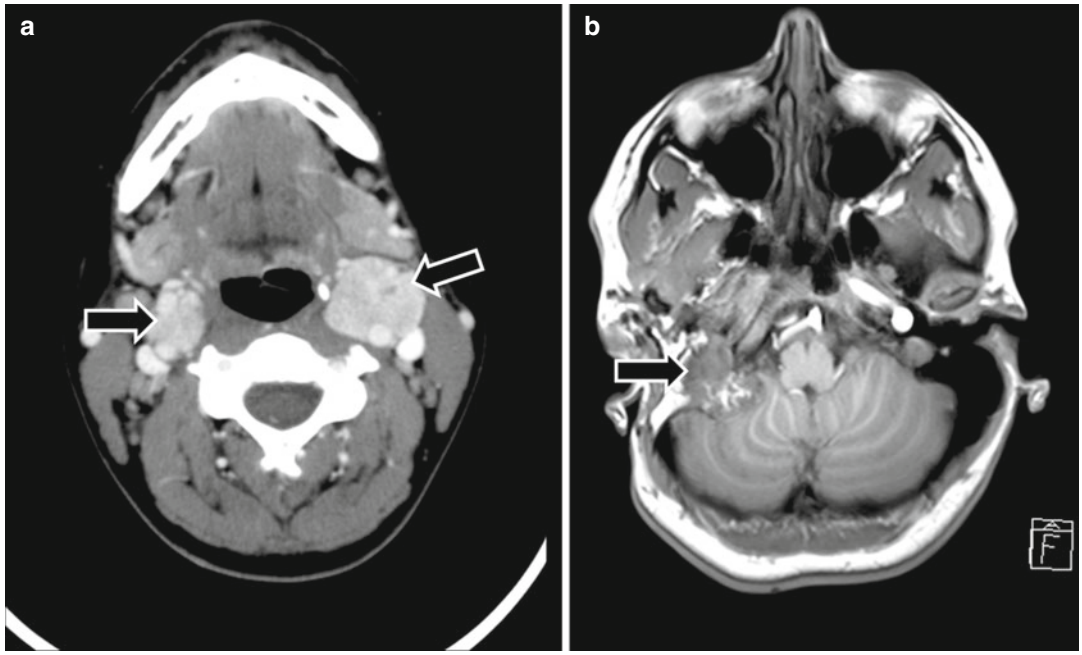

Fig. 3.3 Head and neck paragangliomas (*arrows*) imaged by computed tomography (**a**), showing marked enhancement following contrast administration, and magnetic resonance imaging (**b**).

References

1. Vazquez BJ, Richards ML (2011) Imaging of the thyroid and parathyroid glands. Surg Clin North Am 91:15–32
2. Weber AL, Randolph G, Aksoy FG (2000) The thyroid and parathyroid glands. CT and MR imaging and correlation with pathology and clinical findings. Radiol Clin North Am 38:1105–1129
3. Kirsch E, Hammer B, von Arx G (2009) Graves' orbitopathy: current imaging procedures. Swiss Med Wkly 139:618–623
4. Hopkins CR, Reading CC (1995) Thyroid and parathyroid imaging. Semin Ultrasound CT MR 16:279–295
5. Xue Y-L, Qiu Z-L, Perotti G et al (2013) ^{131}I SPECT/CT: a one-station imaging modality in the management of differentiated thyroid cancer. Clin Transl Imaging 1:163–173
6. Treglia G, Muoio B, Giovanella L et al (2013) The role of positron emission tomography and positron emission tomography/computed tomography in thyroid tumours: an overview. Eur Arch Otorhinolaryngol 270:1783–1787
7. Gotway MB, Higgins CB (2000) MR imaging of the thyroid and parathyroid glands. Magn Reson Imaging Clin N Am 8:163–182
8. Ernst O (2009) Hyperparathyroidism: CT and MR findings. J Radiol 90:409–412
9. Rodgers SE, Hunter GJ, Hamberg LM et al (2006) Improved preoperative planning for directed parathyroidectomy with 4-dimensional computed tomography. Surgery 140:932–940
10. Treglia G, Sadeghi R, Schalin-Jäntii C et al (2015) Detection rate of (99m) Tc-MIBI SPECT/CT in the preoperative planning of patients with primary hyperparathyroidism: a meta-analysis. Head Neck. doi:10.1002/hed.24027
11. Caldarella C, Treglia G, Isgrò MA et al (2013) Diagnostic performance of positron emission tomography using ^{11}C-methionine in patients with suspected parathyroid adenoma: a meta-analysis. Endocrine 43:78–83
12. Taïeb D, Kaliski A, Boedeker CC et al (2014) Current approaches and recent developments in the management of head and neck paragangliomas. Endocr Rev 35:795–819

Percutaneous Minimally Invasive Techniques

4

Massimiliano Andrioli and Roberto Valcavi

Abstract

In the past two decades, percutaneous ultrasound-guided minimally invasive techniques have been proposed in order to produce a volume reduction of the benign thyroid nodules. This chapter describes the main minimally invasive procedures and their indications. Currently available ultrasound-guided minimally invasive procedures can induce a rapid, clinically significant long-term size reduction of benign thyroid nodules with minimal risks. Ethanol injection should preferentially be considered as the first-line treatment for relapsing thyroid cysts. The thermo-ablative techniques, instead, may be used as an alternative to surgery in patients with solid benign thyroid nodules causing aesthetic problems or compressive symptoms, achieving a significant volume reduction. Less appropriate indications are large nodular goiters, multinodular thyroid disease, or deeply positioned lesions.

Keywords

Thyroid nodule • Percutaneous techniques • Ethanol injection • Laser ablation • Radiofrequency ablation • High-intensity focused ultrasound • Microwave

M. Andrioli, MD
EndocrinologiaOggi,
viale Somalia 33, Rome 00199, Italy
e-mail: andrioli@endocrinologiaoggi.it

R. Valcavi, MD (✉)
Endocrinologia, Centro Palmer,
via Fratelli Cervi 75/B, Reggio Emilia 42010, Italy
e-mail: info@robertovalcavi.it

4.1 Introduction

Nodular thyroid disease is very common and thyroid lesions can be found in up to 70 % of the general population by ultrasound. Most of them are benign, asymptomatic, and slowly growing

L. Giovanella et al. (eds.), *Atlas of Head and Neck Endocrine Disorders: Special Focus on Imaging and Imaging-Guided Procedures*, DOI 10.1007/978-3-319-22276-9_4

and do not warrant treatment. On the contrary, large nodules can cause compressive symptoms (dyspnea, dysphagia, tightness) and/or aesthetic problems [1, 2]. Therefore, a minority of the patients with thyroid lesions may benefit from a treatment to address pressure symptoms, local pain, or cosmetic issues.

All the main treatments currently available for benign thyroid lesions present some limitations. Surgery has a risk of complications, usually requires hormone replacement therapy for life, and might not be indicated for patients at high surgical risk. Radiometabolic therapy (I-131) with cytoreductive purpose is not applicable in the preconception status, in pregnancy, and during lactation. Finally, the suppressive therapy with levothyroxine produces results in a few cases only and may cause side effects related to iatrogenic subclinical hyperthyroidism, e.g., reduction in bone mineral density and atrial fibrillation [3].

Due to these limitations, in the past two decades, percutaneous ultrasound-guided minimally invasive techniques have been proposed in order to produce a volume reduction of the benign thyroid nodules.

4.2 Percutaneous Minimally Invasive Techniques

Minimally invasive procedures appear appealing because they most often achieve relief of anterior neck complaints, are relatively inexpensive, and can be performed on outpatients.

Ethanol injection (EI), laser ablation (LA), radiofrequency ablation (RFA), high-intensity focused ultrasound (HIFU), and microwave (MW) represent the main percutaneous ultrasound-guided minimally invasive techniques currently available for thyroid lesions.

EI is currently indicated in the treatment of cystic nodules. It is not applicable in the treatment of solid lesions, for the low efficacy and for the potential risk of uncontrolled spread of alcohol.

Thermo-ablative techniques, instead, are developed for the solid lesions. They all cause the thermal necrosis of the nodular tissue that, with time, undergoes reabsorption, causing a size reduction of the lesion.

LA uses photons released by optical fibers inserted into the tissue to be destroyed. One or more fibers can be inserted (Fig. 4.1). Since its introduction in 2000, there has been extensive evidence about its clinical utility in nodular thyroid disease [2, 4, 5]. Current AACE/AME/ETA guidelines on thyroid nodule indicate its efficacy and safety in patients who refuse surgery or at high surgical risk (Fig. 4.2) [3].

RFA has been introduced in the treatment of thyroid nodules more recently [5, 6]. This technique uses high-frequency radio waves that heat the tissue by ionic friction (Fig. 4.3). Data on its effectiveness are increasing (Figs. 4.4, 4.5, and 4.6).

Globally, many studies highlighted the effectiveness of both, LA and RFA, in reducing thyroid nodule size and in improving the compressive and aesthetic symptoms [7].

HIFU is a new thermo-ablative method which allows the treatment of thyroid nodules with an ultrasonic beam focused in a small area [8]. It has the advantage of being operator-independent and avoids inserting needles into the patient's neck. Since the first case published in 2010, the evidences regarding the effectiveness of this method have been increasing [8].

Finally, ablation with MW was introduced very recently; further studies are needed to assess its real clinical impact [9].

Current use of the thermo-ablative techniques is in the field of treatment of benign nodules. However, some studies reported the use of some of these methods in the treatment of malignancies, such as not surgery-treatable local recurrence of thyroid cancer or isolated lymph node metastasis. A recent pilot study also indicates LA effectiveness on primary treatment of thyroid microcarcinomas [10].

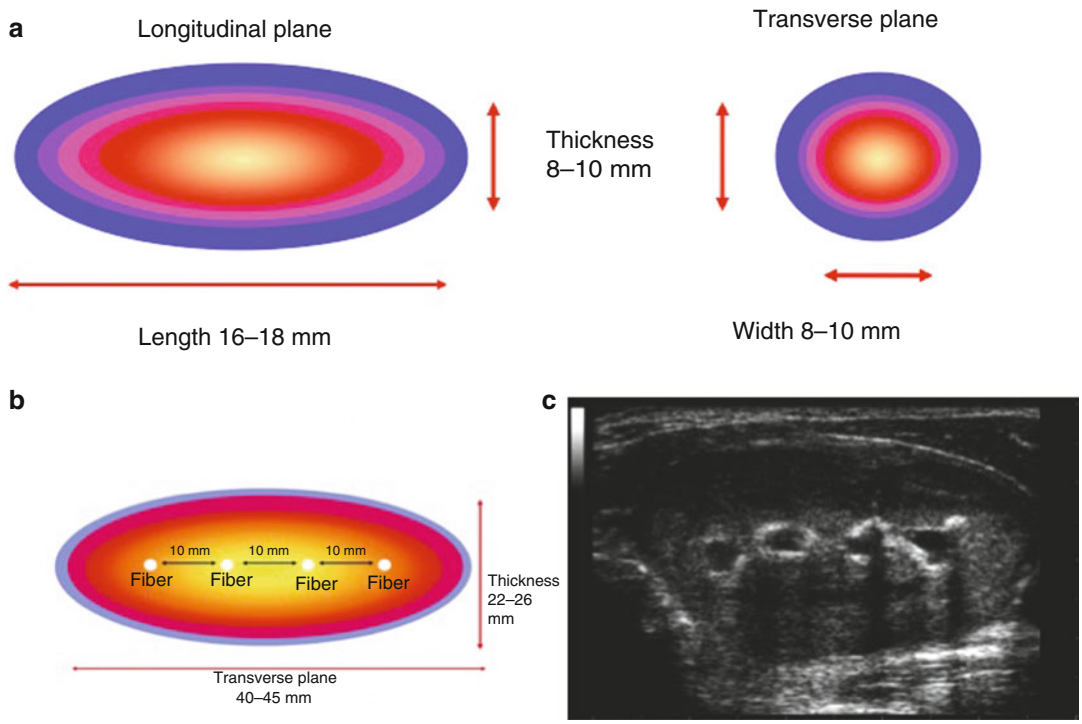

Fig. 4.1 (**a**) A single optic fiber, maintained in a still position, destroys only a small amount of tissue, e.g., 16–18 mm in length, 8–10 mm in width, and 8–10 mm in thickness, i.e., about 1 ml volume (delivered energy 1600–1800 J, output power: 2–4 W). (**b**) More fibers in line configuration may obtain a larger ellipsoid nodule ablation. Cartoon of a transverse scan, showing needles inserted one at a side of the other at a distance of 10 mm in order to match ellipsoid nodule shape. With up to four parallel fibers, a coagulation zone up to 40–45 mm wide and 22–26 mm thick may be obtained. (**c**) Ultrasound transverse scan of a thyroid nodule ablated with four parallel optic fibers. The four laser marks are clearly visible as well as the ablation zone

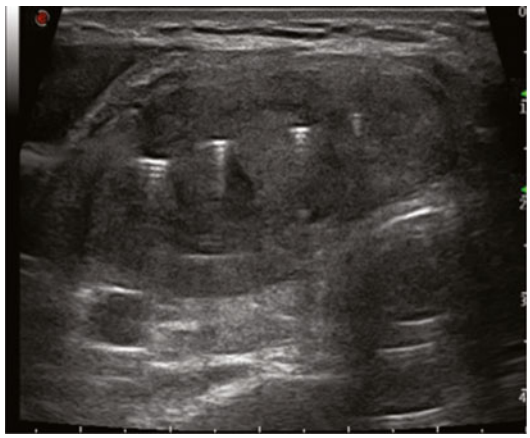

Fig. 4.2 B-mode imaging, transverse scan of thyroid nodule during laser ablation. Heat delivered during laser firing is visible as illumination of four needles at the same time

4.3 Summary of indications

Currently available ultrasound-guided minimally invasive procedures can induce a rapid, clinically significant long-term size reduction of benign thyroid nodules with minimal risks.

EI should preferentially be considered as the first-line treatment for relapsing thyroid cysts. The thermo-ablative techniques, instead, may be used as alternative to surgery in patients with solid benign thyroid nodules causing aesthetic problems or compressive symptoms, achieving a significant volume reduction. Nodules best responsive to the thermal procedures seem to be the spongiform, followed by mixed and compact ones [11]. Less appropriate indications are large nodular goiters, multinodular thyroid disease, or deeply positioned lesions.

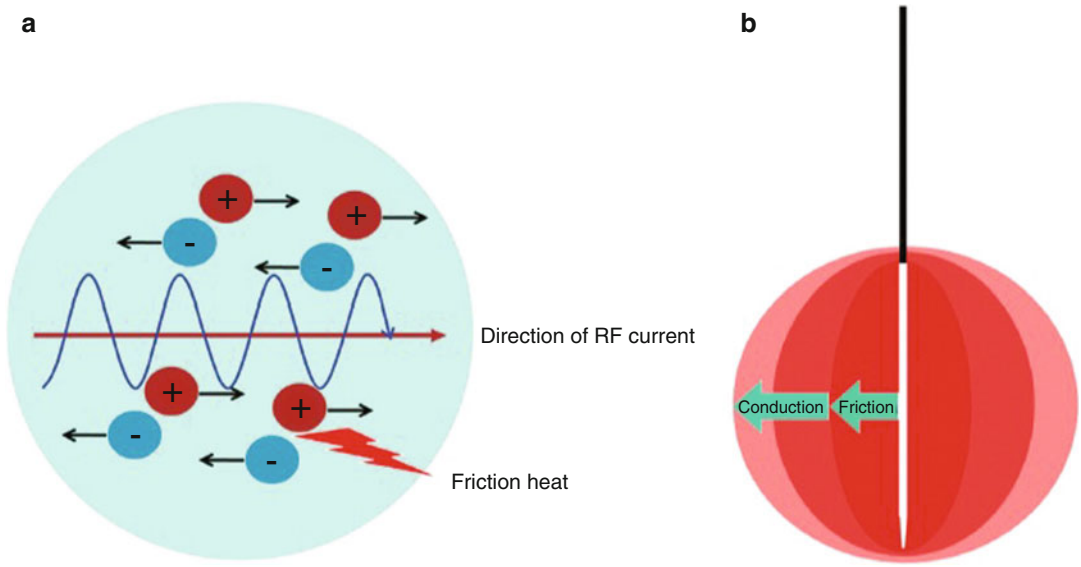

Fig. 4.3 (**a**) Ionic agitation and formation of frictional heat. Tissue ions are agitated by application of alternating electric current. Ionic agitation results in ion friction, which causes heat production. (**b**) Heat propagation through target tumor. Immediate tissue coagulation necrosis is achieved by frictional heat generated in vicinity of electrode, but electrode-remote tumor tissue is ablated more slowly, via conductive heat. Radiofrequency (*RF*) (Modified by reference [5])

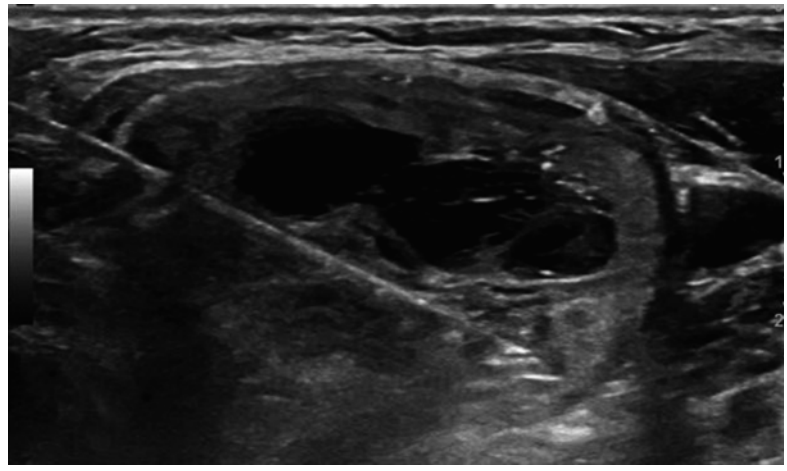

Fig. 4.4 Transverse ultrasound image of the moving-shot radiofrequency ablation technique. The electrode needle is inserted toward the common carotid artery

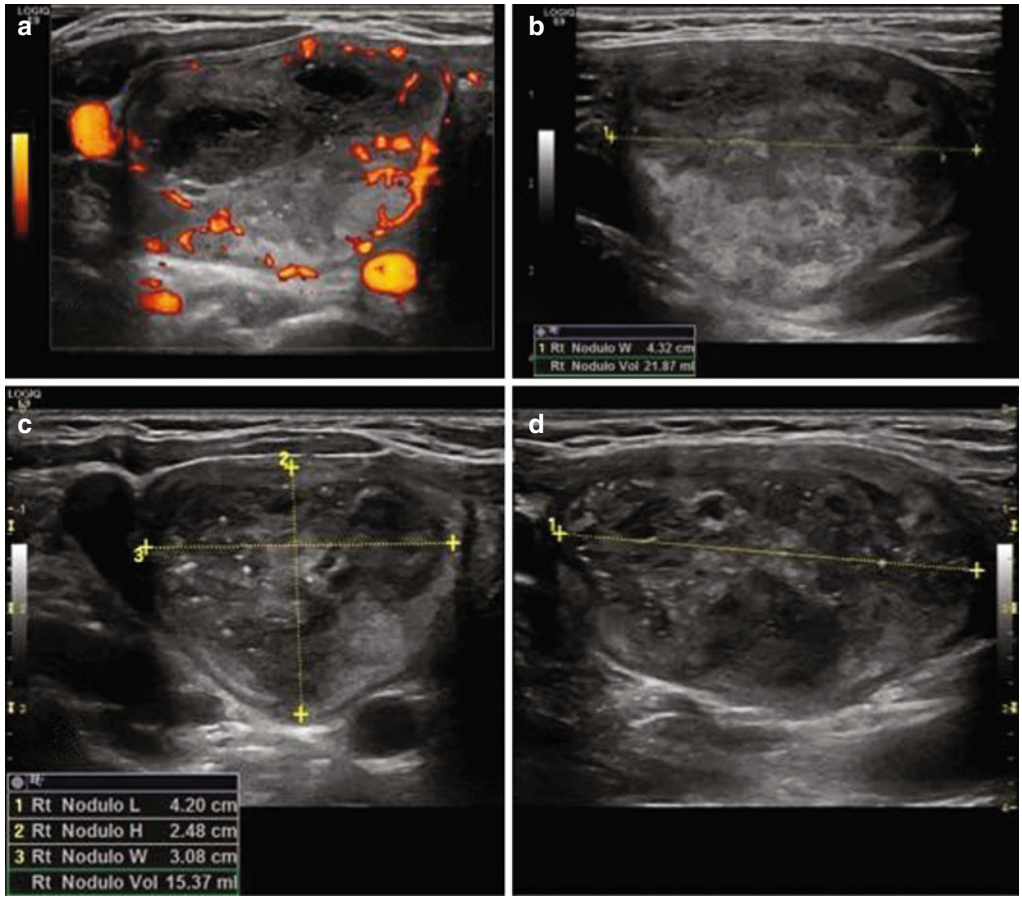

Fig. 4.5 Transverse (**a**) and longitudinal (**b**) ultrasound images of a thyroid nodule before radiofrequency ablation. Transverse (**c**) and longitudinal (**d**) ultrasound images of the same thyroid nodule one month after radiofrequency ablation. Note volume reduction from 21.87 to 15.37 ml (volume reduction of about 30 %)

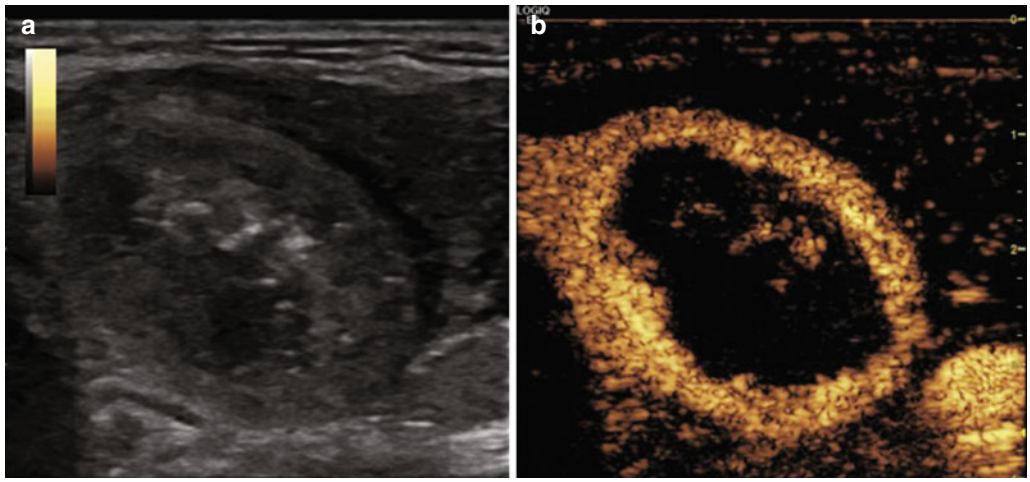

Fig. 4.6 Transverse B-mode (**a**) and CEUS study (**b**) of a thyroid nodule treated with radiofrequency. CEUS demonstrates large ablation of the nodule with minimal residual viable tissue left vital

References

1. Gharib H, Hegedus L, Pacella CM et al (2013) Clinical review: nonsurgical, image-guided, minimally invasive therapy for thyroid nodules. J Clin Endocrinol Metab 98:3949–3957
2. Papini E, Pacella CM, Hegedus L (2014) Thyroid ultrasound and ultrasound-assisted procedures: from the shadows into an array of applications. Eur J Endocrinol 170:133–146
3. Gharib H, Papini E, Paschke R et al (2010) American Association of Clinical Endocrinologists, Associazione Medici Endocrinologi, and European Thyroid Association medical guidelines for clinical practice for the diagnosis and management of thyroid nodules: executive summary of recommendations. J Endocrinol Invest 33:51–56
4. Valcavi R, Riganti F, Bertani A et al (2010) Percutaneous laser ablation of cold benign thyroid nodules: a 3-year follow-up study in 122 patients. Thyroid 20:1253–1261
5. Baek JH, Lee JH, Valcavi R et al (2011) Thermal ablation for benign thyroid nodules: radiofrequency and laser. Korean J Radiol 12:525–540
6. Fuller CW, Nguyen SA, Lohia S et al (2014) Radiofrequency ablation for treatment of benign thyroid nodules: systematic review. Laryngoscope 124:346–353
7. Andrioli M, Valcavi R (2014) The peculiar ultrasonographic and elastographic features of thyroid nodules after treatment with laser or radiofrequency: similarities and differences. Endocrine 47:967–968
8. Korkusuz H, Sennert M, Fehre N et al (2014) Local thyroid tissue ablation by high-intensity focused ultrasound: effects on thyroid function and first human feasibility study with hot and cold thyroid nodules. Int J Hyperthermia 30:480–485
9. Yang YL, Chen CZ, Zhang XH (2014) Microwave ablation of benign thyroid nodules. Future Oncol 10:1007–1014
10. Valcavi R, Piana S, Bortolan GS et al (2013) Ultrasound-guided percutaneous laser ablation of papillary thyroid microcarcinoma: a feasibility study on three cases with pathological and immunohistochemical evaluation. Thyroid 23:1578–1582
11. Valcavi R, Stecconi G, Riganti F et al (2012) Thyroid spongiform nodules are the best candidates for percutaneous laser ablation. A 5-year follow-up study in 72 patients. Endocrine Abstracts 29:OC2.5

Pathology

5

Massimo Bongiovanni and Antoine Nobile

Abstract

The procedures to diagnose head and neck lesions are mostly based on pathological (cytological and histological) evaluation. Cytology is the most accurate and cost-effective method for the initial management of patients with head and neck lesions, above all when performed with the aid of ultrasonographic guidance (i.e., ultrasound guided fine-needle aspiration, US-FNA). US-FNA yields a definitive diagnosis in the great majority of cases: for benign lesions, unnecessary surgery can be avoided; for malignant lesions, preliminary cytological evaluation provides strategies for an optimal surgical treatment. Thanks to the easy accessibility and relatively low cost of this medical equipment, thyroid US-FNA is probably one of the most performed procedures in the world. Histological examination of surgically removed malignant lesions remains the gold standard to assess the extent of the disease and the quality of surgery. In this chapter, we detail the most salient cytohistological features of head and neck neuroendocrine lesions.

Keywords

Fine-needle aspiration • Cytology • Histology • Thyroid • Parathyroid • Paraganglioma

5.1 Thyroid

5.1.1 Graves' Disease

Graves' disease is a thyroid autoimmune disease characterized by the presence in the plasma of anti-

M. Bongiovanni, MD (✉) • A. Nobile, MD
Department of Laboratory,
Institute of Pathology, University Hospital
of Lausanne, Lausanne, Switzerland
e-mail: massimo.bongiovanni@chuv.ch

L. Giovanella et al. (eds.), *Atlas of Head and Neck Endocrine Disorders: Special Focus on Imaging and Imaging-Guided Procedures*, DOI 10.1007/978-3-319-22276-9_5

bodies directed against the thyroid-stimulating hormone receptor (TSH-r). This disease is the most common cause of hyperthyroidism in patients (usually female) younger than 40. The thyroid of patients affected by Graves' disease presents a diffuse parenchymal hyperplasia that macroscopically results in a diffuse, symmetric, and homogenous enlargement of both thyroid lobes that look reddish on cut. Histologically, the characteristic lobular architecture is maintained as well as the general structure of the thyroid follicles that are larger than usual and markedly hyperplastic. Follicles are filled up with watery colloid that characteristically presents clear vacuoles (scalloping) in contact with thyrocytes; in the interfollicular stroma, vessels are prominent. Additional histological features not always visible are hyperplastic papillae, psammoma bodies, chronic inflammation, and dominant hyperplastic nodules [1].

5.1.2 Thyroid Autonomy

Hyperfunction of the thyroid gland can be explained by an isolated adenoma (toxic adenoma, Plummer's disease) or by a multinodular goiter (toxic multinodular goiter). In these situations the thyroid gland shows single or multiple nodules that display various aspects on cut section: cystic, hemorrhagic, fibrotic, or calcified. Microscopically, one can observe an alternance of inactive follicles with no signs of colloid reabsorption and hyperactive follicles with peripheral scalloping of the colloid [1].

5.1.3 Thyroiditis

Inflammation of the thyroid comprises different diseases with specific morphological patterns, possibly of autoimmune etiology in some of them. The most common form of thyroiditis is chronic lymphocytic thyroiditis (Hashimoto thyroiditis), that has an autoimmune etiology. Other forms of thyroiditis can be acute, subacute (de Quervain thyroiditis), and chronic thyroiditis.

Briefly, acute thyroiditis is usually caused by microorganisms that have spread from surrounding organs or structures, such as the pharynx and larynx. Histologically it is characterized by an infiltration of the thyroid parenchyma by abundant necrosis and a large amount of polymorphonuclear neutrophils. Subacute thyroiditis, also known as de Quervain thyroiditis or granulomatous thyroiditis, is usually caused by viral infections. This condition is clinically associated with fever and neck pain and causes hypothyroidism in a first phase followed by hyperthyroidism in a second phase. The histological hallmark is the presence of multiple foreign-body type granulomas accompanied by lymphocytes, plasma cells, histiocytes, and polymorphonuclear neutrophils. Necrosis is absent in the granulomas and fibrosis is variably present. Chronic lymphocytic thyroiditis is an immune-mediated thyroiditis. In its classical form, one can see histologically a variable infiltration of the thyroid parenchyma by lymphocytes that usually form nodular aggregates sometimes with germinal centers. In lymphocytic thyroiditis (Fig. 5.1), the follicular structures are not as hyperplastic as in Graves' disease and oncocytic (Hürthle cells) metaplasia is usually not seen. Thyrocytes usually show nuclear atypia related to inflammation, at a point that it can be misinterpreted for a papillary micro-carcinoma. When the lymphocytic infiltrate, usually with prominent germinal centers, is accompanied by oncocytic (Hürthle cells) metaplasia, then the preferred histological term is Hashimoto thyroiditis. It is usually more frequent in females around 40. Follicles can be atrophic or hyperplastic and different degrees of fibrosis can be seen (fibrous variant). As stated before, the hallmark of Hashimoto thyroiditis is the presence of oncocytes (Hürthle cells), i.e., follicular cells with abundant and characteristically eosinophilic cytoplasm. The accumulation of large mitochondria in the cytoplasm of these cells is responsible for their characteristic morphology. A less frequent form of thyroiditis is Riedel's thyroiditis, also known as silent thyroiditis, a condition characterized histologically by a dense sclerotic fibrous tissue infiltrated by lymphocytes and plasma cells, with occasional images of vasculitis (Fig. 5.2) [1].

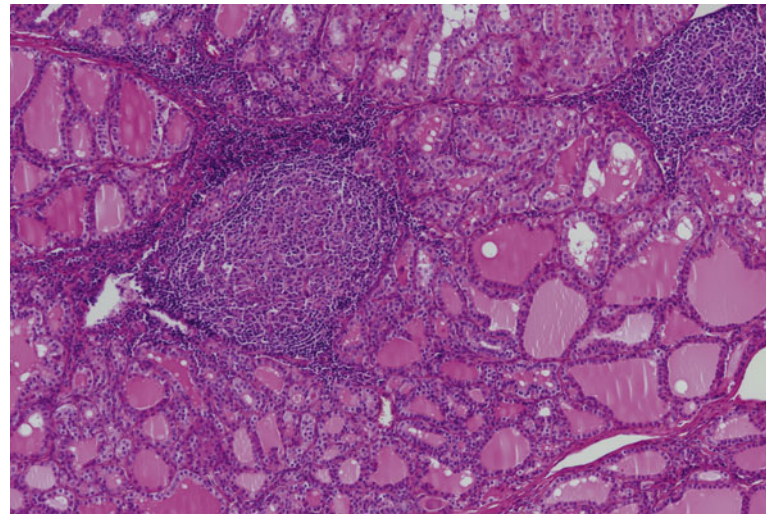

Fig. 5.1 Lymphocytic thyroiditis, histology H&E. In an alternance of macro- and microfollicles bordered by cubic thyrocytes not showing oncocytic changes, one can see large lymphoid follicles with prominent germinal centers, as well as a diffuse interstitial lymphocytic infiltrate

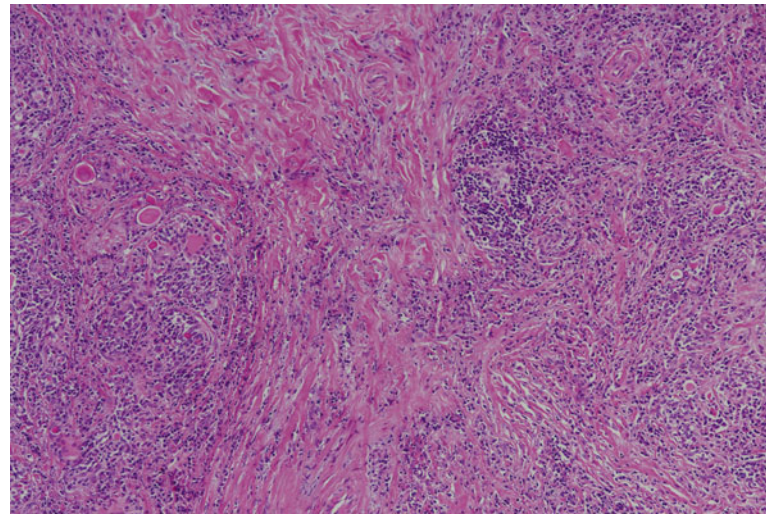

Fig. 5.2 Riedel's thyroiditis, histology H&E. Thyroid parenchyma has almost completely been replaced by dense collagen bands and a mixed, predominantly mononucleated inflammatory infiltrate. An intact and two atrophic thyroid follicles can be seen on the left of the image

5.1.4 Goiter

The term goiter is referring to an abnormal diffuse enlargement of the thyroid gland. Nodular hyperplasia of the thyroid, either uninodular or multinodular, can be the origin of a goiter. It can be endemic (related to iodine deficiency, the most common form) or less commonly sporadic and in this case of unknown etiology. In its early form, hyperplasia is diffuse and limited to the follicles that tend to adopt a macrofollicular architecture. In more advanced forms, the normal thyroid parenchyma is replaced by variously sized nodules that can present a variety of different morphological aspects. It is thus not unusual to observe nodules completely or partially encapsulated as well as areas with solid, colloid, hemorrhagic or cystic, calcified, fibrotic, and degenerated aspects. Microscopically, the thyroid epithelium can present a wide range of variations, from atrophic with flat cells to hyperplastic with cuboidal thyrocytes. Nuclei are usually centrally located, round, with inconspicuous nucleoli, and with coarse granular chromatin [1].

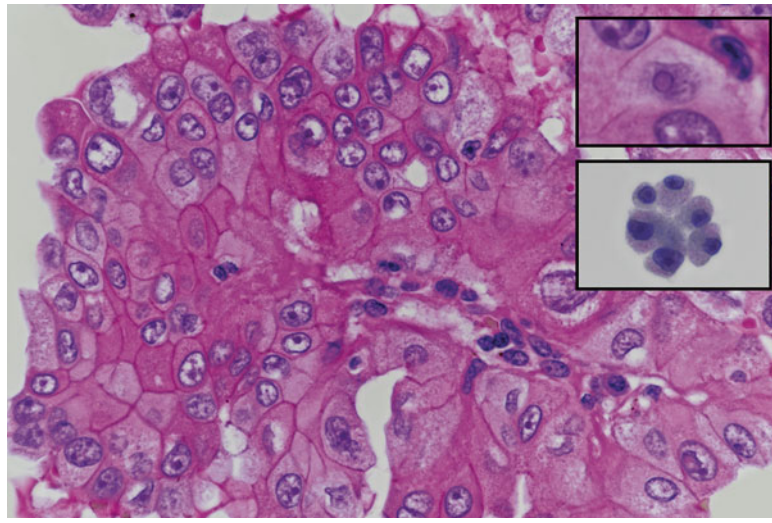

Fig. 5.3 Papillary thyroid carcinoma (PTC), histology H&E and cytology PAP (*lower inset*). In this oncocytic variant of PTC, cells are larger than in the classic variant of PTC, because of an increased content of eosinophilic and granular cytoplasm. Nuclei show the typical atypia of PTC: an irregular nuclear membrane outline, a ground-glass nucleus sometimes containing a pseudo-inclusion (*upper inset*). These cells rest on a true papilla with a vascular core. The *lower inset* shows the typical cytological aspect of thyrocytes with oncocytic cytoplasm and a nucleus of varying size and irregular nuclear membrane suggestive but not specific of PTC

5.1.5 Well-Differentiated Thyroid Carcinomas

Well-differentiated thyroid carcinomas are represented by papillary thyroid carcinoma (PTC), the most common entity, and follicular thyroid carcinoma (FTC). Both forms present excellent prognosis. No precursor lesion is officially identified for both types of carcinoma. However, lesions that have not fully developed the major criteria for malignancy, i.e., typical nuclear characteristics for PTC and unequivocal capsular and/or capsular vascular invasion for FTC are usually identified as lesions of uncertain malignant potential. The most important histological feature of PTC is represented by nuclear atypia (Fig. 5.3): nuclei are raisinoid with clear chromatin, nuclear indentations (grooves), and most characteristically intranuclear cytoplasmic invaginations (nuclear pseudo-inclusions or orphan Annie eyes). Papillary structures (hence the name) are present in the classic variant, but not seen in the follicular variant, where nuclear features are also less pronounced than in the classic variant. The most important histological feature of FTC is represented by infiltration of the tumor capsule (capsular invasion) and/or infiltration of capsular vessels (vascular invasion) (Fig. 5.4). Cytologically, the morphology of the nuclei of follicular cells constituting the tumor is not different from that of normal thyrocytes. These cells are mostly arranged in microfollicular structures.

More and more interest is rising in the field of thyroid carcinogenesis, with several molecular markers identified as initiators: RET/PTC and PAX8/PPAR-gamma rearrangements as well as RAS point mutation. Unknown additional events are required for progression to poorly differentiated or anaplastic forms. The only molecular alteration that has been found so far to be specific for carcinoma (PTC) is the BRAF point mutation. The identification of this anomaly is particularly useful in thyroid fine-needle aspiration (FNA) cytology in case of suspicious features, as its positive predictive value for carcinoma is 100 % [2].

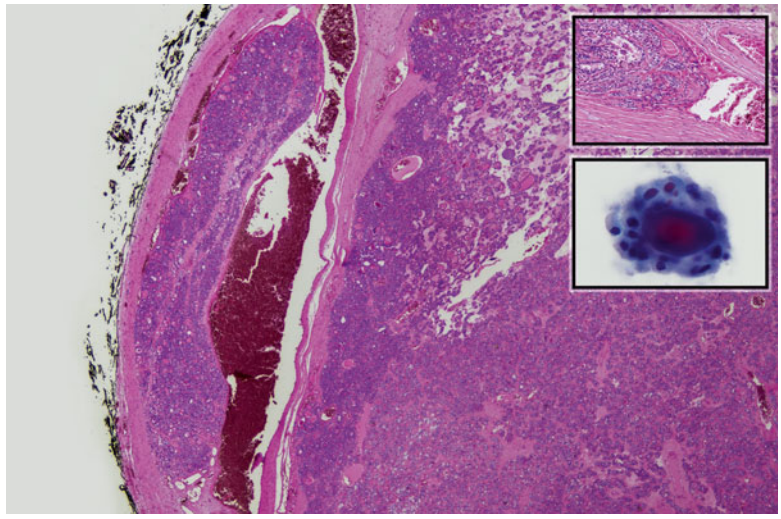

Fig. 5.4 Follicular thyroid carcinoma, histology H&E and cytology PAP (*lower inset*). At low power, one can see a proliferation of small to medium thyroid follicles, bordered on the left by a thick fibrous capsule. An unequivocal capsular vascular invasion is seen in this area and at higher magnification in the *upper inset*. The *lower inset* shows a microfollicle containing a droplet of colloid, as seen cytologically. This cytological image alone could not allow a distinction between a follicular adenoma and a follicular carcinoma, capsular and/or vascular capsular invasion being necessary for the diagnosis

5.1.6 Poorly Differentiated and Undifferentiated Thyroid Carcinomas

The prognosis in these forms of carcinomas drops dramatically in comparison to the well-differentiated forms, both forms being almost always lethal. Fortunately their incidence is low, as compared to well-differentiated carcinomas. Poorly differentiated carcinomas are also named "insular carcinomas," while "anaplastic carcinomas" describe undifferentiated carcinomas. It is not clear if these forms arise "de novo" or if they originate from well-differentiated carcinomas, both theories being probably valid. Additional genetic and epigenetic alterations are required for the progression to less differentiated forms. Histologically, insular carcinomas are characterized by a solid, trabecular, or insular (hence the name) architecture. Essential to pose the correct diagnosis are the presence of necrosis and a high mitotic activity. Anaplastic carcinomas (Fig. 5.5) show no reliable histological features to recognize them as primary cancers of the thyroid gland and thus open a differential diagnosis with locoregional or metastatic cancer: tumor is largely necrotic and cells are highly atypical with monstrous features, sometimes evoking high-grade sarcomas. Expression of basic epithelial cell differentiation markers such as cytokeratins as well as thyroid-specific markers is often lost in anaplastic carcinomas [3, 4].

5.1.7 Medullary Thyroid Carcinoma

Medullary thyroid carcinoma (MTC) arises from the parafollicular thyroid cell, the so-called C-cells, their main role being the production of calcitonin (CT). These cells are thought to be of neural crest origin and the tumor is thus considered to belong to the family of endocrine tumors. It is a rare neoplasm, representing up to 10 % of all thyroid tumor. CT is indeed also used as a powerful diagnostic tool when detected immunohistochemically in FNA or histological specimens. Morphologically, both familial and sporadic forms of MTC have in common a tremendous

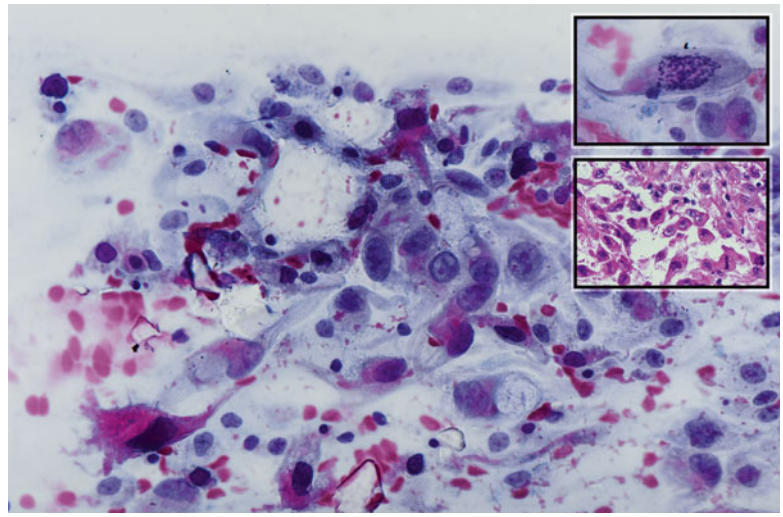

Fig. 5.5 Anaplastic carcinoma, cytology PAP. In this cytological preparation, a population of highly pleomorphic cells, sometimes monstrous, can be appreciated. The cell cytoplasm often displays a keratinized aspect, sometimes mimicking a squamous cell carcinoma. Numerous atypical mitoses can be seen (*upper inset*). The *lower inset* shows the same population as seen histologically after inclusion of the FNA material into a paraffin block (cell block)

variation of growth patterns that makes of this tumor a great mimicker of numerous malignancies. Most frequently, cells are polygonal/cylindrical with salt and pepper nuclear chromatin, a characteristic feature of all neuroendocrine lesions. The stroma is usually eosinophilic as it contains amyloid, evidenced by the Congo red staining, another characteristic diagnostic feature that is unfortunately not always present. In a not neglectable percentage of cases, cytonuclear morphology is different from the one with classical polygonal/cylindrical cells. Forms with small, spindle, clear, oxyphilic, squamoid, giant, binucleated and multinucleated, and pigmented cells are well-known. Architecturally, a great variation is also described with follicular and papillary structures. The possibility of a MTC should always be kept in mind by the pathologist in presence of unusual morphologies. The use of ancillary techniques in this context is fundamental: CT and CEA are positive, while thyroglobulin is negative [5].

5.2 Parathyroid Glands and Related Diseases

Despite considerable variations in their position and rarely in their number, humans usually have 4 parathyroid glands located in close contact with the posterolateral aspect of the thyroid gland. They come in two pairs, the upper pair deriving from the fourth branchial cleft and the lower pair from the third branchial cleft. These endocrine organs measure about 4 mm in their largest dimension and weigh together between 120 and 130 mg.

In physiological conditions, the cells making up these glands monitor blood calcium level. In order to counter a lowered blood calcium level, they produce and secrete parathormone (PTH), a hormone able to stimulate renal reabsorption of calcium and bone lysis. Oppositely, increased blood calcium levels are countered by calcitonin, an antagonistic hormone produced and secreted by C-cells of the thyroid gland. The salient histological and cytological features of the normal parathyroid gland are shown in Fig. 5.6.

Neoplastic conditions of the parathyroid glands can be classified in three categories, each of them often leading to hyperparathyroidism (increased blood level of PTH) and hypercalcemia (increased blood level of calcium): hyperplasia, adenoma, and carcinoma.

Hyperplasia is usually but not always an increase of size of all four glands that can be primary (i.e., not as a consequence of another condition) or secondary to renal insufficiency or impaired intestinal calcium absorption. In primary hyperplasia, blood level of PTH can be normal or increased, whereas in secondary hyperplasia, it is always increased. Histological examination is not

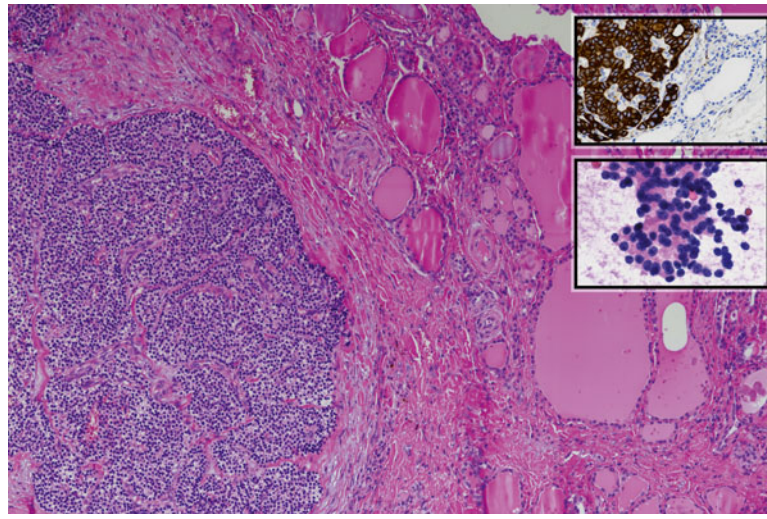

Fig. 5.6 Normal thyroid and parathyroid parenchyma, histology H&E, immunostains, and cytology PAP (*lower inset*). On the *right* of the image, one can see thyroid follicles of varying size containing watery colloid. Separated by the thyroid capsule, the parathyroid parenchyma appears on the *left* of the image as a population of small, very monotonous cubic cells with perfectly round nucleus, arranged in small lobules. Because of their different embryologic origins, thyroid and parathyroid parenchymas differ in their protein expression profile: a strong immunoreactivity of parathyroid cells for CD56 is seen here, thyrocytes being totally negative (*upper inset*). The *lower inset* shows at higher magnification the typical, very regular aspect of parathyroid cells as seen cytologically

reliable to differentiate primary from secondary hyperplasia and should not be interpreted without appropriate clinical data and laboratory findings. Adenomas usually involve one gland and are single. They are responsible of a hyperparathyroidism that is not secondary to other conditions (primary hyperparathyroidism). Histologically, they are surrounded by a thin fibrous capsule and have a hypercellular aspect. These criteria are however insufficient alone to differentiate adenoma from hyperplasia. In this regard, it is said that the diagnosis of adenoma can be secured by the examination of a second histologically normal parathyroid gland. Parathyroid carcinomas are rare findings that are usually suspected clinically on the base of very high blood levels of PTH and calcium. Macroscopically, they are hardened and can adhere to surrounding structures. Microscopically, these tumors characteristically display thick fibrous bands, numerous mitoses, and vascular invasions, these features being very uncommon in hyperplasia and adenoma. In common between hyperplasia, adenoma ,and carcinoma is their occasional occurrence in the context of various MEN syndromes [6, 7].

5.3 Paragangliomas

Paragangliomas are tumors of paraganglia (groups of nonneuronal cells either having endocrine or chemoreceptive functions) that can be found in a wide variety of sites related to sympathetic and parasympathetic chains and organs. Those with endocrine functions (sympathetic) include pheochromocytoma, a tumor of the adrenal medulla, as well as tumors developed in relation with sympathetic ganglia. These tumors secrete norepinephrine, and despite the risks associated with such secretion, they usually have a benign behavior. In the head and neck region, most paragangliomas have a chemoreceptive function (parasympathetic), the most common being carotid body paraganglioma. It is located at the bifurcation of the common carotid artery, in close contact with its wall, and represents a neoplastic transformation of

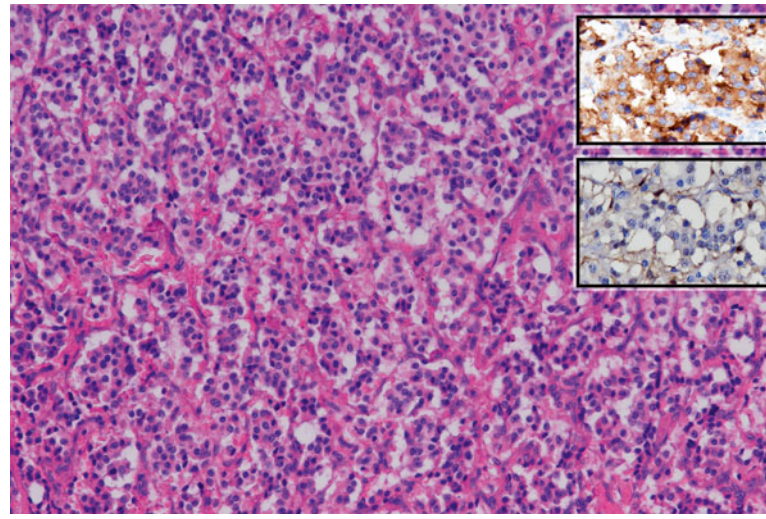

Fig. 5.7 Paraganglioma, histology H&E and immunostains. Small groups of monotonous cells ("Zellballen") with round nuclei and a typical salt and pepper chromatin can be seen. There is no atypia, necrosis, or mitosis. The *upper inset* shows a cytoplasmic immunoreactivity for chromogranin, a neuroendocrine marker. The *lower inset* shows a population of S100 positive sustentacular cells surrounding every group of neuroendocrine cells.

the carotid body, an organ able to detect changes in blood oxygen and carbon dioxide, as well as temperature and pH. There are other paragangliomas in the head and neck region (jugulotympanic, intravagal) that show similar morphological features and that only differ by their location and frequency. Tumors originating from paraganglias in the head and neck usually arise in a familial setting and with a low degree of aggressiveness [8–10]. Histological and cytological features of paraganglia are shown in Fig. 5.7.

References

1. Lloyd RV, Douglas BR, Young WF (2002) In: King DW (ed) Atlas of non tumor pathology. Endocrine diseases. Tumor-like conditions of the thyroid gland. American Registry of Pathology and the Armed Forces Institute of Pathology, Washington, DC
2. Bongiovanni M, Paone G, Ceriani L et al (2013) Cellular and molecular basis for thyroid cancer imaging in nuclear medicine. Clin Transl Imaging 1:149–161
3. Bongiovanni M, Sadow PM, Faquin WC (2009) Poorly differentiated thyroid carcinoma: a cytologic-histologic review. Adv Anat Pathol 16:283–289
4. Bongiovanni M, Bloom L, Krane JF et al (2009) Cytomorphologic features of poorly differentiated thyroid carcinoma: a multi-institutional analysis of 40 cases. Cancer 117:185–194
5. Pusztaszeri MP, Bongiovanni M, Faquin WC (2014) Update on the cytologic and molecular features of medullary thyroid carcinoma. Adv Anat Pathol 21:26–35
6. Baloch ZW, LiVolsi VA (2013) Pathology of the parathyroid glands in hyperparathyroidism. Semin Diagn Pathol 30:165–177
7. Al-Kurd A, Mekel M, Mazeh H (2014) Parathyroid carcinoma. Surg Oncol 23:107–114
8. Tischler AS (2008) Pheochromocytoma and extra-adrenal paraganglioma: updates. Arch Pathol Lab Med 132:1272–1284
9. McNicol AM (2006) Histopathology and immunohistochemistry of adrenal medullary tumors and paragangliomas. Endocr Pathol 17:329–336
10. Pellitteri PK, Rinaldo A, Myssiorek D et al (2004) Paragangliomas of the head and neck. Oral Oncol 40:563–575

Part II

Thyroid Diseases

Graves' Disease

6

Luca Giovanella

Abstract

Graves' disease is a thyroid-specific autoimmune disorder in which autoantibodies to the thyroid-stimulating hormone receptor (TSH-R) bind to TSH-R acting as agonists and stimulating more hormones to be released leading to hyperthyroidism and goiter.

This chapter provides a brief summary on Graves' disease, including some diagnostic and therapeutic aspects. Furthermore typical diagnostic images of Graves' disease are showed.

Keywords

Graves • Basedow • Hyperthyroidism • Thyroid • Autoimmunity • Autoantibodies

6.1 Introduction

Graves' disease is a thyroid-specific autoimmune disorder in which autoantibodies to the thyroid-stimulating hormone receptor (TSH-R) bind to TSH-R acting as agonists and stimulating more hormones to be released leading to hyperthyroidism and goiter [1]. The symptoms of Graves' disease stem partly from hyperthyroidism and partly as a consequence of autoimmunity. Patients can exhibit a variety of symptoms related to hyperthyroidism, including diffuse goiter (enlarged thyroid gland), rapid pulse, weight loss, and trembling. In addition, some patients with Graves' disease exhibit symptoms unique to this form of hyperthyroidism, including endocrine ophthalmopathy (Fig. 6.1) and rarely pretibial myxedema [2]. When thyrotoxicosis, goiter, and ocular signs and symptoms coexist, the diagnosis of Graves' disease appears self-evident. However,

Prof. Dr. med. L. Giovanella, MD, PhD
Department of Nuclear Medicine,
Thyroid and PET/CT Center,
Oncology Institute of Southern Switzerland,
Via Ospedale 12, CH-6500 Bellinzona and Lugano,
Switzerland
e-mail: luca.giovanella@eoc.ch

L. Giovanella et al. (eds.), *Atlas of Head and Neck Endocrine Disorders: Special Focus on Imaging and Imaging-Guided Procedures*, DOI 10.1007/978-3-319-22276-9_6

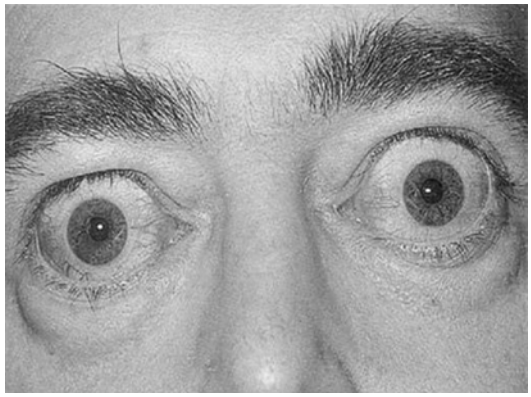

Fig. 6.1 A case of ophthalmopathy related to Graves' disease

50 % of patients with Graves' disease may not have clinically detectable ophthalmopathy at presentation, making the diagnosis less obvious.

6.2 Diagnosis

Once the question of thyrotoxicosis has been raised by clinical history and patient's examination, laboratory data are required to verify the diagnosis, help estimate the severity of the condition, and assist in planning therapy. Hyperthyroidism is confirmed when a suppressed thyrotropin (TSH) level (i.e., <0.1 mUI/L) is found in the face of an elevated free thyroxine (FT4) level. However, 10 % of patients will have an increased total or free triiodothyronine (FT3) level in the face of a normal FT4 and suppressed TSH level, a condition termed "T3 toxicosis." Antibodies to thyroglobulin (TgAb) and thyroid peroxidase (TPOAb) may be present but are not diagnostic. Although TSH receptor antibodies (TRAb) are present in the sera of almost all patients with Graves' disease, their measurement is should be restricted to selected cases (i.e., unclear diagnosis, euthyroid ophthalmopathy, risk of transient neonatal hyperthyroidism) [3].

Thyroid ultrasound shows a reduced echogenicity and heterogeneous echotexture, generally without nodularity (Fig. 6.2), associated with a significantly increased thyroid blood flow at color and power Doppler examination (Fig. 6.3).

Thyroid scan with either ^{99m}Tc-pertechnetate (Figs. 6.4 and 6.5) or ^{123}I (Fig. 6.6) demonstrates homogeneously increased uptake and easily discriminates Graves' disease from other causes of hyperthyroidism such as nodular autonomy (i.e., focally increased uptake), subacute thyroiditis, or iodine overload (depressed uptake) [4].

6.3 Therapy

Current Graves' disease treatments focus on restoring normal thyroid function by compensating for the hyperthyroidism of the disease. This is done either by antithyroid drugs, radioiodine, or surgery. The prevalence of each of these treatments varies regionally; each can be effective but also has potential side effects. Antithyroid drugs act by interfering with thyroid hormone synthesis. It is highly effective in normalizing thyroid hormones, but only 30–35 % of patients treated with them undergo remissions of the disease. Radioiodine is ingested in capsules or solutions, which is absorbed by the thyroid and causes localized death of thyroid tissue, typically counteracting hyperthyroidism within 6–18 weeks. Finally, thyroidectomy is often preferred for patients with a large goiter or an active ophthalmopathy [5].

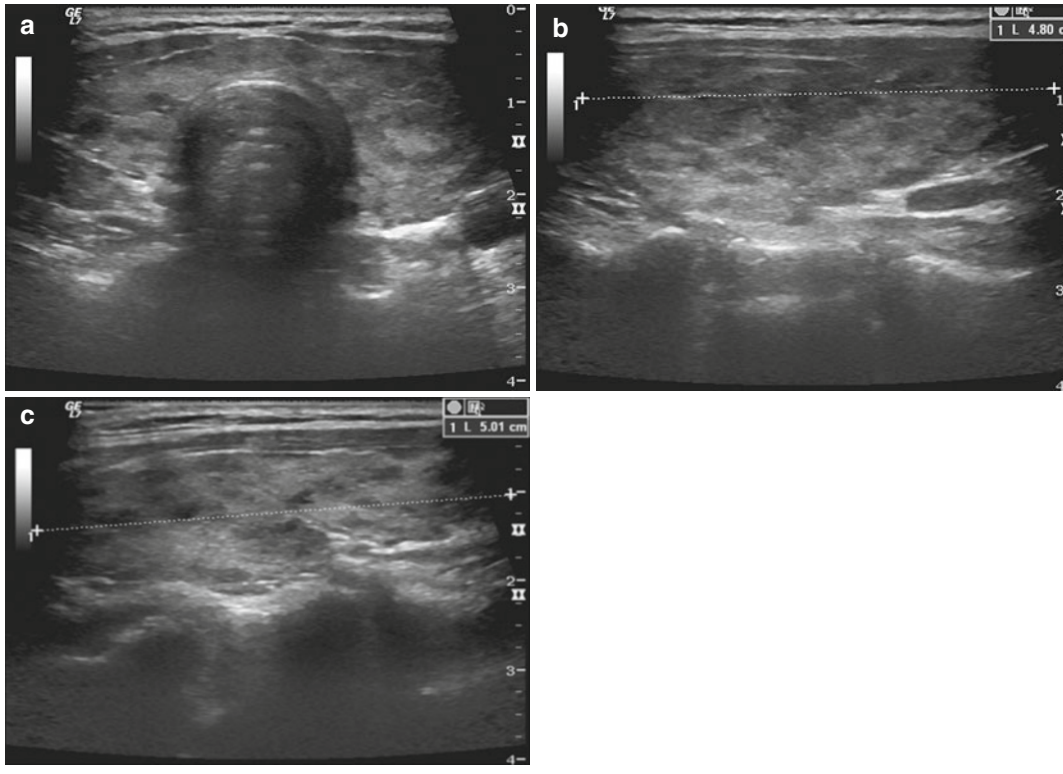

Fig. 6.2 Ultrasonographic (US) findings in a female patient with Graves' disease in axial (**a**) and longitudinal (**b**, **c**) projection. US shows enlarged thyroid lobes with diffusely heterogeneous echotexture

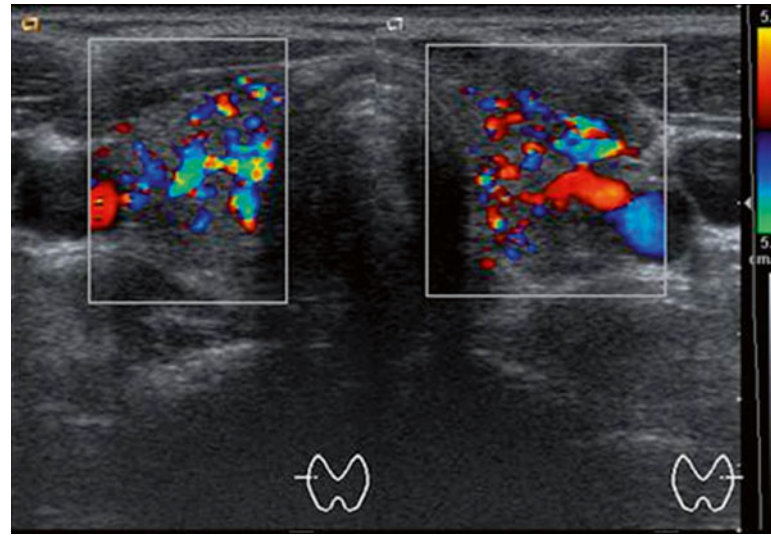

Fig. 6.3 Doppler ultrasonography findings in a patient with Graves' disease showing increased vascularization in both thyroid lobes

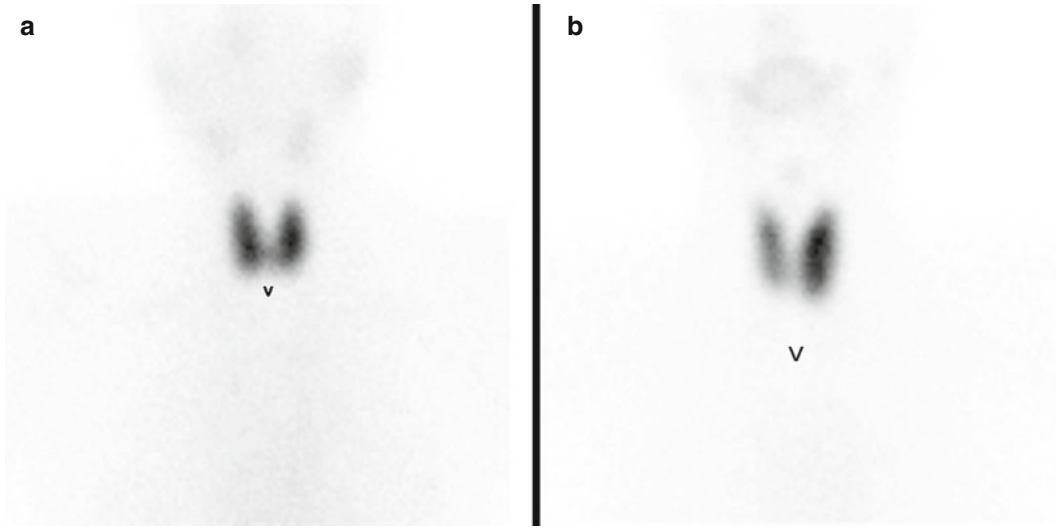

Fig. 6.4 Scintigraphic findings (planar view) in two patients with Graves' disease using ^{99m}TcO4– (**a**, **b**). The thyroid gland was normal sized (**a**) and enlarged (**b**), respectively, with diffuse and homogeneous increased tracer uptake

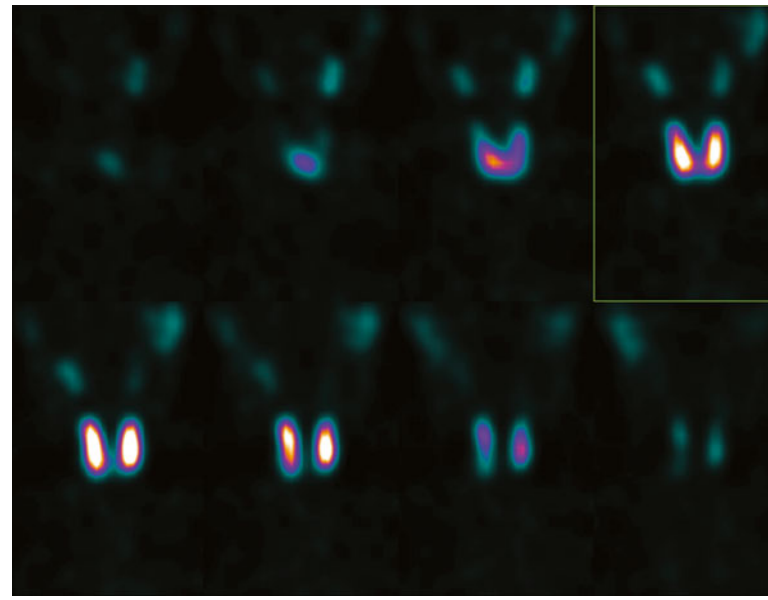

Fig. 6.5 Tomographic scintigraphy (SPECT in coronal views) using ^{99m}TcO4– in a patient with Graves' disease. The thyroid gland was enlarged with diffuse and homogeneous increased tracer uptake

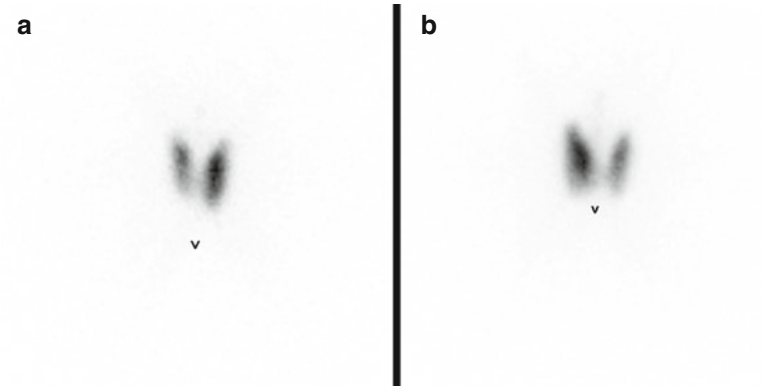

Fig. 6.6 Scintigraphic findings (planar view) in two patients (**a** and **b**, respectively) with Graves' disease using ^{123}I. The thyroid gland was enlarged with diffuse and homogeneous increased tracer uptake

References

1. Giovanella L, Ceriani L, Garancini S (2001) Clinical applications of the 2nd generation assay for anti-TSH receptor antibodies in Graves' disease. Evaluation in patients with negative 1st generation test. Clin Chem Lab Med 39:25–28
2. Brent GA (2008) Graves' disease. N Engl J Med 358:2594–2605
3. Giovanella L, Ceriani L, Ghelfo A (2008) Second-generation thyrotropin receptor antibodies assay and quantitative scintigraphy in autoimmune hyperthyroidism. Horm Metab Res 40:484–486
4. Meller J, Becker W (2002) The continuing importance of thyroid scintigraphy in the era of high-resolution ultrasound. Eur J Nucl Med 29(Suppl 2):425–438
5. Bahn RS, Burch HB, Cooper DS et al (2011) Hyperthyroidism and other causes of thyrotoxicosis: management guidelines of the American Thyroid Association and American Association of Clinical Endocrinologists. Endocr Pract 17:456–520

Thyroid Autonomy

7

Luca Giovanella

Abstract

Hyperfunctioning thyroid adenomas are benign monoclonal tumors characterized by their capacity to grow and produce thyroid hormone autonomously independently from thyrotropin feedback.

This chapter provides a brief summary on thyroid autonomy, including some diagnostic and therapeutic aspects. Furthermore typical diagnostic images of thyroid autonomy are discussed.

Keywords

Autonomy • Toxic nodule • Toxic adenoma • Hyperthyroidism • Plummer • Thyroid

7.1 Introduction

Solitary hyperfunctioning thyroid adenomas are benign monoclonal tumors characterized by their capacity to grow and produce thyroid hormone autonomously independently from thyrotropin (TSH) feedback. Mutations of the TSH receptor (TSH-R) have been found in most solitary hyperfunctioning thyroid adenomas. Toxic multinodular goiters were believed to differ in their nature and pathogenesis from toxic adenoma. The incidence of toxic multinodular goiters has been demonstrated to be related to iodine deficiency. However, TSH receptor mutations were demonstrated in microscopic autonomously functioning areas in euthyroid goiters, and it is therefore very likely that toxic thyroid nodules originate from small autonomous areas in iodine-deficient euthyroid goiters that contain a TSH receptor mutation [1].

Prof. Dr. med. L. Giovanella, MD, PhD
Department of Nuclear Medicine,
Thyroid and PET/CT Center,
Oncology Institute of Southern Switzerland,
Via Ospedale 12, CH-6500 Bellinzona, Switzerland
e-mail: luca.giovanella@eoc.ch

L. Giovanella et al. (eds.), *Atlas of Head and Neck Endocrine Disorders: Special Focus on Imaging and Imaging-Guided Procedures*, DOI 10.1007/978-3-319-22276-9_7

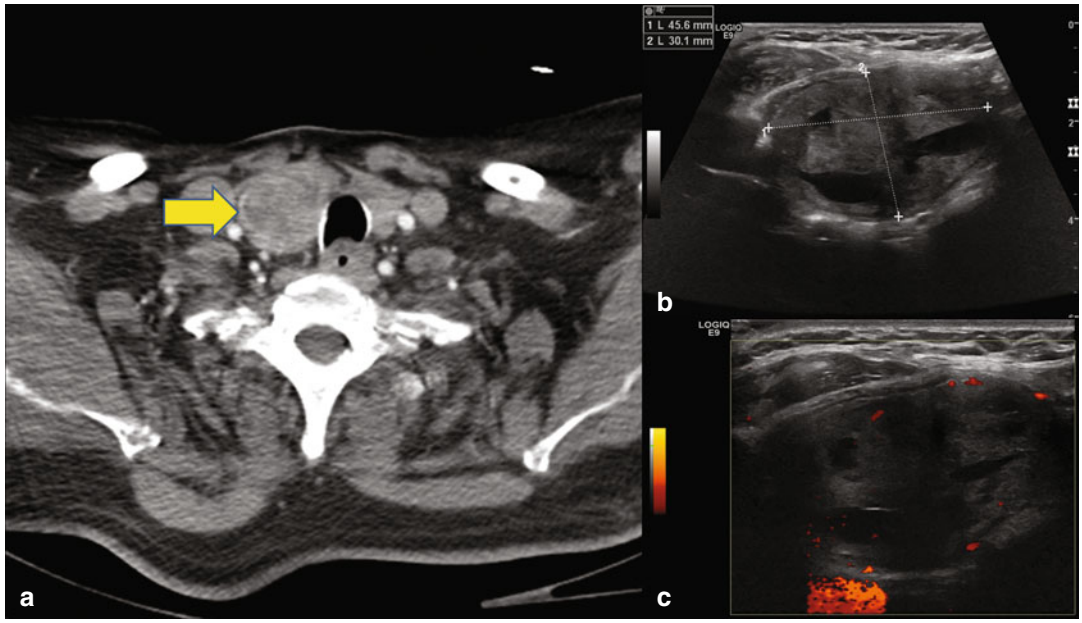

Fig. 7.1 Axial computed tomography (**a**), ultrasonography (**b**), and color Doppler ultrasonography (**c**) images in a 70-year-old male patient with hyperthyroidism. Computed tomography (**a**) showed a large nodule (diameter of 4.5 cm) in the right thyroid lobe (*arrow*). The thyroid nodule was hypoechoic and inhomogeneous at ultrasonography (**b**) with low intranodular blood flow (**c**). These morphological findings were not specific for hyperfunctioning thyroid nodules

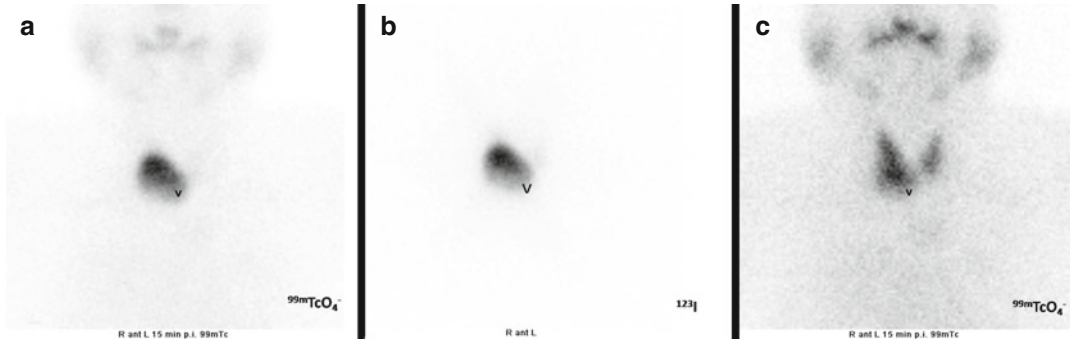

Fig. 7.2 Scintigraphic findings in the same patient of Fig. 7.1. Thyroid scan with $^{99m}TcO_4^-$ (**a**) showed a large hyperfunctioning thyroid nodule in the right thyroid lobe with functional suppression of the remaining thyroid parenchyma (**b**). These findings are confirmed by scintigraphy with ^{123}I performed for dosimetric purpose. After radiometabolic treatment with ^{131}I, euthyroid status was reached and posttreatment thyroid scan with $^{99m}TcO_4^-$ showed homogeneous uptake in the thyroid gland (**c**)

7.2 Diagnosis

Thyroid ultrasound pattern is not specific in hyperfunctioning nodules, and thyroid scintigraphy with either ^{99m}Tc-pertechnetate ($^{99m}TcO_4^-$) or ^{123}I-natrium iodide (^{123}I) is the only examination able to demonstrate the presence of autonomously functioning thyroid nodules (AFTN) (Figs. 7.1, 7.2, 7.3, 7.4, and 7.5). In turn, the identification of a lesion as an AFTN almost certainly excludes malignancy. Accordingly, current clinical guidelines suggest refraining from fine needle aspiration cytology (FNAC) of hyperactive nodules diagnosed by thyroid scan with either

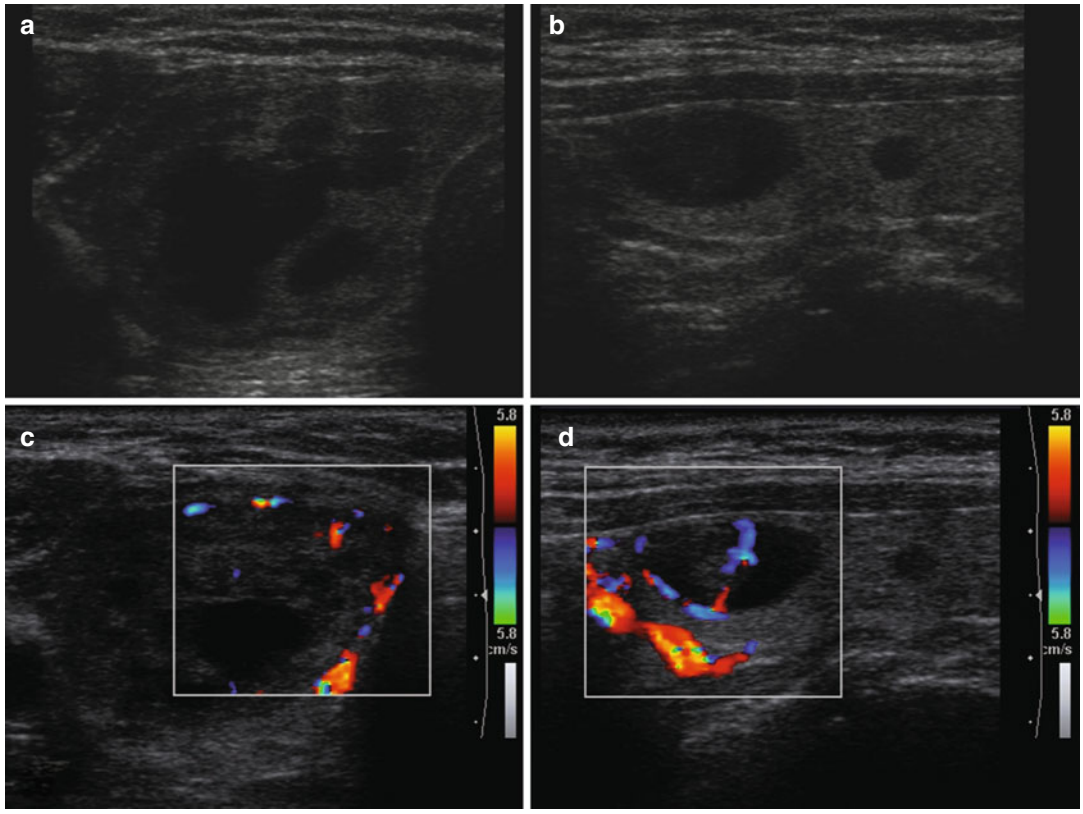

Fig. 7.3 Ultrasonography (**a**, **b**) and color Doppler ultrasonography (**c**, **d**) images in a 66-year-old female patient with hyperthyroidism. Ultrasonography showed two hypoechoic and inhomogeneous nodules in the right thyroid lobe (**a**, **b**) with increased blood flow (**c**, **d**). These ultrasonography findings are not specific for hyperfunctioning thyroid nodules

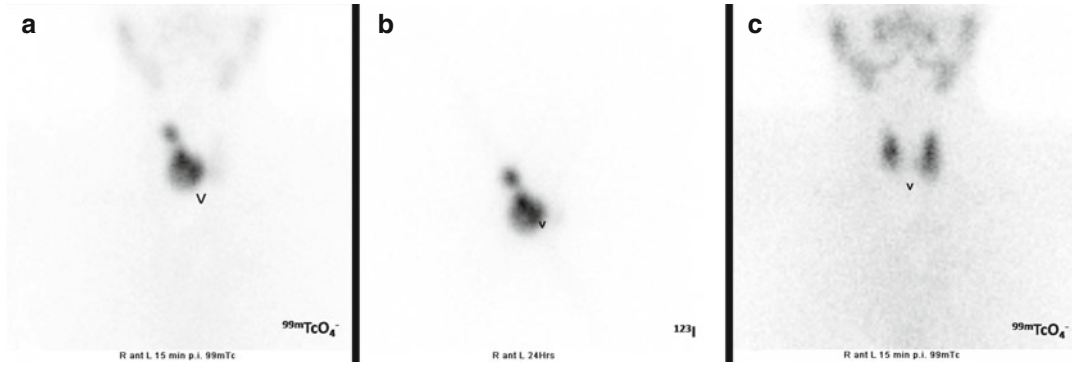

Fig. 7.4 Scintigraphic findings in the same patient of Fig. 7.3. Thyroid scan with $^{99m}TcO_4^-$ (**a**) showed two hyperfunctioning thyroid nodules in the right thyroid lobe with functional suppression of the remaining thyroid parenchyma (**b**). These findings were confirmed by scintigraphy with ^{123}I performed for dosimetric purpose. After radiometabolic treatment with ^{131}I, euthyroid status was reached and posttreatment thyroid scan with $^{99m}TcO_4^-$ showed homogeneous uptake in the thyroid gland (**c**)

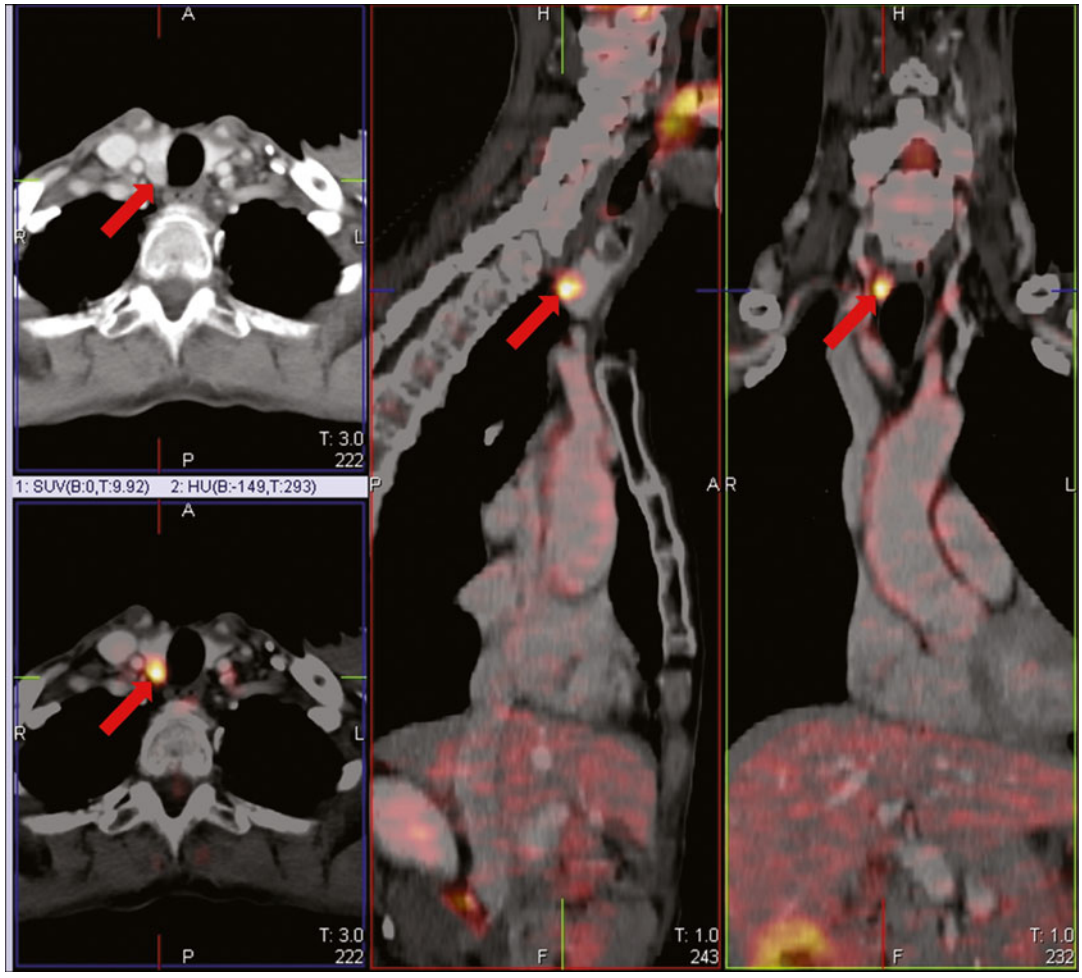

Fig. 7.5 Hyperfunctioning thyroid nodule (*arrow*) incidentally detected by fluorine-18 fluorodeoxyglucose positron tomography/computed tomography (^{18}F-FDG PET/CT) as focal area of increased thyroid uptake in the right thyroid lobe. This focal uptake pattern is not specific for thyroid autonomy but it may represent a thyroid tumor in about one third of cases

$^{99m}TcO_4^-$ or ^{123}I [2]. Furthermore, a timely diagnosis of thyroid autonomy allows early treatment avoiding progression toward manifest hyperthyroidism. Despite that, thyroid scintigraphy is now used more rarely in the management of thyroid nodules based on the assumption that serum TSH levels are always subnormal in the presence of an AFTN. However, especially in geographic areas that formerly had or still show dietary iodine deficiency, serum TSH may remain normal even if AFTN is present because, especially in the early phases, the bulk of autonomous tissue, the low proliferation rate of thyroid epithelial cells, and the low synthesis rate of thyroid hormones may be insufficient to suppress the TSH. Accordingly, normal TSH is encountered in up to 40–70 % of European patients with AFTN at thyroid scan [3].

7.3 Therapy

Radioiodine and surgery are the two most effective treatment options for permanently decreasing the production of thyroid hormone [4, 5]. Antithyroid drugs decrease thyroid hormone

production but do not induce remission (i.e., discontinuation results in recurrence of hyperthyroidism). Thioamides are often used to treat hyperthyroidism in patients with unifocal or multifocal autonomy in preparation for definitive radioiodine treatment or surgery. However, in patients with increased surgical risk and/or inability to comply with radiation safety guidelines, long-term treatment with thioamides is an option. Radioiodine is given as primary therapy to most patients with AFTN while surgery is generally indicated for patients with obstructive goiters or very large goiters, those who need rapid and definitive correction of hyperthyroidism, and patients with coexisting malignancy or primary hyperparathyroidism. Surgery could also be considered in patients with coexistent nonfunctioning nodules, especially if the goiters are large. Ultrasound-guided percutaneous ethanol injection, interstitial laser photocoagulation or radiofrequency ablation were also evaluated with sparse results and their use is not recommended in daily clinical practice.

References

1. Giovanella L (2009) Thyroid nodules: clinical management and differential diagnosis. Praxis 98:83–90
2. Giovanella L, Ceriani L, Treglia G (2014) Role of isotope scan, including positron emission tomography/computed tomography, in nodular goitre. Best Pract Res Clin Endocrinol Metab 28:507–518
3. Treglia G, Trimboli P, Verburg FA et al (2015) Prevalence of normal TSH value among patients with autonomously functioning thyroid nodule. Eur J Clin Invest 45:739–744
4. Ross DS (2011) Radioiodine therapy for hyperthyroidism. N Engl J Med 364:542–550
5. Vidal-Trecan GM, Stahl JE, Eckman MH (2004) Radioiodine or surgery for toxic thyroid adenoma: dissecting an important decision. A cost-effectiveness analysis. Thyroid 14:933–945

Thyroiditis

8

Pierpaolo Trimboli and Luca Giovanella

Abstract

Thyroiditis is an inflammation of the thyroid gland that has several etiologies and can be associated with normal, elevated, or depressed thyroid function, often with evolution from one condition to another. Basing on clinical presentation, different subtypes of thyroiditis can be divided into those associated with thyroid pain and tenderness, and those that are painless. The most frequent painful form is subacute thyroiditis, while the most frequent painless form is autoimmune thyroiditis (i.e., Hashimoto's disease). In this chapter, some principles of differential diagnosis, therapy, and follow-up of thyroiditis are briefly discussed. Furthermore, some typical images of thyroiditis are provided.

Keywords

Subacute thyroiditis • Autoimmune thyroiditis • Hashimoto's disease • Inflammation • Thyroiditis • Thyroid

P. Trimboli, MD
Section of Endocrinology and Diabetology, Ospedale Israelitico, Rome, Italy

Department of Nuclear Medicine, Thyroid and PET/CT Centre, Oncology Institute of Southern Switzerland, Via Ospedale 12, Bellinzona and Lugano CH-6500, Switzerland

Prof. Dr. med. L. Giovanella, MD, PhD (✉)
Department of Nuclear Medicine, Thyroid and PET/CT Centre, Oncology Institute of Southern Switzerland, Via Ospedale 12, Bellinzona and Lugano CH-6500, Switzerland
e-mail: luca.giovanella@eoc.ch

8.1 Introduction

Thyroiditis is an inflammation of the thyroid gland that has several etiologies and can be associated with normal, elevated, or depressed thyroid function, often with evolution from one condition to another. Although there is considerable overlap, different subtypes of thyroiditis can be divided into those associated with thyroid pain and tenderness, and those that are painless.

L. Giovanella et al. (eds.), *Atlas of Head and Neck Endocrine Disorders: Special Focus on Imaging and Imaging-Guided Procedures*, DOI 10.1007/978-3-319-22276-9_8

8.2 Painful Thyroiditis

8.2.1 Subacute Thyroiditis

Also named subacute granulomatous thyroiditis, giant cell thyroiditis, or de Quervain's thyroiditis, subacute thyroiditis is attributed to a viral infection being the most common cause of thyroid pain. It affects more women than men, and most often occurs at 40–50 years of age. Clinical presentation includes a tender, diffuse goiter and neck pain that often radiates up to the ear associated to myalgia, pharyngitis, low-grade fever, and fatigue [1]. C-reactive protein (CRP) and erythrocyte sedimentation rate (ESR) are typically increased. Thyroid follicular cell damage leads to a transient unregulated release of large amounts of thyroid hormones into the circulation. This process usually is transient (i.e., 3–6 weeks), and patients usually return to euthyroidism within 3–12 months. However, in 10–15 % of patients, hypothyroidism persists, requiring long-term levothyroxine therapy [1]. Treatment for subacute granulomatous thyroiditis is firstly based on nonsteroidal anti-inflammatory drugs (NSAIDs). If no improvement occurs within 1 week, prednisone may be given in a dosage of 40–60 mg daily tapered to discontinuation over 4–6 weeks [1–3]. Beta-blockers may be given to treat symptoms of thyrotoxicosis.

8.2.2 Radiation-Induced Thyroiditis

Approximately 1 % of patients who have radioactive iodine for hyperthyroidism develop radiation thyroiditis between 5 and 10 days after the procedure. Clinical presentation resembles subacute thyroiditis. A brief course of NSAIDs or, rarely, prednisone in dosages of 40–60 mg per day may be used to alleviate pain; a beta-blocker often is required to block the peripheral effects of the thyroid hormone [1].

8.2.3 Suppurative Thyroiditis

This is an extremely rare form of thyroiditis caused by bacterial, fungal, or parasitic infection of the thyroid. Infection usually spreads to the thyroid from the adjacent structures directly or through the blood or lymphatic system or from a distant focus. Suppurative thyroiditis commonly present with acute unilateral anterior neck pain and erythema of the skin overlying an exquisitely tender thyroid. ESR is elevated, and the white blood cell count generally shows a marked increase with a left shift. Fine-needle aspiration of the lesion with Gram stain and culture is the most useful diagnostic test. Parenteral antibiotics should be given, and surgical drainage may also be required [1, 2].

8.3 Painless Thyroiditis

8.3.1 Autoimmune Thyroiditis

Also known as chronic lymphocytic thyroiditis or Hashimoto's thyroiditis, autoimmune thyroiditis (AIT) is a T-cell mediated autoimmune disorder in which thyroid-specific autoantibodies are produced [1, 2, 4]. This thyroid-specific pathway affects thyroid structure, and thyroid gland damage leads over time to an impaired gland function (i.e., hypothyroidism) [3]. The course of the disease varies, and there are no specific symptoms of AIT until hypothyroidism is achieved [5]. High circulating levels of antithyroid peroxidase antibodies (TPOAb) are a hallmark of AIT [1]. The indications for treatment of Hashimoto's disease with levothyroxine are goiter or clinical hypothyroidism [2].

8.3.2 Painless Sporadic Thyroiditis and Postpartum Thyroiditis

Painless sporadic thyroiditis (also known as subacute lymphocytic thyroiditis or silent sporadic thyroiditis) and postpartum thyroiditis are similar, but the former occurs in the absence of pregnancy. They appear to be autoimmune in origin as the thyroid contains a lymphocytic infiltrate and TPOAb are generally positive [3]. Most patients present (2–6 months after delivery in postpartum type) with a small, nontender goiter in the absence of pain. Hyperthyroidism is frequently asymptomatic and may be followed

by transient hypothyroidism in about 25 % of patients. Many patients finally develop permanent hypothyroidism 2–10 years after the first episode [1, 2].

8.3.3 Drug-Induced Thyroiditis

Amiodarone, interferon-alfa, interleukin-2, and lithium may cause a destructive thyroiditis with hyperthyroidism or hypothyroidism, low radioiodine uptake, and variable presence of TPOAb. Treatment is similar to that of subacute granulomatous or lymphocytic thyroiditis. The thyroid abnormalities usually resolve with discontinuation of the responsible drug.

8.3.4 Riedel's Thyroiditis

Riedel's thyroiditis (also known as fibrous thyroiditis) is a rare condition characterized by an extensive fibrotic process of unknown etiology involving the thyroid and adjacent structures. It may be associated with a diffuse fibrotic process affecting multiple tissues (idiopathic multifocal fibrosclerosis). Patients present with a rock-hard, fixed, painless goiter, often accompanied by symptoms of esophageal or tracheal compression [6].

8.4 Diagnosis and Follow-Up of Thyroiditis

Laboratory test (thyroid function, CRP, ESR, blood cell count), thyroid ultrasound (Figs. 8.1, 8.2, 8.3, 8.4, and 8.5), and thyroid scintigraphy (Figs. 8.6 and 8.7) are employed to differentiate thyroiditis providing the basis for a specific treatment. Overt or subclinical hyperthyroidism is generally found in painful and painless destructive thyroiditis, while thyroid function varies in autoimmune and Riedel's thyroiditis. Positive TPOAb are detected in autoimmune, painless, and postpartum thyroiditis. CRP and ESR are increased in subacute and suppurative thyroiditis. White blood cells are typically increased in suppurative thyroiditis. Ultrasound pattern is aspecific showing a diffusely reduced echogenicity and heterogeneity of thyroid echotexture with diffuse pseudonodular pattern. Moderate to increased thyroid vascularity frequently occurs even if a reduction in vascular signal is detected in subacute, painless, and drug-induced thyroiditis. Thyroid scan with ^{123}I or ^{99m}Tc-pertechnetate demonstrates homogeneously reduced uptake in destructive thyroiditis, while large variability is reported in AIT. Sometimes thyroiditis can be incidentally detected as diffuse fluorodeoxyglucose (FDG) uptake by positron emission tomography/computed tomography (Fig. 8.8).

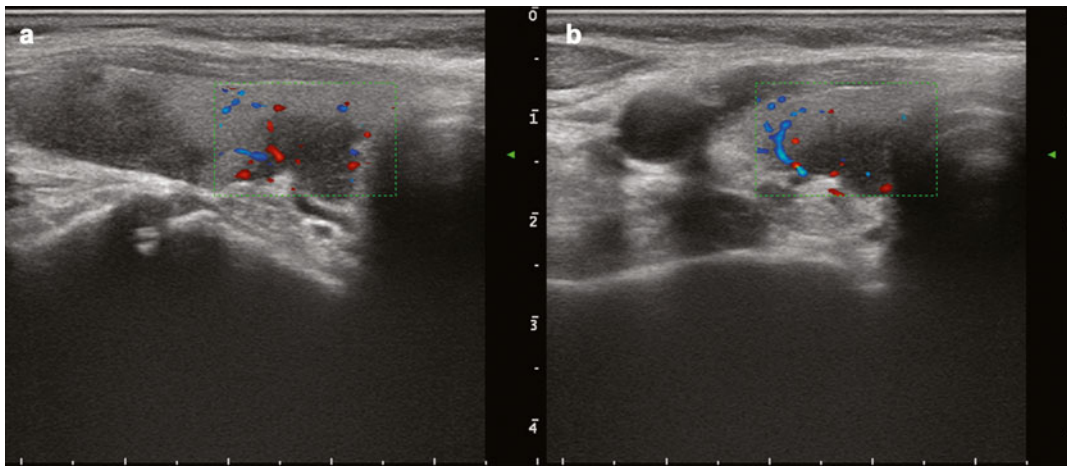

Fig. 8.1 Ultrasound presentation of a subacute de Quervain thyroiditis. Two hypoechoic areas with undefined margins and vascular spots are present at the superior and inferior thirds of the right thyroid lobe (**a**, longitudinal scan; **b**, transversal scan). Mild-moderate pain is detectable at physical examination and ultrasound evaluation

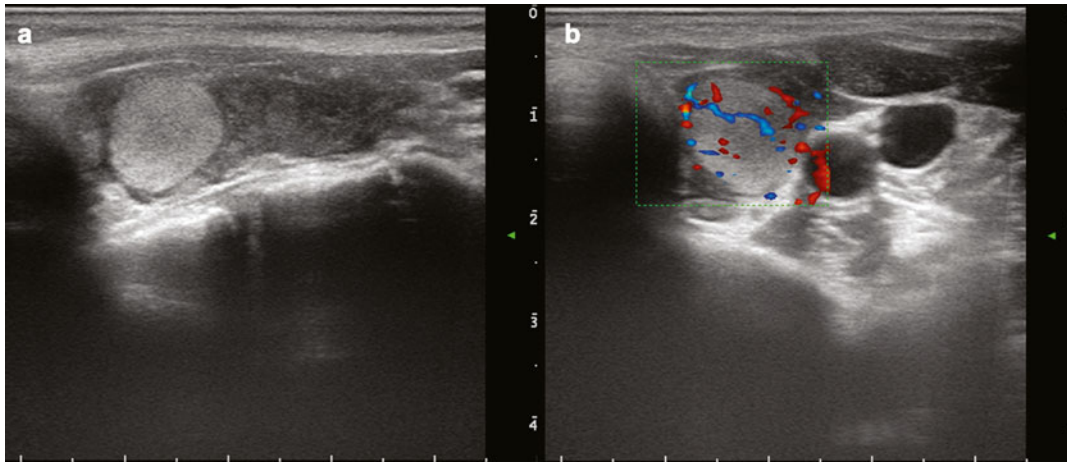

Fig. 8.2 Ultrasound presentation of a case of Hashimoto thyroiditis with a well defined hyperechoic area. The gland has an extended hypoechogenicity as a sign of tissue destruction by Hashimoto disease. At the base of left lobe there is a normoechoic (hyperechoic with respect to the surrounding tissue) nodular area (**a**) with normal vascularization (**b**) of about 1 cm. This area is not a "true" nodule but represents a part of the gland not involved by Hashimoto autoimmune pathways

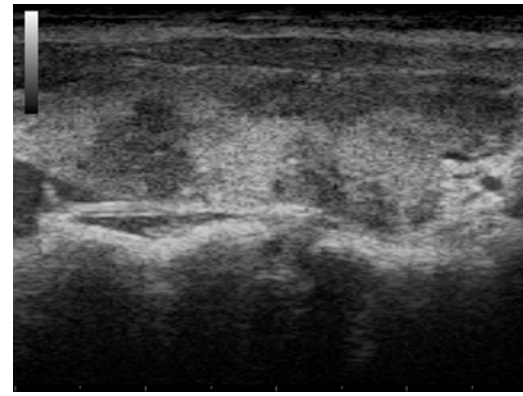

Fig. 8.3 Longitudinal ultrasonography scan of right thyroid lobe with Hashimoto's thyroiditis. The structure is inhomogeneously damaged, the majority of the tissue appears hypoechoic due to the damage by autoimmune pathway. Normoechoic areas represent the normal (normofunctioning) tissue

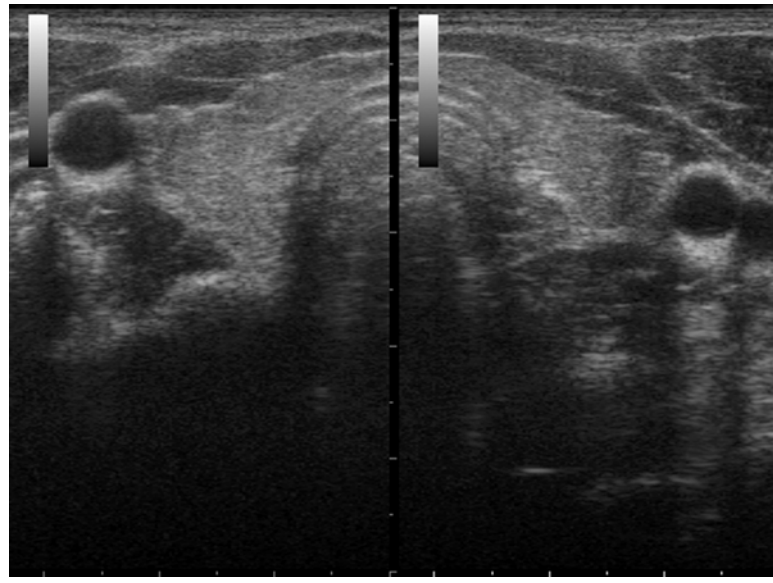

Fig. 8.4 Transverse ultrasonography scan of thyroid gland with thyroiditis. Thyroid volume is reduced, margins are irregular, echostructure is slightly inhomogeneous, echogenicity is poor. This thyroid US aspect frequently correlates with hypofunction (hypothyroidism)

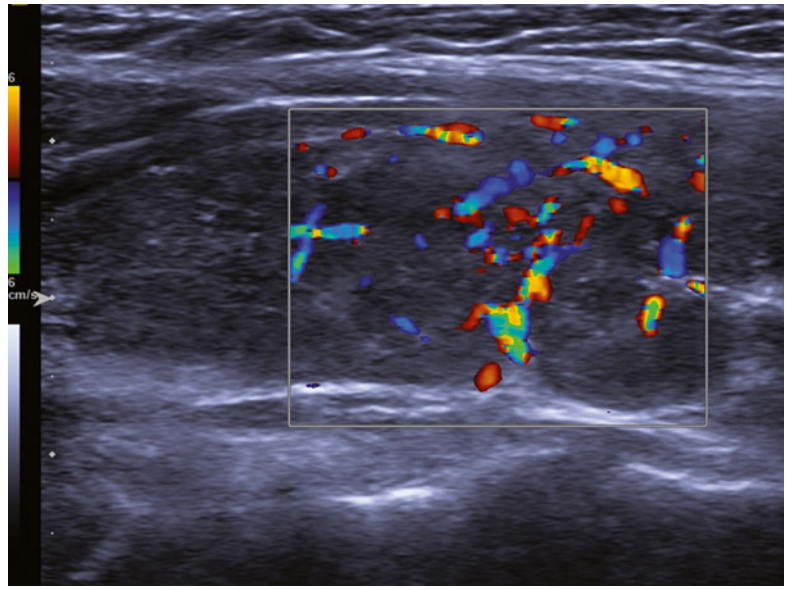

Fig. 8.5 Doppler US demonstrating moderate increased thyroid vascularity in a case of autoimmune thyroiditis

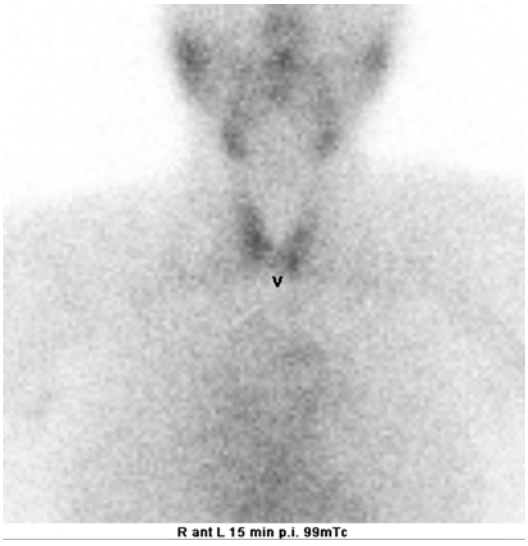

Fig. 8.6 Thyroid scintigraphy with ^{99m}Tc showing global reduced tracer uptake in a patient with autoimmune thyroiditis

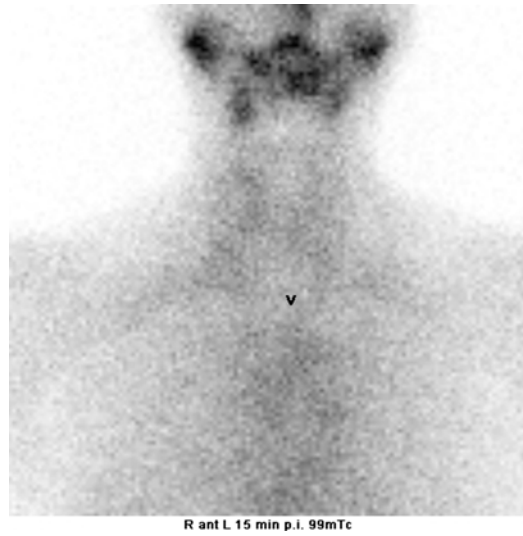

Fig. 8.7 Thyroid scintigraphy with ^{99m}Tc showing absent tracer uptake in a patient with subacute thyroiditis

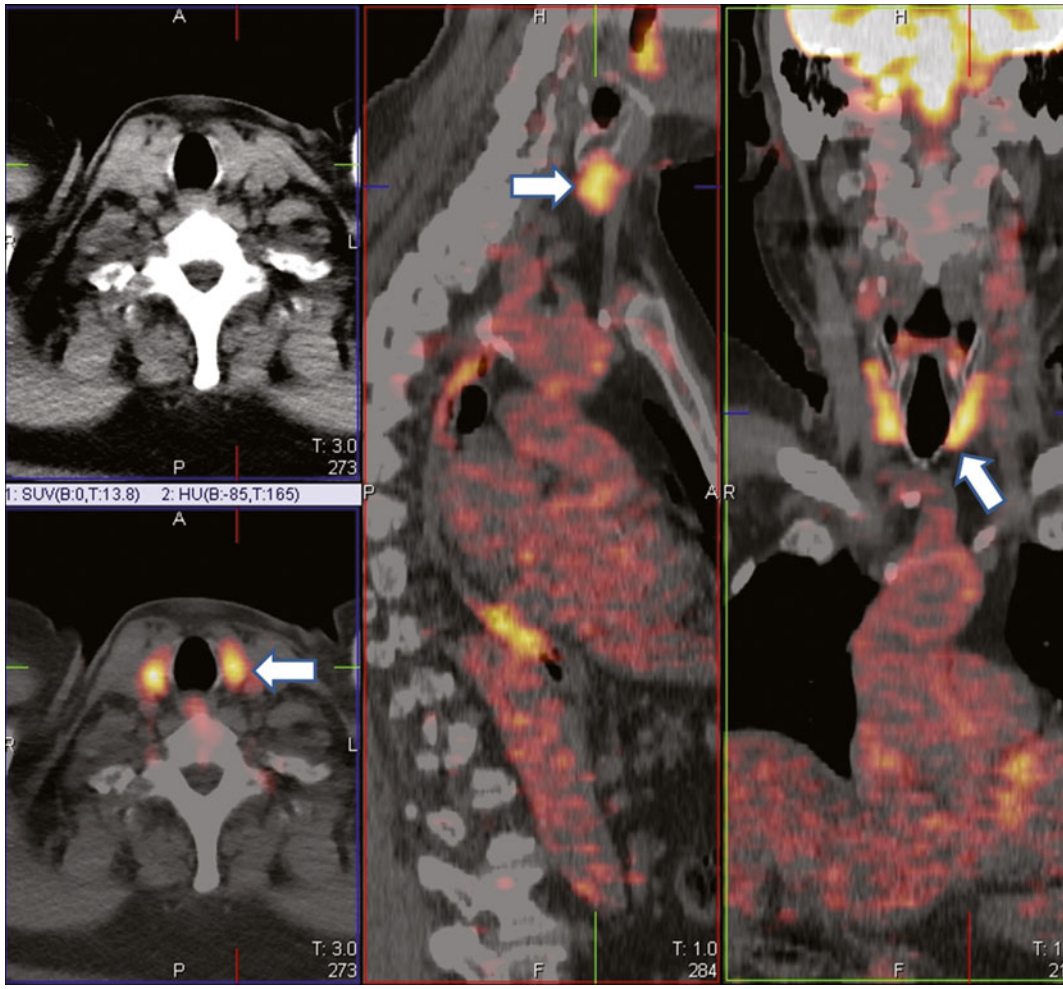

Fig. 8.8 Thyroiditis incidentally detected by fluorine-18 fluorodeoxyglucose positron emission tomography/computed tomography showing diffuse tracer uptake in the thyroid gland (*arrows*)

References

1. Pearce EN, Farwell AP, Braverman LE (2003) Thyroiditis. N Engl J Med 348:2646–2655
2. Lazarus J, Hennessey DJ (2012) Subacute thyroiditis. In: De Groot LJ, Beck-Peccoz P, Chrousos G et al (eds) Endotext [Internet]. MDText.com, Inc., South Dartmouth
3. Alfadda AA, Sallam RM, Elawad GE et al (2014) Subacute thyroiditis: clinical presentation and long term outcome. Int J Endocrinol 2014:794943
4. Caturegli P, De Remigis A, Rose NR (2014) Hashimoto thyroiditis: clinical and diagnostic criteria. Autoimmun Rev 13:391–397
5. Walsh JP, Bremner AP, Feddema P et al (2010) Thyrotropin and thyroid antibodies as predictors of hypothyroidism: a 13-year, longitudinal study of a community-based cohort using current immunoassay techniques. J Clin Endocrinol Metab 95:1095–1104
6. Hennessey JV (2011) Clinical review: Riedel's thyroiditis: a clinical review. J Clin Endocrinol Metab 96:3031–3041

Nontoxic Uninodular Goiter

9

Massimiliano Andrioli and Roberto Valcavi

Abstract

This chapter describes imaging findings in patients with nontoxic uninodular goiter. Thyroid ultrasonography is the first-line diagnostic procedure for characterizing uninodular goiter providing immediate information about the degree of suspicion of a thyroid lesion. Position, extracapsular relationships, internal content, shape, echogenicity, echotexture, presence of calcifications, margins, vascularity, hardness, and size of a thyroid lesion are the ultrasonographic features commonly used for risk stratification. Scintigraphic techniques may have a supporting role in this setting.

Keywords

Thyroid nodule • Goiter • Thyroid cancer • Ultrasonography • Scintigraphy

9.1 Introduction

Nodular thyroid disease is a common finding and malignancy comprises less than 5 % of all thyroid nodules [1]. Cytological examination of material obtained by fine-needle cytology (FNC) is the best single test for tumor diagnosis [2]. To identify the nodule that should be cytologically analyzed represents the main challenge for clinicians. Thyroid ultrasonography (US) gives immediate information about the degree of suspicion of a thyroid lesion and is widely recognized as the first-line diagnostic procedure for characterizing thyroid lesions [3]. Scintigraphy also

M. Andrioli, MD
EndocrinologiaOggi,
v.le Somalia 33, 00199 Rome, Italy
e-mail: andrioli@endocrinologiaoggi.it

R. Valcavi, MD (✉)
Endocrinologia, Centro Palmer,
v. Fratelli Cervi 75/B, 42010 Reggio Emilia, Italy
e-mail: info@robertovalcavi.it

L. Giovanella et al. (eds.), *Atlas of Head and Neck Endocrine Disorders: Special Focus on Imaging and Imaging-Guided Procedures*, DOI 10.1007/978-3-319-22276-9_9

plays a role in this field, most of all in toxic thyroid nodules.

Position, extracapsular relationships, internal content, shape, echogenicity, echotexture, presence of calcifications, margins, vascularity, hardness, and size of a thyroid lesion are the ultrasonographic features commonly used for risk stratification.

9.2 Position

Any thyroid lesion may be placed in one-third superior, medium, or inferior of each thyroid lobe or in the isthmus. Seldom, they may be located in the pyramidal lobe and more rarely can be ectopic. The localization of a thyroid lesion has no diagnostic importance in distinguishing between benign and malignant nodules.

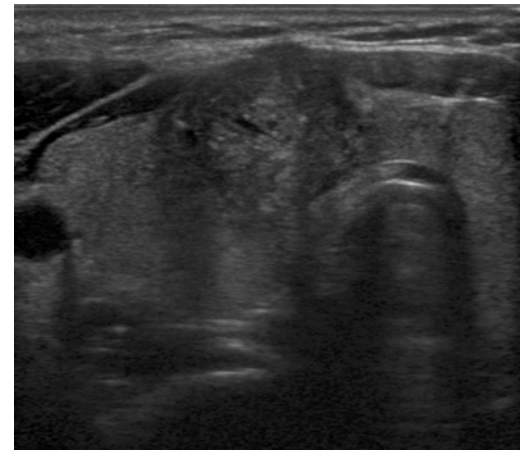

Fig. 9.1 A papillary thyroid carcinoma (PTC) in the isthmus (transverse scan). The cancer appears as an isohypoechoic lesion, infiltrating the thyroid capsule and invading the adjacent muscles. The lesion presents irregular spiculated edges and its echostructure is inhomogeneous for microcalcifications

9.3 Extracapsular Relationships

A nodule may deform, infiltrate, or cross the thyroid capsule. Deformation of the thyroid capsule without interruption of its hyperechogenicity does not necessarily indicate malignancy. Infiltration of the thyroid capsule, defined as an interruption of its hyperechogenicity (Fig. 9.1), instead, is highly suspicious for malignancy. Finally, diagnosis of cancer is certain in case of invasion, when the thyroid capsule is interrupted and the tumoral tissue penetrates the surrounding structures (Fig. 9.1). The latter represents a rare event in differentiated thyroid cancer.

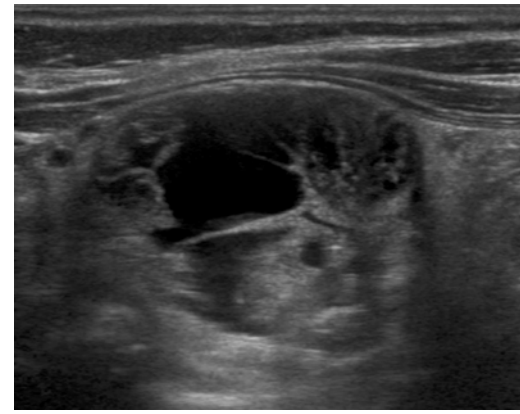

Fig. 9.2 A mixed thyroid nodule in the right lobe (longitudinal scan). This oval lesion is mainly liquid but presents an isoechoic solid component with septa, conferring a typical heterogeneous appearance

9.4 Internal Content

A thyroid nodule can be: solid (liquid portion ≤10 % of the nodule volume), mixed predominantly solid (liquid portion between 10 % and ≤50 % of the nodule volume), mixed predominantly cystic (liquid portion >50 % but ≤90 % of the nodule volume) (Fig. 9.2), cystic (liquid portion >90 % of the nodule volume), and spongiform (nodule characterized by aggregation of multiple microcystic areas <5 mm separated by thin septations that are interspersed within solid tissue) (Fig. 9.3). Generally, cystic lesions are always benign. Mixed polyconcamerated cysts, instead, may harbor a risk of malignancy. The spongiform pattern is usually associated to benignancy, but globally, the internal content does not give certainty about the nature of a thyroid lesion.

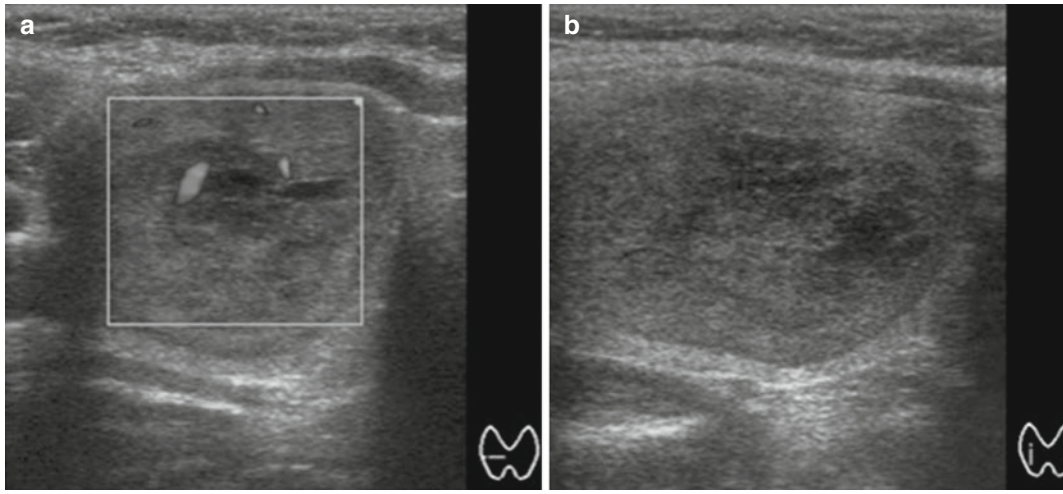

Fig. 9.3 A large ovoid spongiform nodule of the right thyroid lobe, transverse (**a**) and longitudinal (**b**) sections. The lesion is hypoechoic and finely heterogeneous and presents regular and well-defined margins

9.5 Shape

Thyroid nodules can be: ovoid (anteroposterior diameter less than its transverse diameter) (Fig. 9.3), round (anteroposterior diameter equal to transverse diameter), taller-than-wide (anteroposterior diameter longer than transverse diameter), and irregular (nodule neither ovoid/round nor taller-than-wide). Ovoid and round shapes may be present in both benign and malignant lesions. A taller-than-wide shape, instead, is reported to be more strongly associated with thyroid malignancy [4].

9.6 Echogenicity

A thyroid lesion can be: markedly hypoechoic (hypoechoic relative to the adjacent strap muscles), hypoechoic (hypoechoic relative to the thyroid parenchyma) (Fig. 9.3), isoechoic (the same echogenicity of the thyroid parenchyma), hyperechoic (more echoic than thyroid parenchyma), and anechoic (in cystic lesions). Pure anechoic cysts are usually benign. Isoechoic or hyperechoic nodules are often benign lesions. Hypoechogenicity is frequently reported in thyroid malignancies but unfortunately is also reported in almost a third of benign thyroid lesions. A marked hypoechogenicity, instead, seems to be more specific for malignancy [5].

9.7 Echotexture

A nodule can be homogeneous, finely inhomogeneous (Fig. 9.3), or markedly inhomogeneous (Fig. 9.1). Malignancy cannot be excluded in homogeneous lesions, and, similarly, the heterogeneous echotexture is not exclusive of malignancies. It follows that the echotexture cannot be considered a useful tool in distinguishing malignant from benign lesions [6].

9.8 Calcifications

Calcifications can be classified as microcalcifications, macrocalcifications, and peripheral rim calcifications (eggshell calcifications). Microcalcifications appear as small (<1 mm) intranodular punctate hyperechoic spots without posterior acoustic shadowing (Fig. 9.1) and are highly suggestive of papillary thyroid cancer. Macrocalcifications are coarse and large calcifications (>1 mm) with posterior acoustic shadowing most frequently occurring in old degenerating

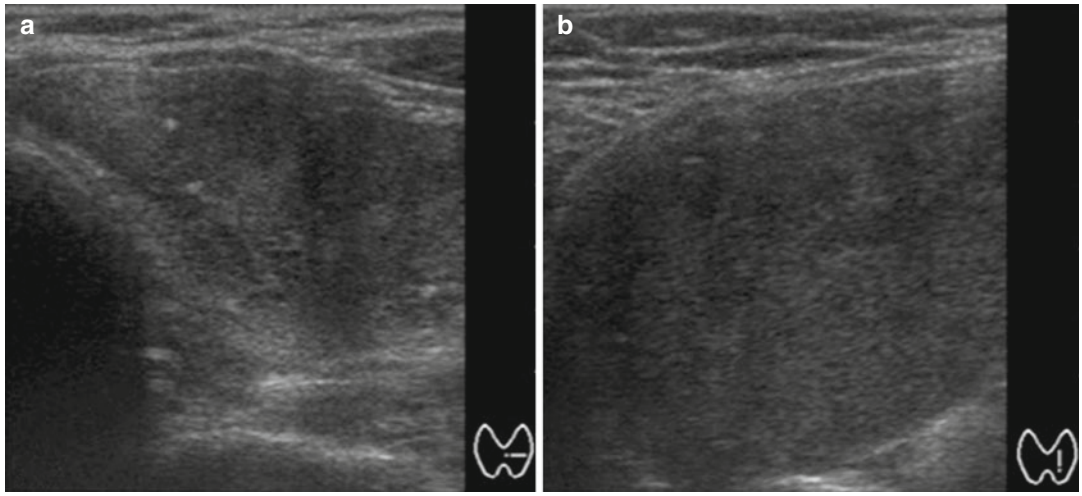

Fig. 9.4 A large solid nodule in the left thyroid lobe, transverse (**a**) and longitudinal (**b**) sections. The lesion is hypoechoic and heterogeneous, presents regular edges, and deforms the thyroid capsule without interrupting its hyperechogenicity

nodules. Peripheral rim calcifications surround the thyroid lesion and are usually thought to indicate a benign nodule. However, in case of an interruption of the rim calcification, the possibility of cancer should be considered.

9.9 Margins

The definition of nodules' margins is highly operator-dependent. Nevertheless, the edges of a thyroid nodule may be described as: well-defined (when there is a clear demarcation with normal thyroid tissue) (Fig. 9.4) or ill-defined (lack of clear demarcation with normal thyroid parenchyma) (Fig. 9.1) and regular (without irregularities and imperfections) (Fig. 9.3) or irregular (with edges and irregularities), the latter further divided into spiculated (presence of one or more spiculations on its surface) (Fig. 9.1) and microlobulated (presence of one or more smooth lobules on its surface). Ill-defined and irregular, both spiculated and microlobulated, margins are usually reported to be suggestive of malignancy [5].

The halo sign, a hypo-anechoic ring that may completely or incompletely surround a nodule, can be a regular thin halo (Fig. 9.5) or an irregular thick halo. The first is usually suggestive of benignancy [7, 8]; the latter, instead, may also represent the fibrous capsule surrounding a neoplastic growth.

9.10 Vascularity

Power Doppler and color Doppler are the preferred imaging techniques for assessing the vascularity of thyroid nodules [8]. Nodule vascularity can be: absent (no or scarce blood flow), perinodular (vascular predominance in the periphery of the nodule), further divided into complete or partial, intranodular (vascular predominance within the nodule) (Fig. 9.6), and peri-intranodular (flow in the periphery and within the nodule). Most benign nodules have absent or perinodular flow. Intralesional vascularity does not necessarily indicate a tumor, because the specificity of this feature is low [8]. Generally, nodular vascularity is not particularly useful in the diagnosis of thyroid cancer.

9.11 Size

The risk of malignancy does not change with the size of the nodule [9]. A nodule growth, defined as a 20 % increase in the nodule diam-

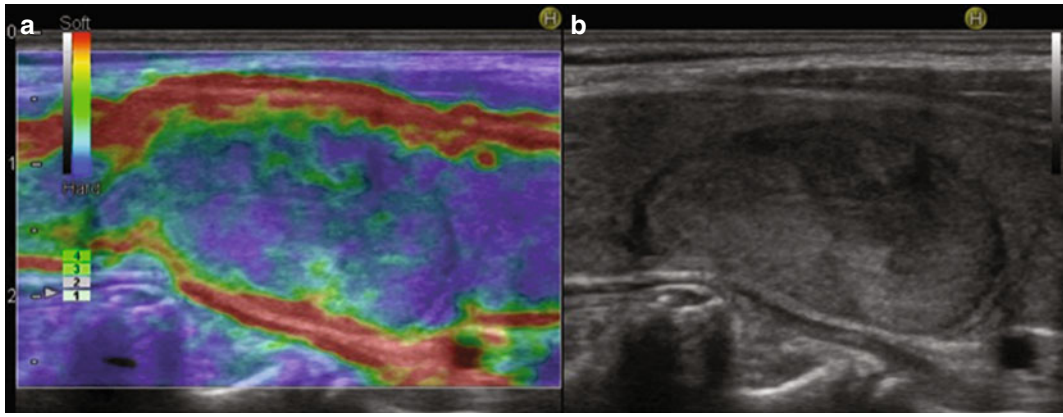

Fig. 9.5 Qualitative elastography (USE) of a solid, isoechoic thyroid nodule with thin hypoechoic halo (longitudinal scans). The USE technique combines anatomic B-mode (**b**) and elasticity images (**a**). The elastogram is displayed over the B-mode image in a color scale depending on the magnitude of strain, usually *red* (soft tissue), *green* (intermediate degree of stiffness), and *blue* (hard, inelastic tissue). The nodule in the figure, appearing mainly blue at elastographic evaluation, is classified as a hard lesion

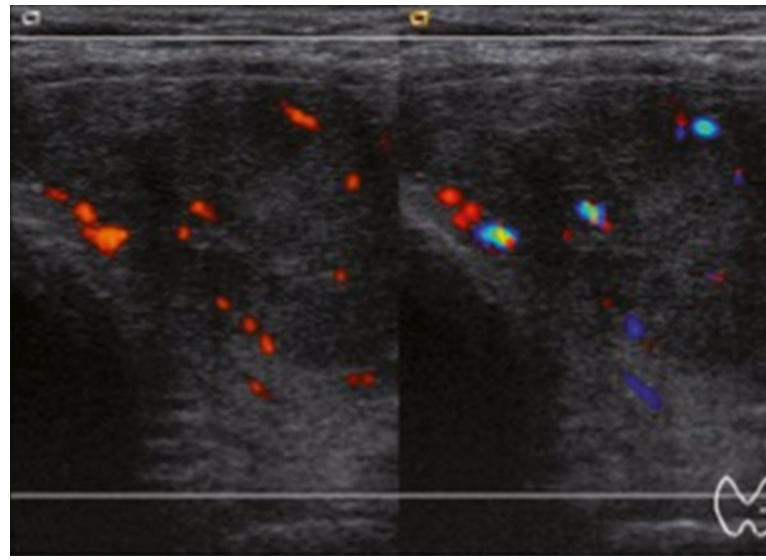

Fig. 9.6 The same nodule in Fig. 9.4 presents minimal intralesional blood flow at color Doppler evaluation (transverse sections)

eter (with a minimum increase in two dimensions of at least 2 mm) or a 50 % increase in the nodule volume [3], is thought to be usually associated to malignancy. But, although malignancy is believed to grow more frequently than benignancy, also the majority of benign thyroid nodules grow with time [9]. Moreover, differentiated thyroid cancers may remain unchanged in size for years. Instead, a rapidly growing solid nodule should be considered suspicious [10].

9.12 Elastosonography

Elastosonography (USE) is a new method that provides an estimation of tissue stiffness, being malignant lesions harder than normal tissue [11]. USE seems to be a useful tool for differential diagnosis if associated with standard ultrasonography, although, with lower sensitivity and specificity [12] than that previously reported (Fig. 9.5). The role of elastography in indeterminate lesions, instead, is still a matter of debate [13].

9.13 Combination of US and Scintigraphic Findings

No single US feature of thyroid nodules retains a sufficient predictive value for the suspicion diagnosis of thyroid cancer. Only a combination of these features may be useful to stratify the risk [14], but when multiple patterns suggestive of malignancy are simultaneously present in a nodule, the specificity increases, but the sensitivity decreases [15]. In this context scintigraphy with technetium-99m pertechnetate and technetium-99m sestamibi may have a supporting role (Figs. 9.7, 9.8, and 9.9) [16].

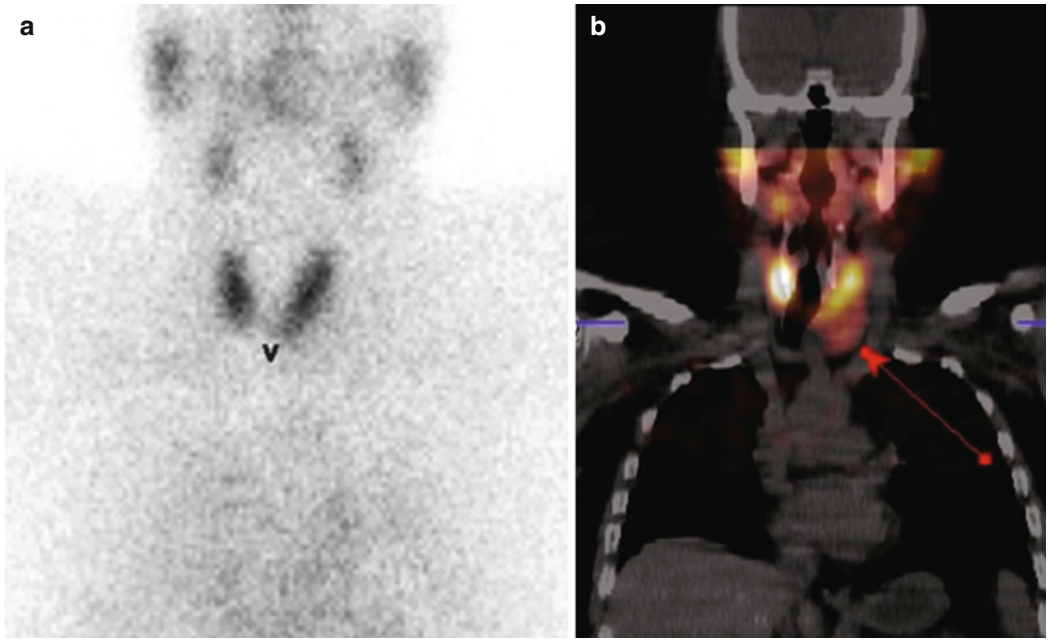

Fig. 9.7 The same lesion in the left thyroid lobe in Figs. 9.4 and 9.6 appears as a hypofunctioning ("cold") nodule at technetium-99m pertechnetate scintigraphic evaluation (**a**). The hybrid tomographic imaging (SPECT/CT) shows the mediastinal position of the lesion and the right dislocation of the trachea (**b**)

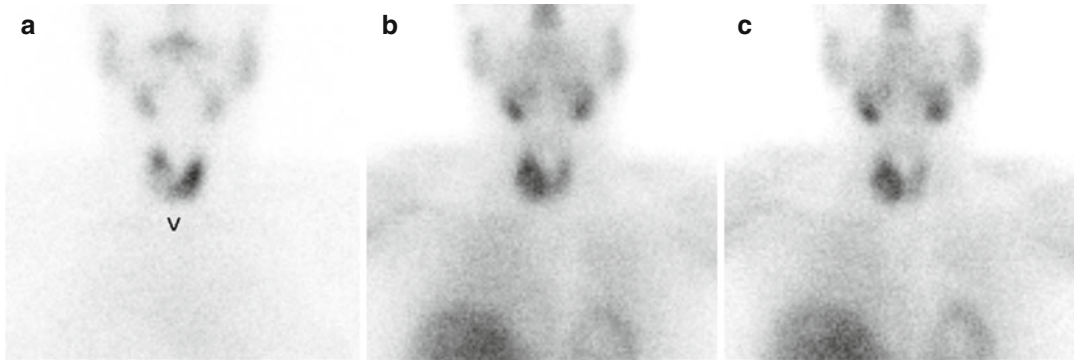

Fig. 9.8 A "cold" nodule of the right thyroid lobe at technetium-99m pertechnetate scintigraphy (**a**) with increased uptake of technetium-99m sestamibi at both early (**b**) and delayed (**c**) images. These findings demonstrate the presence of a hypofunctioning but high-proliferating thyroid nodule, suspicious for malignancy

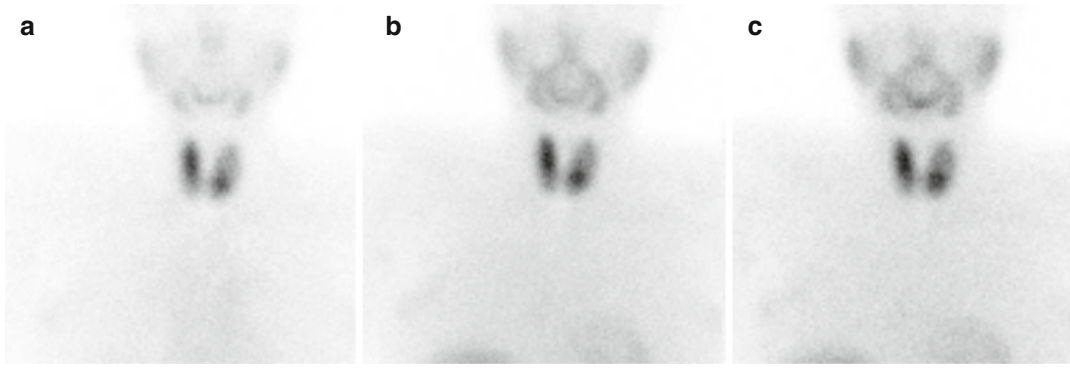

Fig. 9.9 A "cold" nodule of the left thyroid lobe at technetium-99m pertechnetate scintigraphy (**a**) with low uptake of technetium-99m sestamibi at both early (**b**) and delayed (**c**) images. These findings demonstrate the presence of a hypofunctioning and low-proliferating thyroid nodule, suggesting a benign lesion

References

1. Mazzaferri EL (1993) Management of a solitary thyroid nodule. N Engl J Med 328:553–559
2. Gharib H (1994) Fine-needle aspiration biopsy of the thyroid nodules: advantages, limitations and effect. Mayo Clin Proc 69:44–49
3. Gharib H, Papini E, Paschke R et al (2010) AACE/AME/ETA task force on thyroid nodules. American Association of Clinical Endocrinologists, Associazione Medici Endocrinologi, and European Thyroid Association Medical guidelines for clinical practice for the diagnosis and management of thyroid nodules. Endocr Pract 16(suppl 1):1–43
4. Cappelli C, Castellano M, Pirola I et al (2006) Thyroid nodule shape suggests malignancy. Eur J Endocrinol 155:27–31
5. Kim EK, Park CS, Chung WY et al (2002) New sonographic criteria for recommending fine-needle aspiration biopsy of nonpalpable solid nodules of the thyroid. AJR Am J Roentgenol 178:687–691
6. Moon WJ, Jung SL, Lee JH et al (2008) Thyroid Study Group, Korean Society of Neuro-and Head and Neck Radiology Benign and malignant thyroid nodules: US differentiation-multicenter retrospective study. Radiology 247:762–770
7. Andrioli M, Carzaniga C, Persani L (2013) Standardized ultrasound report for thyroid nodules: the Endocrinologist's viewpoint. Eur Thyroid J 2:37–48
8. Cerbone G, Spiezia S, Colao A et al (1999) Power Doppler improves the diagnostic accuracy of color Doppler ultrasonography in cold thyroid nodules: follow-up results. Horm Res 52:19–24
9. Hegedüs L (2004) Clinical practice. The thyroid nodule. N Engl J Med 351:1764–1771
10. Hoang JK, Lee WK, Lee M et al (2007) US features of thyroid malignancy: pearls and pitfalls. Radiographics 27:847–860
11. Andrioli M, Persani L (2014) Elastographic techniques of thyroid gland: current status. Endocrine 46:455–461
12. Unlütürk U, Erdogan MF, Demir O et al (2012) Ultrasound-elastography is not superior to gray-scale ultrasound in predicting malignancy in thyroid nodules. Thyroid 22:1031–1038
13. Trimboli P, Treglia G, Sadeghi R et al (2014) Reliability of real-time elastography to diagnose thyroid nodules previously read at FNAC as indeterminate: a meta-analysis. Endocrine. doi:10.1007/s12020-014-0510-9
14. Andrioli M (2014) Nodulo tiroideo. In: Andrioli M (ed) Ecografia della tiroide – un approccio specialistico. Griffin Editore, Como
15. Papini E, Guglielmi R, Bianchini A et al (2002) Risk of malignancy in nonpalpable thyroid nodules: predictive value of ultrasound and color-Doppler features. J Clin Endocrinol Metab 87:1941–1946
16. Treglia G, Caldarella C, Saggiorato E et al (2013) Diagnostic performance of (99m)Tc-MIBI scan in predicting the malignancy of thyroid nodules: a meta-analysis. Endocrine 44:70–78

Nontoxic Multinodular Goiter

10

Luca Giovanella

Abstract

Nodular goiter is caused by excessive replication of thyroid epithelial cell with formation of new follicles. The clinical presentation of patients with nontoxic multinodular goiter is variable and depends on the volume and location of the thyroid. In this chapter some principles of diagnosis and management of nontoxic multinodular goiter are briefly discussed. Furthermore some typical images of patients with nontoxic multinodular goiter are showed.

Keywords

Goiter • Multinodular • Thyroid • Nontoxic goiter • Neck mass

Prof. Dr. med. L. Giovanella, MD, PhD
Department of Nuclear Medicine, Thyroid
and PET/CT Center, Oncology Institute
of Southern Switzerland, Via Ospedale 12,
CH-6500 Bellinzona and Lugano, Switzerland
e-mail: luca.giovanella@eoc.ch

L. Giovanella et al. (eds.), *Atlas of Head and Neck Endocrine Disorders: Special Focus on Imaging and Imaging-Guided Procedures*, DOI 10.1007/978-3-319-22276-9_10

10.1 Introduction

Nodular goiter is caused by excessive replication of thyroid epithelial cell with formation of new follicles [1]. Generally, there is a gradual increase in goiter size with simultaneous development of thyroid nodules and, later, thyroid autonomy [2]. The clinical presentation of patients with nontoxic multinodular goiter (NT-MNG) is variable and depends on the volume and location of the thyroid. Most euthyroid patients with a small goiter are completely asymptomatic. Others may have a visible goiter (Fig. 10.1) in the absence of other clinical symptoms [3]. However, occasionally, the thyroid may extend into the thoracic cavity (substernal goiter) resulting in obstruction or pressure of structures within the cavity. Tracheal compression can result in exertional or positional dyspnea and dysphagia may also be reported in patients with large goiters [4].

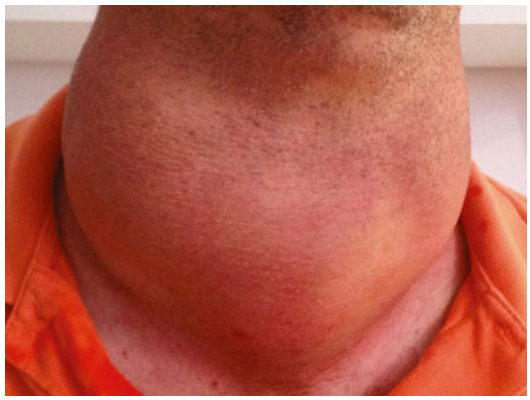

Fig. 10.1 Large goiter in a 57-year-old man with euthyroid status

10.2 Diagnosis and Management of Nontoxic Multinodular Goiter

Beyond clinical examination, all patients with NT-MNG should have serum thyrotropin (TSH) measured to assess functional thyroid status and ultrasound (US) examination to evaluate the number, size, and sonographic features of the nodules and assist in the selection of nodules that may need fine-needle aspiration biopsy [5]. Conventional radiography of the trachea and of the esophagus or, even better, computed tomography (CT) or magnetic resonance imaging (MRI) can be used to confirm compression, especially in symptomatic patients [6]. Patients with nodules yielding malignant cytology should be referred for surgery. Given the lack of reliable markers to predict biological behavior of nodules with indeterminate cytology, patients with such nodules are generally addressed to surgery, unless autonomous function of these nodules can be confirmed by scintigraphy.

Some typical morphological and functional images of patients with NT-MNG are showed in Figs. 10.1, 10.2, 10.3, 10.4, 10.5, 10.6, and 10.7.

In the absence of malignancy, the mere presence of goiter does not mean that treatment is necessary and asymptomatic patients may be observed. Many patients with benign but large goiters may experience clinical symptoms of pressure, such as dysphagia, choking sensation, or airway obstruction. Such patients will often require surgery for alleviation of symptoms [7]. Radioactive iodine is safe and effective and may be a reasonable option in older patients, when surgery is unfeasible and/or at high risk or refuted by the patients [8].

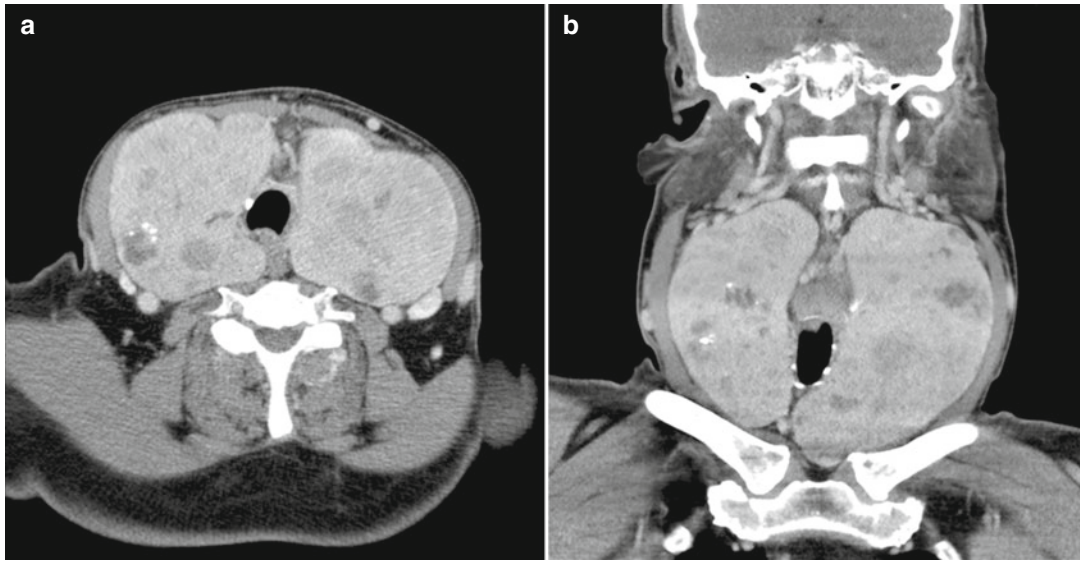

Fig. 10.2 Neck computed tomography (CT) of the same patient showed in Fig. 10.1. CT in axial (**a**) and coronal (**b**) projection showed a large goiter with multiple nodules, some of them with macroscopic calcifications

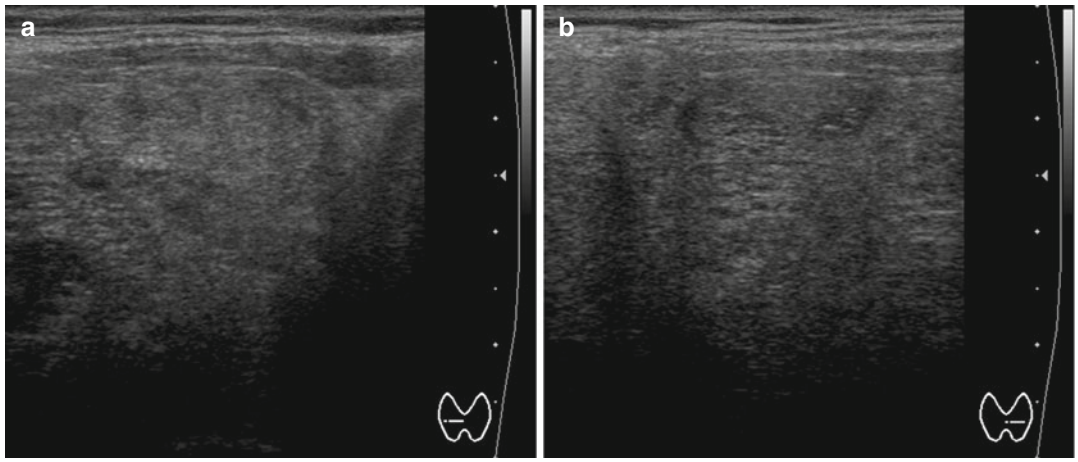

Fig. 10.3 Thyroid ultrasonography (US) of the same patient showed in Fig. 10.1. US showed large *right* (**a**) and *left* (**b**) thyroid lobes with diffusely inhomogeneous echotexture and regular margins

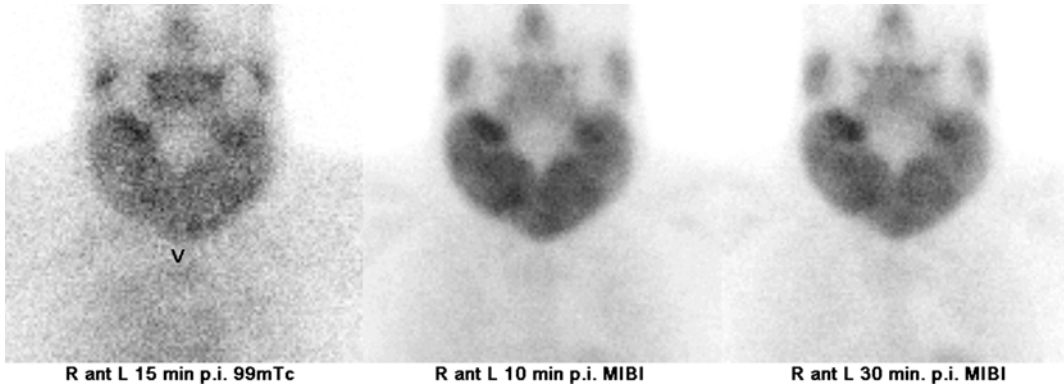

Fig. 10.4 Thyroid scans with ^{99m}Tc-pertechnetate (**a**) and ^{99m}Tc-MIBI using early (**b**) and delayed (**c**) acquisitions in the same patient of Fig. 10.1. ^{99m}Tc-pertechnetate scan showed an enlarged thyroid gland with multiple normofunctioning nodules. ^{99m}Tc-MIBI scan did not reveal thyroid nodules with increased proliferation. Final diagnosis was nontoxic multinodular goiter

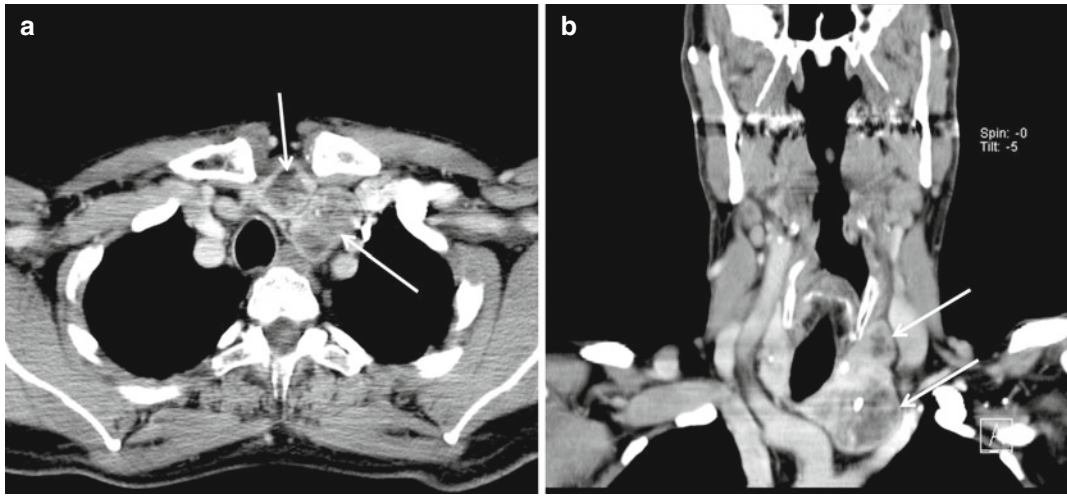

Fig. 10.5 Axial (**a**) and coronal (**b**) computed tomography (CT) of a 62-year-old male patient showing an enlarged thyroid gland with multiple hypodense nodules in the left thyroid lobe (*arrows*), some of them located in the retrosternal region

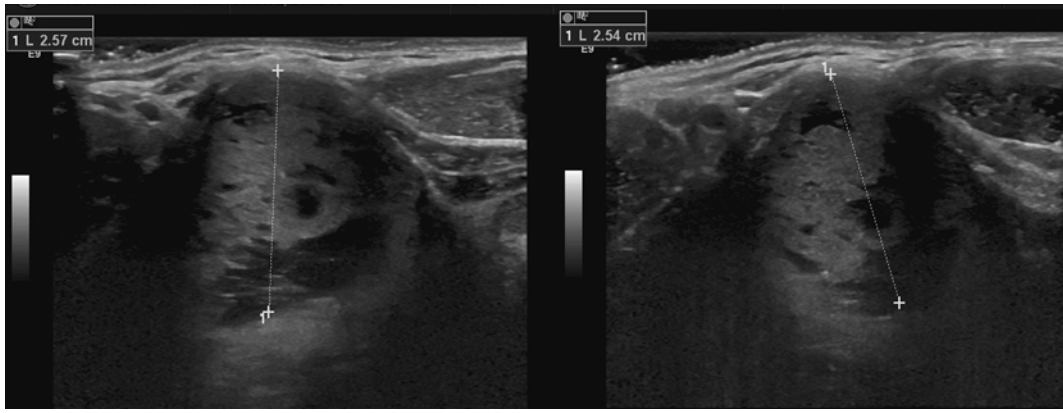

Fig. 10.6 Thyroid ultrasonography (US) of the same patient showed in Fig. 10.5. US showed multiple nodules in the left thyroid lobe with inhomogeneous echotexture

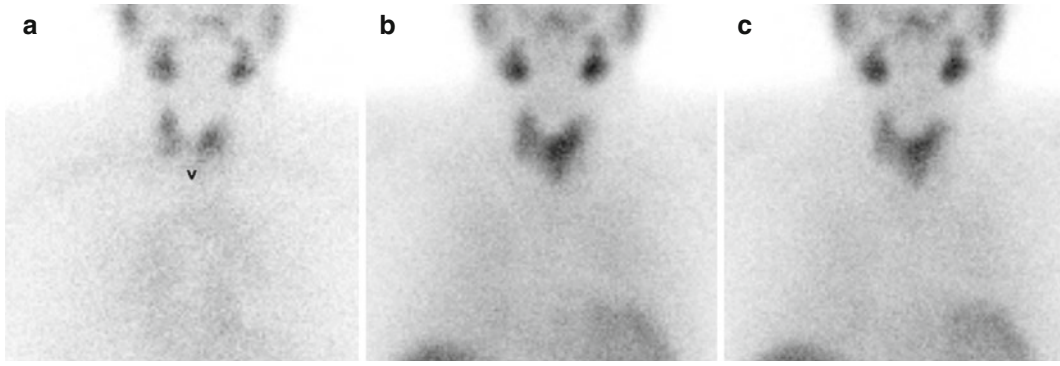

Fig. 10.7 Thyroid scans with ^{99m}Tc-pertechnetate (**a**) and ^{99m}Tc-MIBI using early (**b**) and delayed (**c**) acquisitions in the same patient of Fig. 10.5. ^{99m}Tc-pertechnetate scan showed an enlarged left thyroid lobe with multiple hypofunctioning nodules. ^{99m}Tc-MIBI scan did not reveal significant uptake of the proliferation tracer in the left thyroid nodules. Final diagnosis was nontoxic multinodular goiter

References

1. Maenhaut C, Lefort A, Libert F et al (1990) Function, proliferation and differentiation of the dog and human thyrocyte. Horm Metab Res 23:S51–S61
2. Berghout A, Wiersinga WM, Smits NJ et al (1990) Interrelationship between age, thyroid volume, thyroid nodularity and thyroid function in patients with sporadic non-toxic goiter. Am J Med 89:602–608
3. Wartofsky L (1998) Diseases of the thyroid. In: Fauci AS, Braunwald E (eds) Harrison's principles of internal medicine. McGraw-Hill, New York, pp 2012–2034
4. Elte JW, Bussemaker JK, Haak A (1990) The natural history of euthyroid multinodular goitre. Postgrad Med J 66:186–190
5. Brkljacić B, Cuk V, Tomić-Brzac H et al (1994) Ultrasonic evaluation of benign and malignant nodules in echographically multinodular thyroids. J Clin Ultrasound 22:71–76
6. Cooper JC, Nakielny R, Talbot CH (1991) The use of computed tomography in the evaluation of large multinodular goitres. Ann R Coll Surg Engl 73:32–35
7. Muller PE, Kabus S, Robens E et al (2001) Indications, risks and acceptance of total thyroidectomy for multinodular benign goiter. Surg Today 31:958–962
8. Manders JMB, Corstens FHM (2002) Radioiodine therapy of euthyroid multinodular goitres. Eur J Nucl Med 29:S466–S470

Differentiated Thyroid Carcinoma

11

Luca Giovanella and Giorgio Treglia

Abstract

Differentiated thyroid cancer (DTC), arising from thyroid follicular epithelial cells, is the most common endocrine malignancy. DTC is characterized by low morbidity and mortality because its clinical course is generally indolent.

This chapter provides a brief summary on the management of DTC. Some diagnostic images of DTC are also provided.

Keywords

Differentiated thyroid carcinoma • Papillary • Follicular • Thyroid cancer

11.1 Introduction

Differentiated thyroid cancer (DTC), arising from thyroid follicular epithelial cells, is the most common endocrine malignancy. Of DTC, papillary cancer comprises about 85 % of cases compared to about 10 % that have follicular histology and 3 % that are Hürthle cell or oxyphil tumors [1].

Prof. Dr. med. L. Giovanella, MD, PhD (✉)
G. Treglia, MD, MSc
Department of Nuclear Medicine,
Thyroid and PET/CT Center, Oncology Institute
of Southern Switzerland, Via Ospedale 12,
CH-6500 Bellinzona and Lugano, Switzerland
e-mail: luca.giovanella@eoc.ch;
giorgio.treglia@eoc.ch

DTC is characterized by low morbidity and mortality because its clinical course is generally indolent [2].

11.2 Management of DTC

After diagnosis of DTC, initial treatment consists of total thyroidectomy, except in patients with microcarcinoma when lobectomy may be an option if no other nodules in the neck are detected by ultrasonography (US). Preoperative neck US for the contralateral lobe and cervical (central and especially lateral neck compartments) lymph nodes is recommended for all patients undergoing

L. Giovanella et al. (eds.), *Atlas of Head and Neck Endocrine Disorders: Special Focus on Imaging and Imaging-Guided Procedures*, DOI 10.1007/978-3-319-22276-9_11

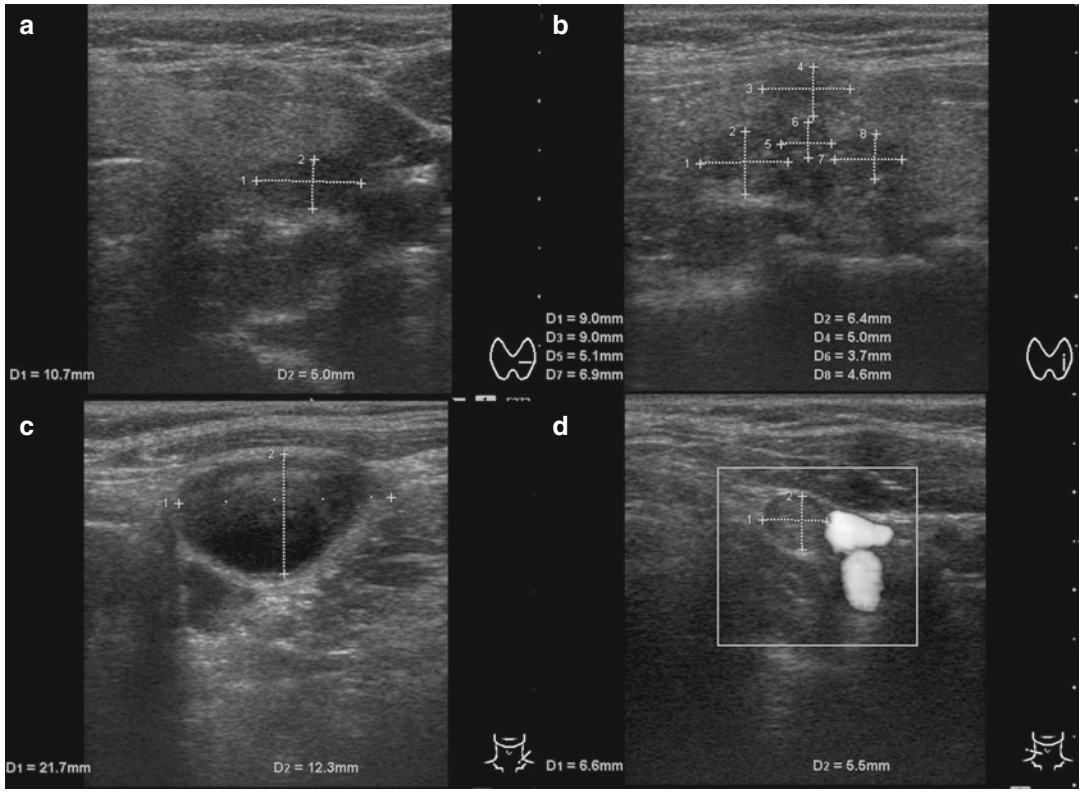

Fig. 11.1 A patient with differentiated thyroid carcinoma of the left thyroid lobe with bilateral cervical lymph nodal metastases demonstrated by fine-needle cytology. Ultrasonography demonstrates multiple nodules with irregular margins in the left thyroid lobe (**a**, **b**), cystic left cervical lymph nodes (**c**), and solid right cervical lymph nodes (**d**)

thyroidectomy for malignant cytologic findings on biopsy (Figs. 11.1 and 11.2) [1].

Primary differentiated thyroid carcinoma or metastases from this tumor may also be incidentally detected by several diagnostic imaging methods (Figs. 11.3, 11.4, 11.5, and 11.6).

Sonographic features suggestive of abnormal metastatic lymph nodes include loss of the fatty hilus, a rounded rather than oval shape, hypoechogenicity, cystic change, calcifications, and peripheral vascularity. No single sonographic feature is adequately sensitive for detection of lymph nodes with metastatic thyroid cancer [1]. US-guided fine-needle aspiration (FNA) of sonographically suspicious lymph nodes should be performed to confirm malignancy if this would change the management [1].

After thyroidectomy, most patients receive ablative iodine-131 (^{131}I) therapy, depending on the individual patient's situation and physician preference [2, 3]. A third element of DTC treatment, levothyroxine therapy (L-T4), aims to achieve either a low-normal thyrotropin (TSH) concentration or TSH suppression, depending on the disease stage [4].

With treatment, most patients with DTC have an excellent prognosis with normal life expectancy. However, some show persistent disease after initial therapy or develop recurrent disease during follow-up [2]. Postsurgical follow-up of DTC aims to identify early the small proportion of patients with residual disease or who will develop recurrence (Figs. 11.7, 11.8, 11.9, 11.10, and 11.11).

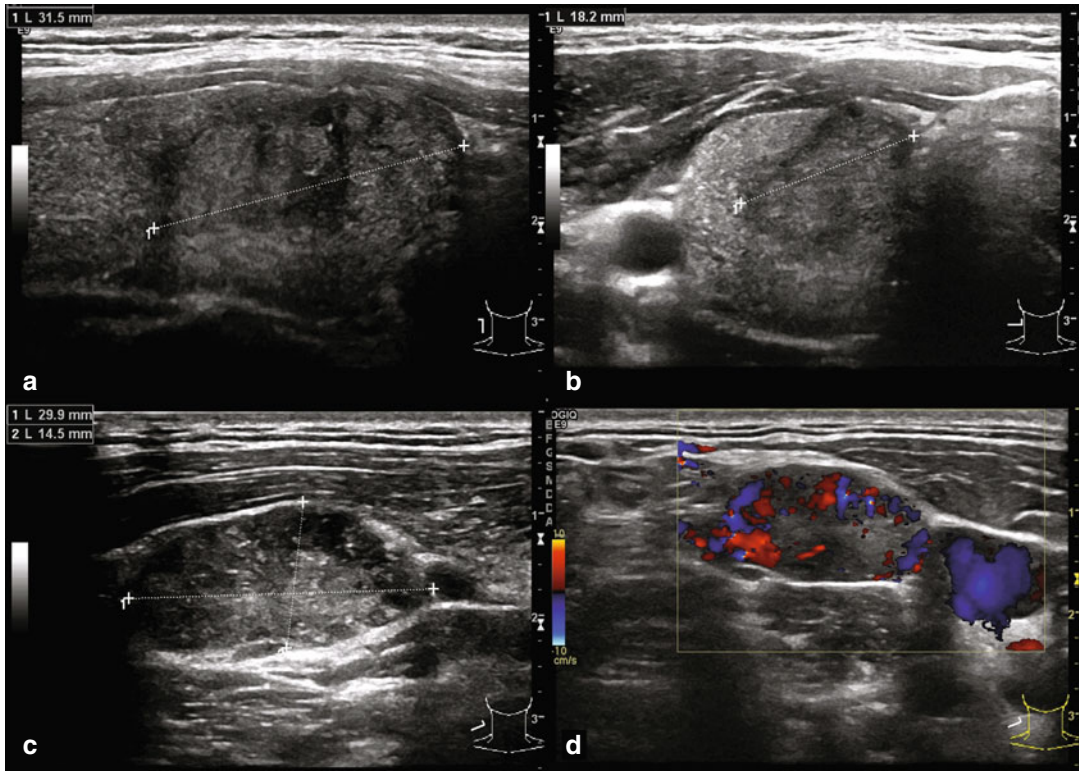

Fig. 11.2 A patient with differentiated thyroid carcinoma of the right thyroid lobe with cervical lymph nodal metastasis demonstrated by fine-needle cytology. Ultrasonography demonstrates a large nodule in the right thyroid lobe with irregular margins and inhomogeneous echotexture (**a**, **b**) and an enlarged right cervical lymph node (**c**) with increased vascularity at Doppler ultrasonography (**d**)

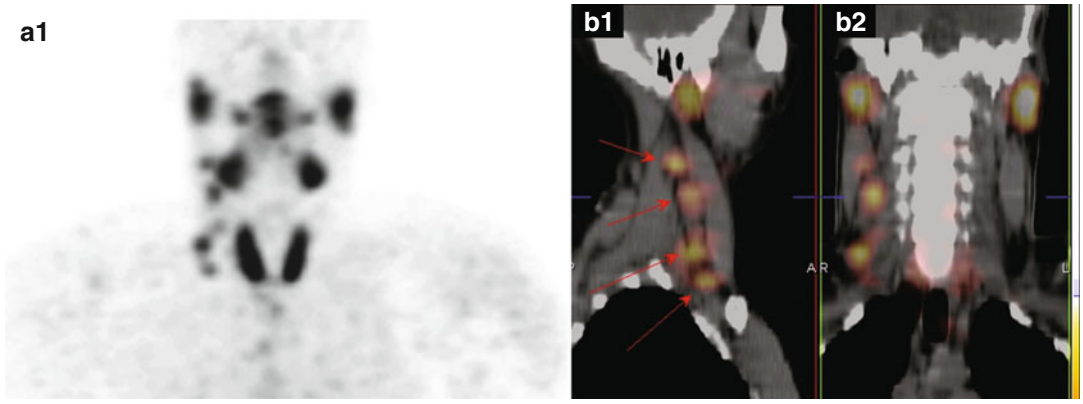

Fig. 11.3 Right cervical lymph nodal metastases of differentiated thyroid cancer detected by ^{99m}Tc-MIBI scintigraphy both at planar (**a**) and fused tomographic single-photon emission computed tomography/computed tomography (SPECT/CT) images (**b1**, **b2**, *arrows*)

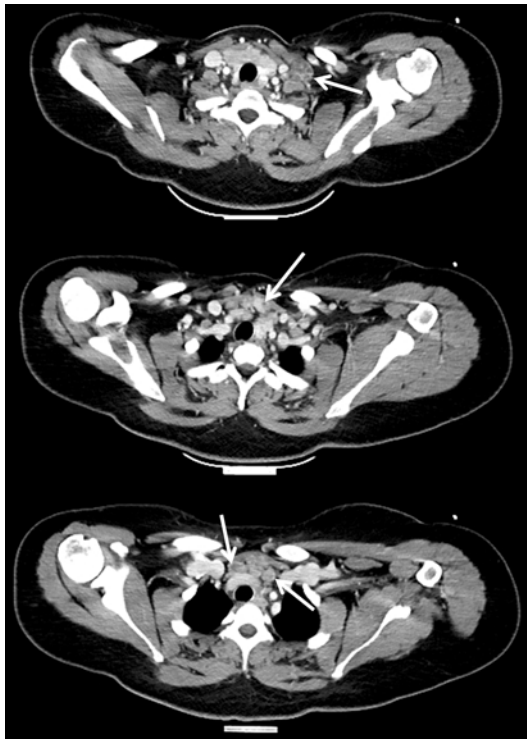

Fig. 11.4 Cervical and upper mediastinal metastatic lymph nodes from differentiated thyroid carcinoma detected by contrast-enhanced computed tomography (*arrows*)

Thyroglobulin (Tg) is produced by normal or well-differentiated malignant thyrocytes only; its tissue-specific origin makes it eminently suitable for use as a tumor marker [5]. In the absence of interfering anti-Tg and/or heterophile antibodies, Tg measurement is the reference standard for clinical management of patients previously treated for DTC combined with the use of cervical US and diagnostic ^{131}I-whole body scan (dxWBS) [6]. If no DTC foci are identified on conventional imaging or ^{131}I dxWBS in face of increased serum Tg, fluorine-18 fluorodeoxyglucose positron emission tomography/computed tomography (^{18}F-FDG PET/CT) should be performed to detect recurrent or metastatic disease (Fig. 11.11) [7]. Another emerging indication of ^{18}FDG PET/CT is the selection of patients with advanced radioiodine-refractory DTC for targeted therapies (i.e., tyrosine kinase inhibitors) and the evaluation of the response to such treatments [2].

Finally, empiric administration of therapeutic ^{131}I activities should be considered in highly selected DTC cases in order to better detect sites of disease using the improved sensitivity of post-treatment ^{131}I-WBS and for the therapy of disease not amenable to surgery [8].

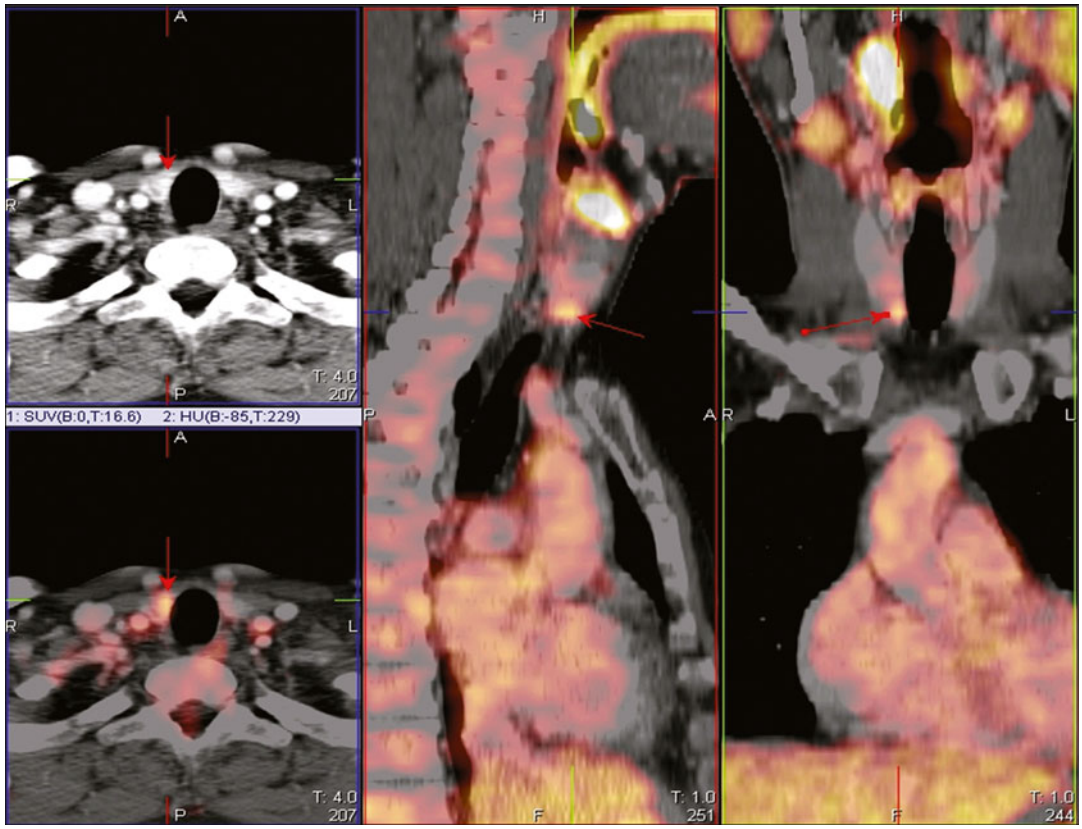

Fig. 11.5 Differentiated thyroid carcinoma of the right thyroid lobe incidentally detected by fluorine-18 fluorodeoxyglucose positron emission tomography/computed tomography (^{18}F-FDG PET/CT). Axial CT (*upper left image*) and axial (*lower left image*), sagittal (*central image*), and coronal (*right image*) fused PET/CT images show focal radiopharmaceutical uptake corresponding to a small thyroid nodule of the right thyroid lobe (*arrows*)

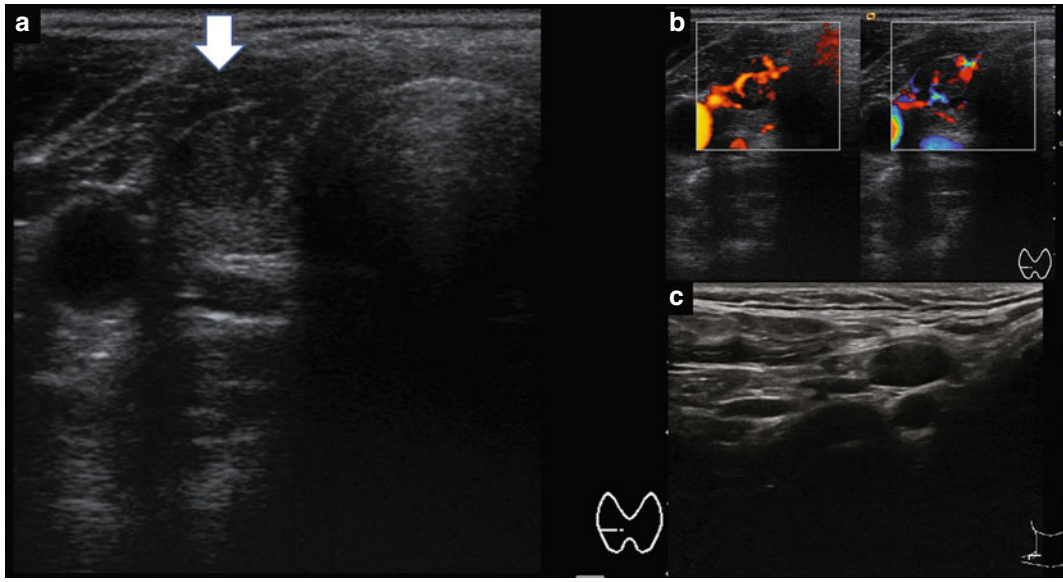

Fig. 11.6 Ultrasonographic findings of the same patient of Fig. 11.5. Ultrasonography (US) shows a mixed right thyroid nodule (**a**, *arrow*) with increased vascularity at Doppler US (**b**) and hypoechoic right cervical lymph nodes (**c**). Fine-needle aspiration cytology demonstrated a differentiated thyroid carcinoma with right cervical lymph nodal metastases

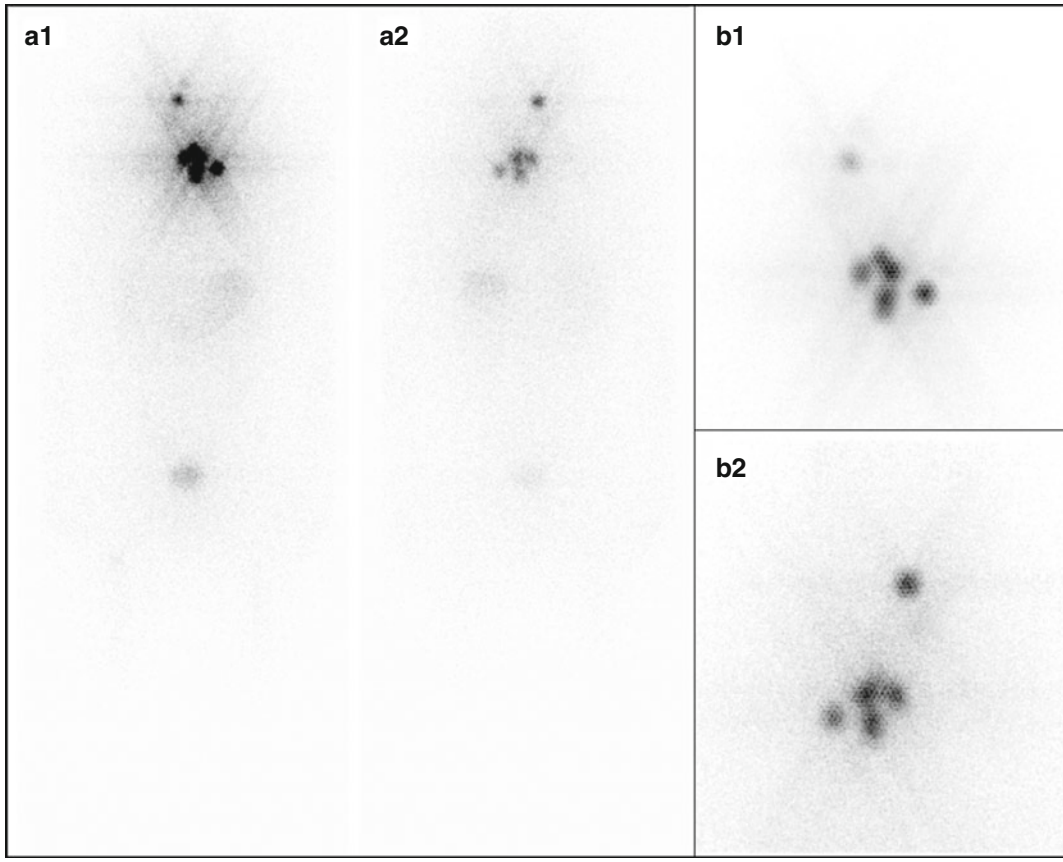

Fig. 11.7 Iodine-131 whole body scintigraphy ($^{131I\text{-}WBS}$) performed after radioiodine therapy in a patient with differentiated thyroid carcinoma treated with thyroidectomy and central neck lymphadenectomy. Planar ^{131}I-WBS images in anterior (**a1**, **b1**) and posterior view (**a2**, **b2**) show several focal areas of increased radiopharmaceutical uptake corresponding to residual thyroid tissue and metastatic cervical lymph nodes

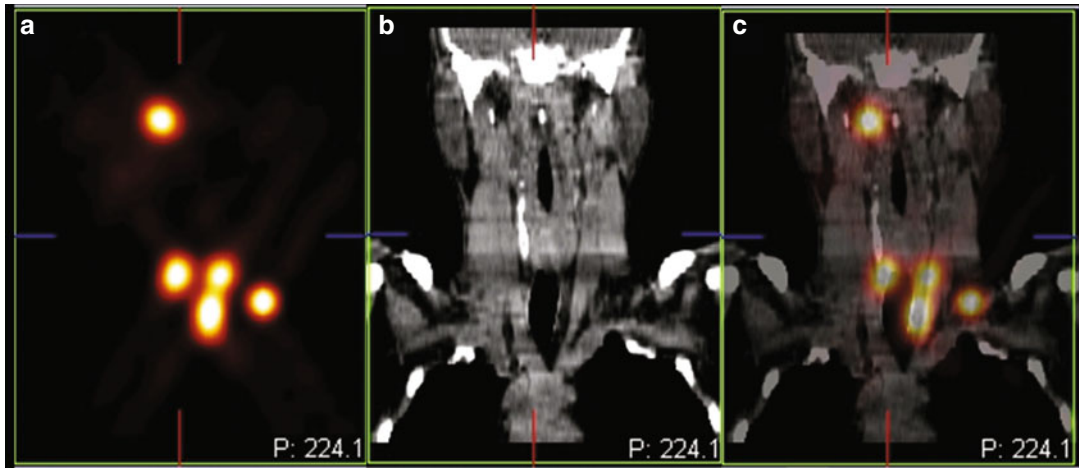

Fig. 11.8 Iodine-131 single-photon emission computed tomography/computed tomography (^{131}I-SPECT/CT) in the same patient of Fig. 11.7. Coronal SPECT (**a**), CT (**b**), and fused SPECT/CT (**c**) images show several focal areas of increased radiopharmaceutical uptake corresponding to residual thyroid tissue and metastatic cervical lymph nodes, with higher accuracy compared to planar images

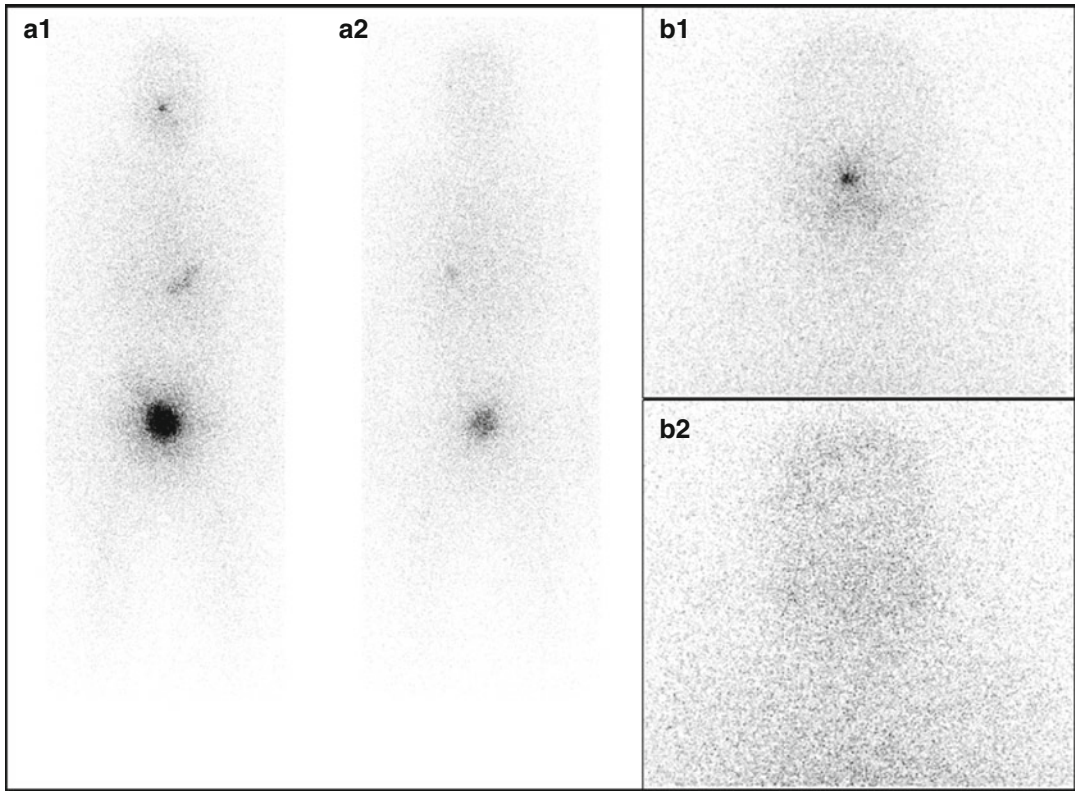

Fig. 11.9 Follow-up diagnostic iodine-131 whole body scintigraphy (^{131}I-WBS) performed in the same patient of Figs. 11.7 and 11.8 shows absence of areas of abnormal radiopharmaceutical uptake in anterior (**a1**, **b1**) and posterior view (**a2**, **b2**) demonstrating complete response to radioiodine therapy

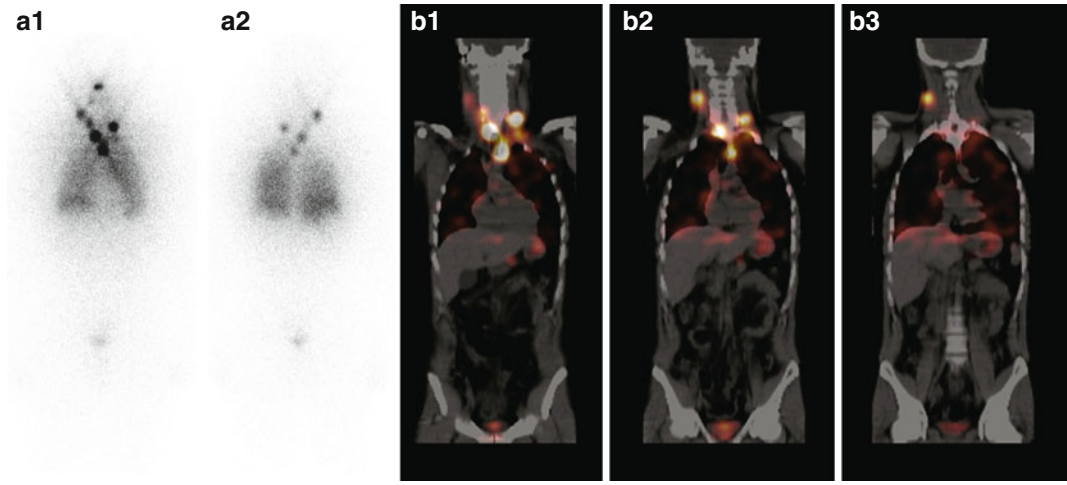

Fig. 11.10 Iodine-131 whole body scintigraphy ($^{131I\text{-}WBS}$) performed after radioiodine therapy in a patient with differentiated thyroid carcinoma treated with thyroidectomy and central neck lymphadenectomy. Planar ^{131}I-WBS images in anterior (**a1**) and posterior view (**a2**) and fused tomographic single-photon emission computed tomography/computed tomography (SPECT/CT) images (**b1**–**b3**) show several focal areas of increased radiopharmaceutical uptake corresponding to multiple cervical and mediastinal metastatic lymph nodes and bilateral lung micrometastases

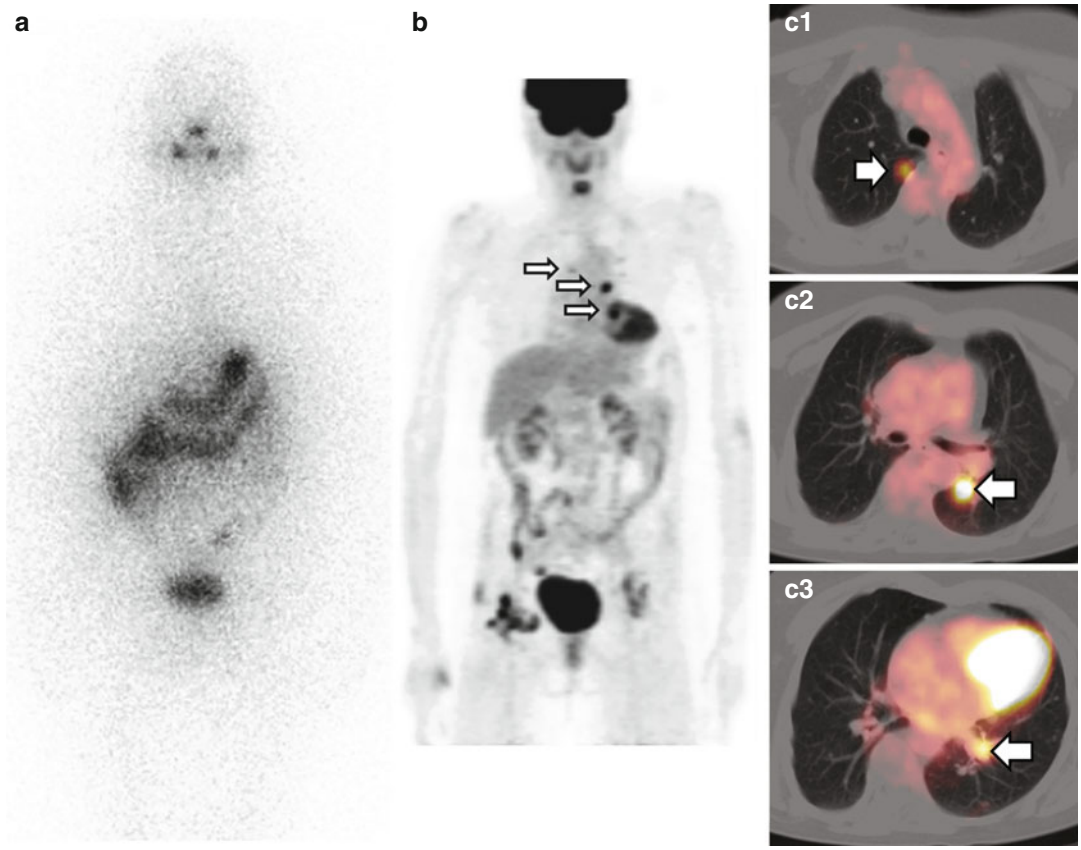

Fig. 11.11 Iodine-131 whole body scintigraphy ($^{131I\text{-}WBS}$) and fluorine-18-fluorodeoxyglucose positron emission tomography (^{18}F-FDG PET/CT) performed for restaging due to increased serum thyroglobulin levels in a patient with differentiated thyroid carcinoma treated with thyroidectomy and bilateral cervical lymphadenectomy.$^{131I\text{-}WBS}$ (**a**) was normal, whereas ^{18}F-FDG PET (**b**) and axial fused PET/CT images (**c**1–**c3**) show bilateral lung metastases of differentiated thyroid carcinoma (*arrows*) due to dedifferentiation (flip-flop phenomenon)

References

1. American Thyroid Association (ATA) Guidelines Taskforce on Thyroid Nodules and Differentiated Thyroid Cancer, Cooper CS, Doherty GM, Haugen BR et al (2009) Revised American Thyroid Association management guidelines for patients with thyroid nodules and differentiated thyroid cancer. Thyroid 19:1167–1214
2. Verburg FA, Mader U, Tanase K et al (2013) Life expectancy is reduced in differentiated thyroid cancer patients ≥ 45 years old with extensive local tumour invasion, lateral lymph node, or distant metastases at diagnosis and normal in all other DTC patients. J Clin Endocrinol Metab 98:172–180
3. Reiners C, Hanscheid H, Luster M et al (2011) Radioiodine for remnant ablation and therapy of metastatic disease. Nat Rev Endocrinol 7: 589–595
4. Diessl S, Holzberger B, Mäder U et al (2012) Impact of moderate vs stringent TSH suppression on survival in advanced differentiated thyroid carcinoma. Clin Endocrinol 76:586–592
5. Giovanella L (2008) Highly sensitive thyroglobulin measurements in differentiated thyroid carcinoma management. Clin Chem Lab Med 46:1067–1073
6. Giovanella L, Trimboli P, Verburg FA et al (2013) Thyroglobulin levels and thyroglobulin doubling time independently predict a positive ^{18}F-FDG PET/CT scan in patients with biochemical recurrence of differentiated thyroid carcinoma. Eur J Nucl Med Mol Imaging 40:874–880
7. Giovanella L, Treglia G, Ceriani L et al (2014) Detectable thyroglobulin with negative anatomical imaging and radioiodine scan in differentiated thyroid cancer patients: what to do? Nuklearmedizin 53:1–10
8. Schlumberger M, Mancusi F, Baudin E et al (1997) 131I therapy for elevated thyroglobulin levels. Thyroid 7:273–276

Medullary Thyroid Carcinoma

12

Pierpaolo Trimboli and Luca Giovanella

Abstract

Medullary thyroid carcinoma (MTC) is an infrequent thyroid malignancy deriving from parafollicular thyroid C cells.

This chapter provides a brief summary on MTC, including some diagnostic and therapeutic aspects. Furthermore typical diagnostic images of medullary thyroid carcinoma are discussed.

Keywords

Medullary thyroid carcinoma • Calcitonin • Thyroid • Cancer • Neuroendocrine

P. Trimboli, MD
Section of Endocrinology and Diabetology,
Ospedale Israelitico of Rome, Rome, Italy

Department of Nuclear Medicine,
Thyroid and PET/CT Centre,
Oncology Institute of Southern Switzerland,
Via Ospedale 12, CH-6500
Bellinzona and Lugano, Switzerland

Prof. Dr. med. L. Giovanella, MD, PhD (✉)
Department of Nuclear Medicine,
Thyroid and PET/CT Centre,
Oncology Institute of Southern Switzerland,
Via Ospedale 12, CH-6500
Bellinzona and Lugano, Switzerland
e-mail: luca.giovanella@eoc.ch

L. Giovanella et al. (eds.), *Atlas of Head and Neck Endocrine Disorders: Special Focus on Imaging and Imaging-Guided Procedures*, DOI 10.1007/978-3-319-22276-9_12

12.1 Diagnosis

Medullary thyroid carcinoma (MTC) is an infrequent thyroid malignancy (about 5 % of all thyroid cancers) deriving from parafollicular thyroid C cells. One in five MTC is part of an autosomal dominant inherited disorder (MEN-2A, MEN-2B, or familial MTC), while it manifests as sporadic tumor in the remaining cases [1].

The presurgical diagnosis of MTC should be difficult due to many reasons. Calcitonin measurement is the most accurate tool when value is above 100 pg/ml, but intermediate results (i.e., value comprised between upper reference limit and 100 pg/ml) are frequent, false-positive findings (calcitonin levels >100 pg/ml) are possible, and calcitonin-negative MTC have been reported [2, 3]. Also, routine test of serum calcitonin in workup of thyroid nodule is still a matter of debate.

Fine-needle aspiration biopsy (FNA) of thyroid nodules is the most accurate tool for detecting thyroid cancers; nevertheless, only about 50 % of MTC may be correctly identified at cytology, while the other cases are assessed as indeterminate (Thy 3), inadequate (Thy 1), benign (Thy 2), or undefined malignancy [4, 5].

Finally, ultrasound (US) examination has lower sensitivity than other thyroid cancers because MTC US presentation may be heterogeneous (Figs. 12.1 and 12.2). Analysis of RET gene is mandatory in all patients with MTC, even when apparently sporadic [1].

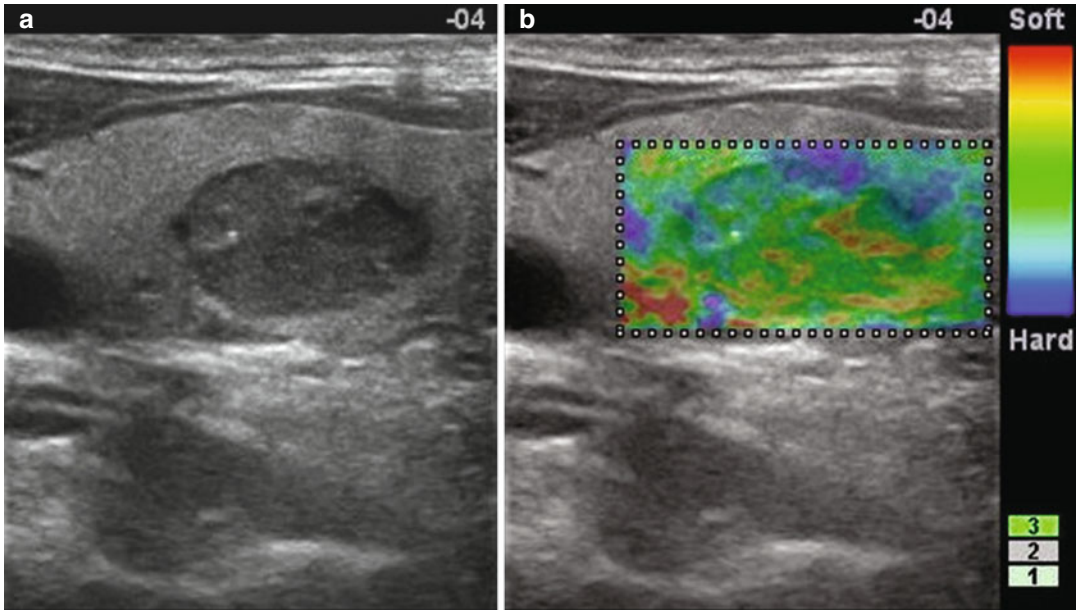

Fig. 12.1 Medullary thyroid cancer in the right lobe. Nodule was assessed at ultrasonography as not suspicious: echotexture was spongiform and margins were regular (**a**). Elastography showed *green color* (**b**)

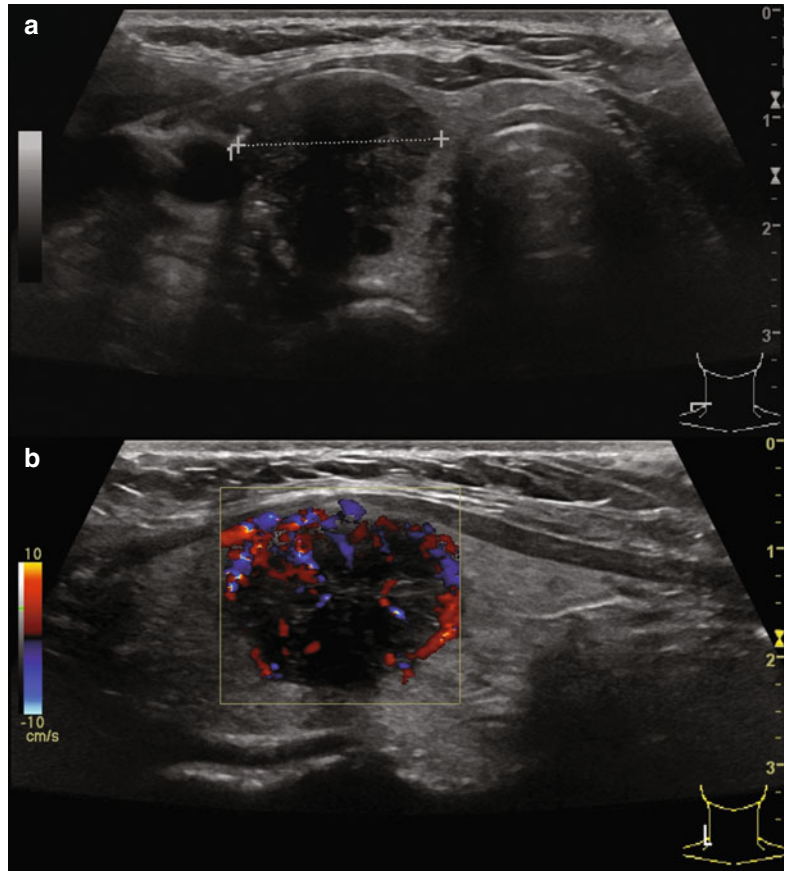

Fig. 12.2 Medullary thyroid cancer of the right lobe presenting as mixed nodule at ultrasonography with irregular margins (**a**) and mixed vascularity at Doppler ultrasonography (**b**)

12.2 Therapy and Follow-Up

The initial treatments of MTC include total thyroidectomy and central neck nodal and, in selected cases, lateral neck nodal dissection. This approach is needed for an appropriate treatment which strongly affects on patient prognosis [1].

Overall, prognosis of patients affected by MTC is poorer than that of subjects with differentiated thyroid malignancy. As above mentioned, these data depend on initial surgical removal of thyroid gland and eventual cervical metastases and the delay of the diagnosis.

Follow-up of these patients is based on periodical measurement of serum calcitonin and other potential markers, such as CEA and procalcitonin [6, 7]. Neck ultrasonography over time is the main imaging tool, while computed tomography (CT) and PET/CT could improve the localization and stratification of the risk of more aggressive disease (Figs. 12.3 and 12.4) [8]. Generally, imaging is required only in patients with postoperative calcitonin >150 pg/ml.

More recently, new chemotherapies have been introduced for metastatic MTC. These drugs, vandetanib and cabozantinib, tyrosine kinase inhibitors (TKI), should improve prognosis of patients even if adverse effects are not rare. To date, TKI are indicated in patients with advanced and symptomatic MTC.

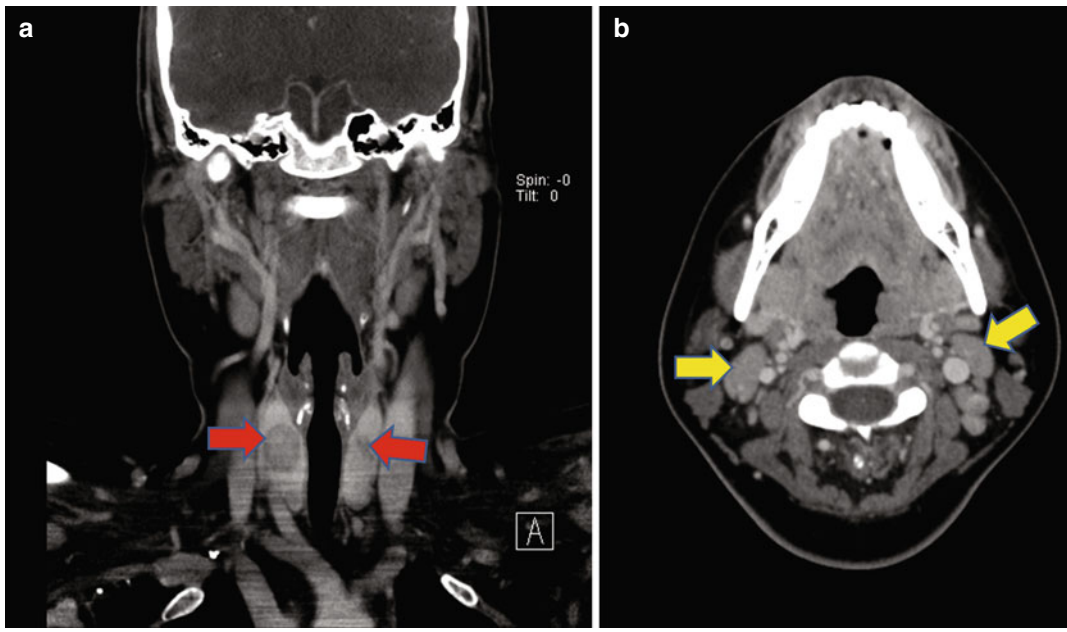

Fig. 12.3 CT performed for staging in a patient with medullary thyroid carcinoma demonstrates bilateral hypodense nodules (*red arrows*). The larger nodule was located in the right thyroid lobe (**a**). Bilateral enlarged cervical lymph nodes were also evident (*yellow arrows*) at CT imaging (**b**). Final diagnosis after surgery was multifocal medullary thyroid carcinoma with cervical lymph nodal metastases

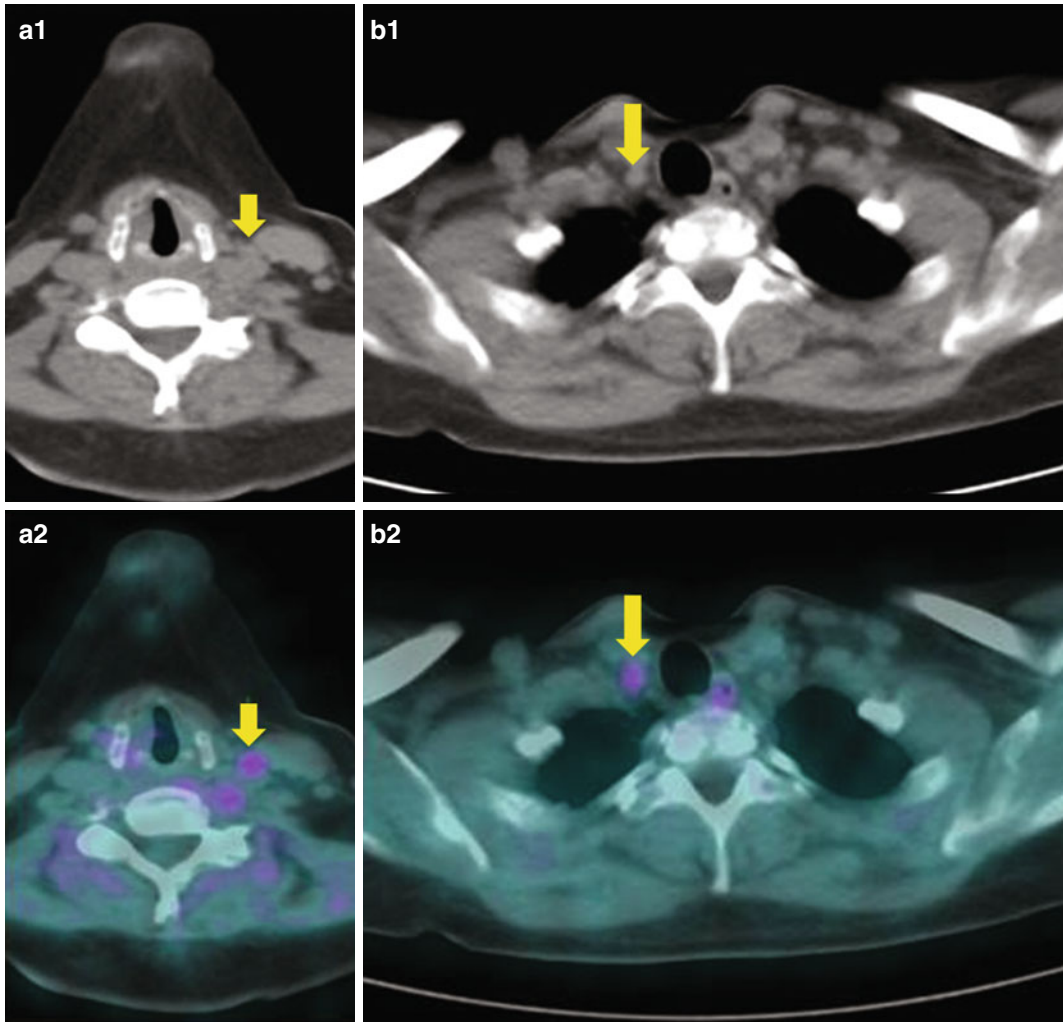

Fig. 12.4 CT (**a1**, **b1**) and ^{18}F-DOPA PET/CT (**a2**, **b2**) performed for restaging in a patient surgically treated for medullary thyroid carcinoma who showed increased serum calcitonin levels (calcitonin > 150 mg/dl). The images show small lymph nodes (diameter < 1 cm) with increased tracer uptake suspicious for recurrence of medullary thyroid cancer (*arrows*). Medullary thyroid cancer metastases were found after removal of these PET-positive lymph nodes

References

1. American Thyroid Association Guidelines Task Force, Kloos RT, Eng C, Evans DB et al (2009) Medullary thyroid cancer: management guidelines of the American Thyroid Association. Thyroid 19:565–612
2. Elisei R, Bottici V, Luchetti F et al (2004) Impact of routine measurement of serum calcitonin on the diagnosis and outcome of medullary thyroid cancer: experience in 10,864 patients with nodular thyroid disorders. J Clin Endocrinol Metab 89:163–168
3. Trimboli P, Giovanella L (2015) Serum calcitonin negative medullary thyroid carcinoma: systematic review of the literature. Clin Chem Lab Med 53: 1507–1514
4. Trimboli P, Treglia G, Guidobaldi L et al (2015) Detection rate of FNA cytology in medullary thyroid carcinoma: a meta-analysis. Clin Endocrinol 82:280–285
5. Pusztaszeri MP, Bongiovanni M, Faquin WC (2014) Update on the cytologic and molecular features of medullary thyroid carcinoma. Adv Anat Pathol 21:26–35
6. Trimboli P, Giovanella L, Crescenzi A et al (2014) Medullary thyroid cancer diagnosis: an appraisal. Head Neck 36:1216–1223
7. Trimboli P, Seregni E, Treglia G et al (2015) Procalcitonin for detecting medullary thyroid carcinoma: a systematic review. Endocr Relat Cancer 22:R157–R164
8. Treglia G, Rufini V, Salvatori M et al (2012) PET imaging in recurrent medullary thyroid carcinoma. Int J Mol Imaging 2012:324686

Anaplastic Carcinoma and Other Tumors

13

Luca Giovanella and Giorgio Treglia

Abstract

This chapter provides a brief summary on more rare thyroid tumors, including anaplastic thyroid carcinoma and thyroid lymphomas. Some diagnostic images of these thyroid tumors including ultrasonography, computed tomography, magnetic resonance imaging, and positron emission tomography are discussed.

Keywords

Anaplastic • Undifferentiated • Thyroid cancer • Lymphoma • Aggressive tumor

Prof. Dr. med. L. Giovanella, MD, PhD (✉)
G. Treglia, MD, MSc
Department of Nuclear Medicine,
Thyroid and PET/CT Center,
Oncology Institute of Southern Switzerland,
Via Ospedale 12, CH-6500
Bellinzona and Lugano, Switzerland
e-mail: luca.giovanella@eoc.ch;
giorgio.treglia@eoc.ch

L. Giovanella et al. (eds.), *Atlas of Head and Neck Endocrine Disorders: Special Focus on Imaging and Imaging-Guided Procedures*, DOI 10.1007/978-3-319-22276-9_13

13.1 Introduction

Beyond well-differentiated thyroid carcinoma and medullary thyroid carcinoma, other malignant tumors may affect the thyroid gland, including anaplastic carcinoma, lymphomas, and metastases from other tumors. Several imaging methods including ultrasonography, computed tomography, magnetic resonance imaging, and positron emission tomography may be used to evaluate these rare thyroid tumors (Figs. 13.1, 13.2, 13.3, 13.4, 13.5, 13.6, and 13.7).

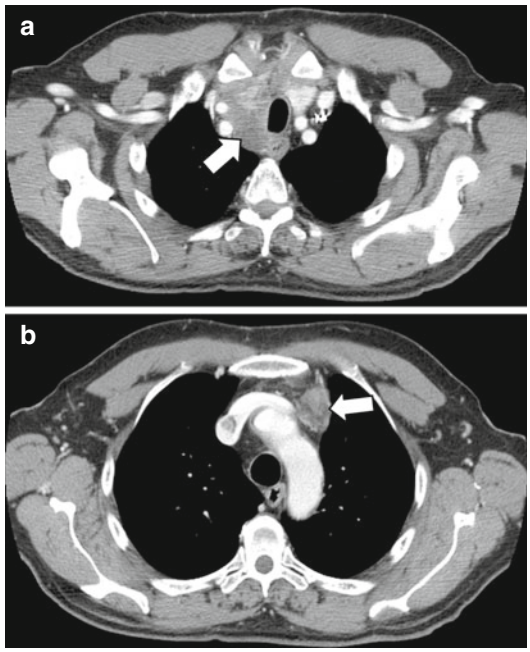

Fig. 13.1 Computed tomography in a patient with anaplastic thyroid carcinoma showing a large mass of the right thyroid lobe (*arrow*) (**a**) with mediastinal lymph nodal metastases (*arrow*) (**b**)

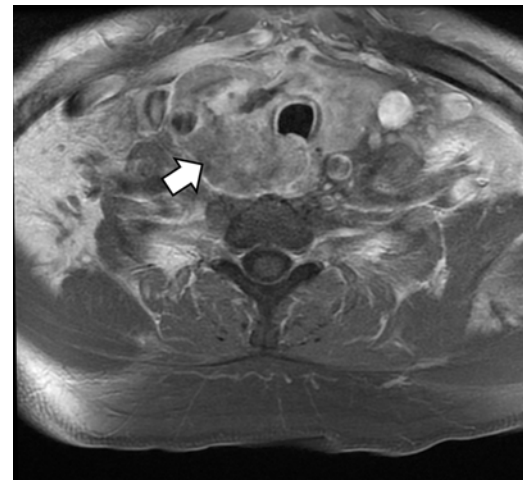

Fig. 13.2 Magnetic resonance imaging in a case of anaplastic thyroid carcinoma showing an inhomogeneous mass of the right thyroid lobe with invasion of adjacent anatomic structures

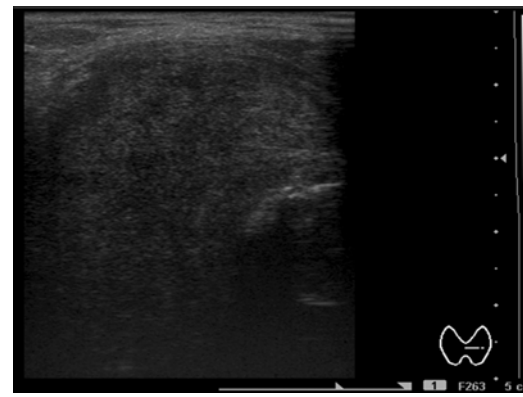

Fig. 13.3 Ultrasonography shows a 5 cm hypoechogenous nodule of the left thyroid lobe with calcifications. Final diagnosis was anaplastic thyroid carcinoma

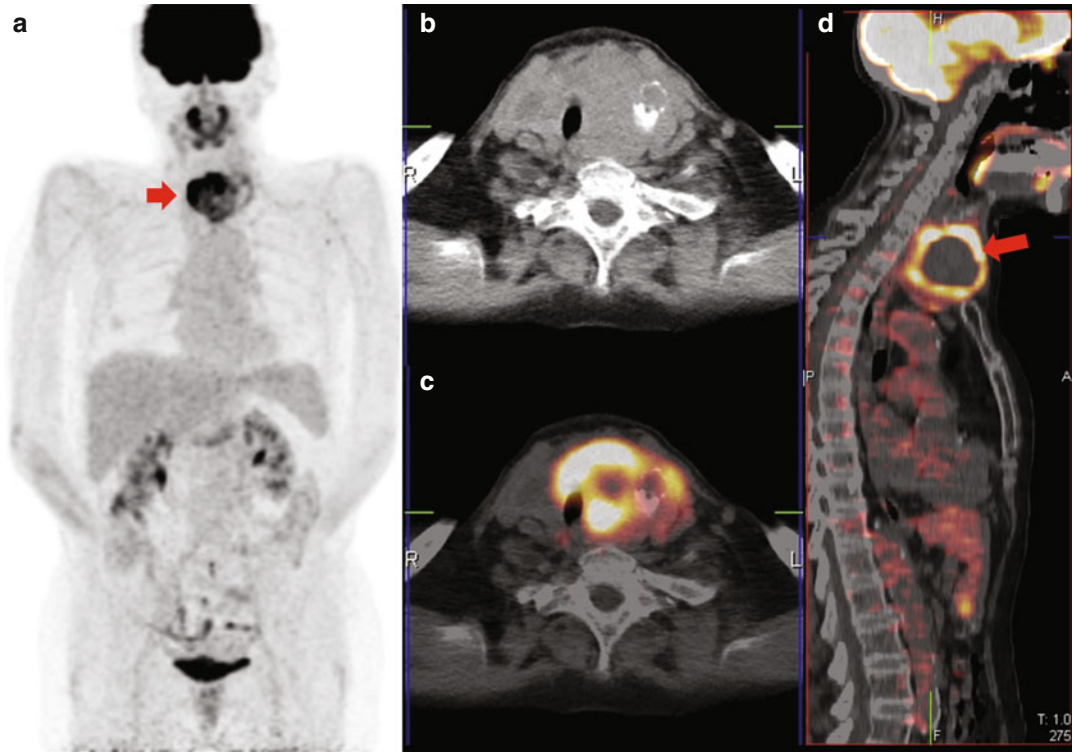

Fig. 13.4 Fluorine-18 fluorodeoxyglucose positron emission tomography/computed tomography (^{18}F-FDG-PET/CT) in a patient with anaplastic thyroid carcinoma. ^{18}F-FDG-PET shows an area of increased metabolism in the neck (**a**) corresponding to a large and inhomogeneous thyroid mass at co-registered CT (**b**), as even demonstrated by fused PET/CT images (**c**). The thyroid mass shows a central area of reduced metabolism due to necrosis and an external ring of increased metabolism as demonstrated by fused PET/CT images (**d**)

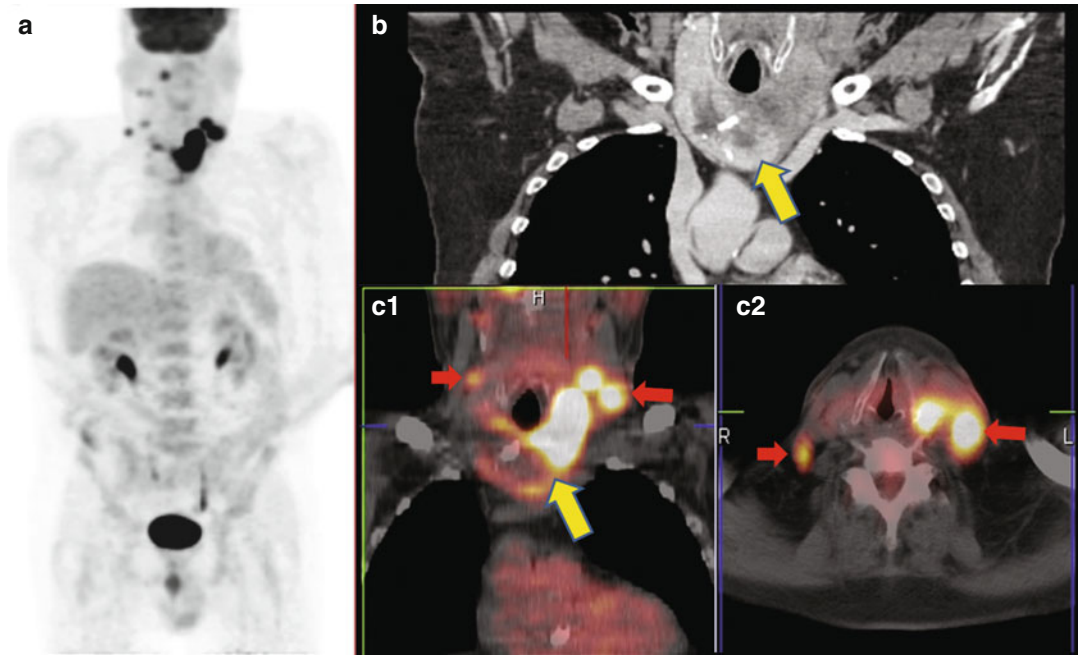

Fig. 13.5 Fluorine-18 fluorodeoxyglucose positron emission tomography/computed tomography ($^{18F\text{-}FDG\text{-}PET}$/CT) in a patient with anaplastic thyroid carcinoma and lymph nodal metastases. ^{18}F-FDG-PET shows several areas of increased metabolism in the neck (**a**) corresponding to a large and inhomogeneous thyroid mass at contrast-enhanced CT (**b**). Fused PET/CT images (**c1**, **c2**) showed a large thyroid tumor with increased metabolism (*yellow arrow*) and several lymph nodal metastases (*red arrows*)

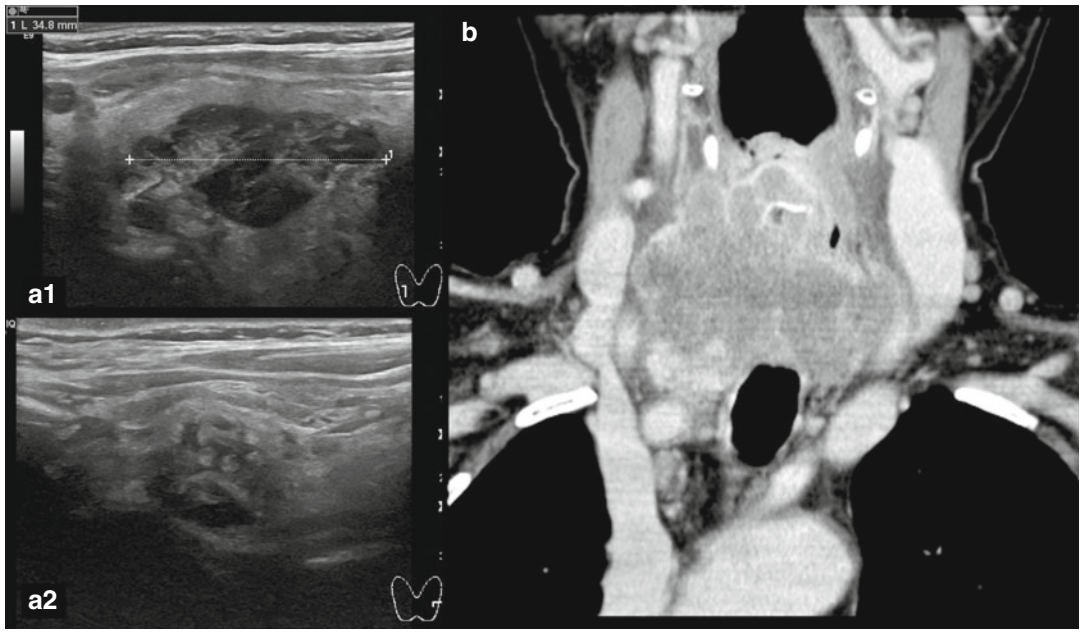

Fig. 13.6 Ultrasonography (**a1**, **a2**) and computed tomography (**b**) findings in a patient with large B-cell lymphoma of the thyroid gland. Large hypoechogenous nodules with inhomogeneous echotexture involving both thyroid lobes are evident at ultrasonography (**a1**, **a2**). Contrast-enhanced computed tomography shows a large and inhomogeneous thyroid mass with compression of the near structures

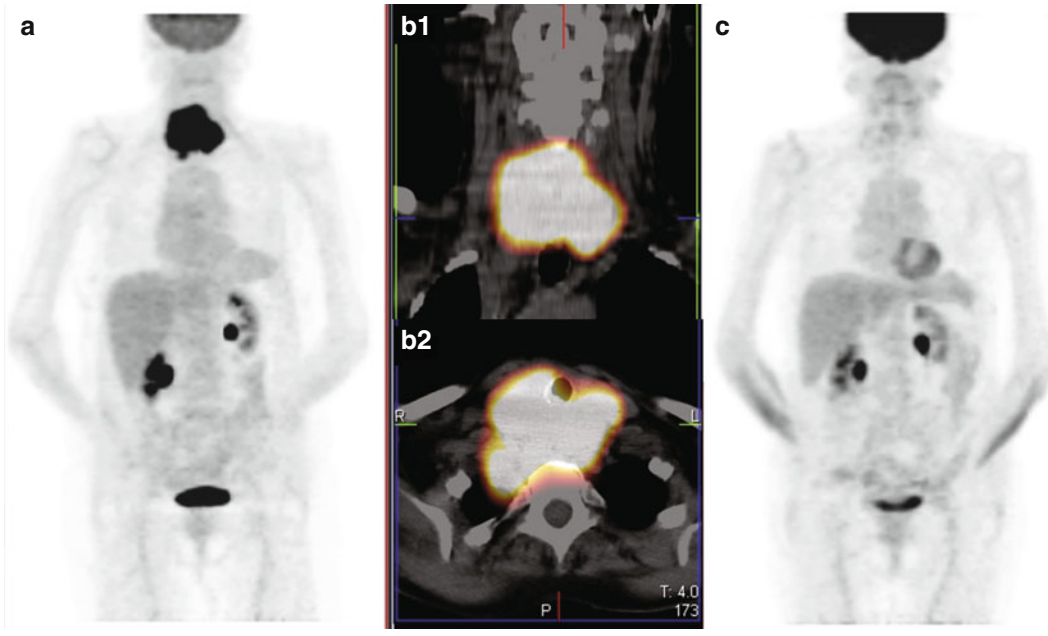

Fig. 13.7 Fluorine-18 fluorodeoxyglucose positron emission tomography/computed tomography ($^{18F\text{-}FDG\text{-}PET}$/CT) performed before (**a**, **b1**, **b2**) and after chemotherapy (**c**) in a patient with large B-cell lymphoma of the thyroid gland. ^{18}F-FDG-PET shows an area of increased metabolism in the neck (**a**) corresponding to a large thyroid mass at co-registered CT, as demonstrated by fused PET/CT images in coronal (**b1**) and axial projection (**b2**). PET/CT performed after 2 cycles of immunochemotherapy shows a dramatic metabolic response to the treatment (**c**)

13.2 Anaplastic Thyroid Carcinoma

Anaplastic thyroid carcinoma (ATC) is a rare disease, accounting for less than 1–2 % of all thyroid tumors. Nevertheless, it is one of the most lethal human malignant tumors, accounting for about one-half of all thyroid carcinoma deaths. ATC usually presents as a rapidly enlarging neck mass, often associated with vocal cord paralysis, dyspnea, and/or dysphagia with a female/male ratio of 1.5:1 and a peak of incidence in the sixth and seventh decades of life [1]. ATC typically follows a rapid and lethal clinical course, with median survival below 6 months in the majority of series reported. The disease is usually advanced at the time of diagnosis, with extensive local disease and direct invasion into adjacent organs, such as the trachea, esophagus, blood vessels, and muscles, in a high percentage of patients (Figs. 13.1, 13.2, 13.3, 13.4, and 13.5). In addition, about half of patients present with distant metastases, the lung being the most commonly involved site [2]. Patients usually die from local and regional progression of the tumor, with airway and esophageal obstruction. The options for treatment of ATC include surgery, chemotherapy, and radiotherapy. All of these, especially if used alone, most often fail to control local disease. Multimodal therapy, combining surgery, chemotherapy, and radiation therapy, can give better results, avoiding death from local invasion and suffocation and improving survival of some ATC patients [3].

13.3 Lymphomas

Primary thyroid lymphomas are rare and generally they derive from B cell. There was great difficulty in distinguishing thyroid lymphoma from anaplastic thyroid carcinoma, but, due to the new immunocytochemical staining techniques, diagnostic accuracy has improved drastically over the past decade. The more indolent lymphomas are the subgroup of mucosa-associated lymphoid tissue (MALT) lymphomas (6–27 % of thyroid lymphomas). Diffuse large B-cell lymphoma (DLBCL), the more common subtype of thyroid lymphoma (i.e., up to 70 % of cases), shows an aggressive behavior with almost 60 % of these tumors diagnosed with disseminated disease (Figs. 13.6 and 13.7) [4]. Surgery that was once the mainstay of treatment for this disease now plays a minimal role. Current treatment regimens for primary thyroid lymphoma consist of immunochemotherapy and external beam radiation. The overall 5-year survival for thyroid DLBCL group is less than 50 % [5].

13.4 Thyroid Metastases

Thyroid metastases are clinically rare and the kidney represents the most common primary site of origin. They usually occur when there are metastases elsewhere, sometimes many years after diagnosis of the original primary tumor. However, thyroid gland metastasis was reported as the initial manifestation of metastatic disease in some patients [6]. The treatment planning is dictated by the histotype and staging of the primary cancer.

References

1. Are C, Shaha AR (2006) Anaplastic thyroid carcinoma: biology, pathogenesis, prognostic factors and treatment approaches. Ann Surg Oncol 13:453–464
2. Kebebew E, Greenspan FS, Clark OH et al (2005) Anaplastic thyroid carcinoma. Treatment outcome and prognostic factors. Cancer 103:1330–1335
3. De Crevoisier R, Baudin E, Bachelot A et al (2004) Combined treatment of anaplastic thyroid carcinoma with surgery, chemotherapy and hyperfractionated accelerated external radiotherapy. Int J Radiat Oncol Biol Phys 60:1137–1143
4. Widder S, Pasieka JL (2004) Primary thyroid lymphomas. Curr Treat Options Oncol 5:307–313
5. Mack LA, Pasieka JL (2007) An evidence-based approach to the treatment of thyroid lymphoma. World J Surg 31:978–986
6. Wood K, Vini L, Harmer C (2004) Metastases to the thyroid gland: the Royal Marsden experience. Eur J Surg Oncol 30:583–588

Part III

Parathyroid Diseases

Primary Hyperparathyroidism

14

Jukka Schildt, Virpi Tunninen, Marko Seppänen, and Camilla Schalin-Jäntti

Abstract

Primary hyperparathyroidism (PHPT) is a common endocrine disorder that especially affects women over 50–60 years [1]. The combination of increased serum calcium and parathyroid hormone (PTH) concentrations confirms the diagnosis. Surgery is the only potentially curative treatment, and there is universal agreement regarding which patients should be referred for surgery and for whom surveillance is sufficient. If the patient is scheduled for surgery, preoperative localization of the abnormal parathyroid gland(s) should be performed in order to help the surgeon plan the surgical strategy. It has been estimated that 60–70 % of patients with PHPT are candidates for unilateral neck exploration. If surgery is not planned, there is no reason to perform preoperative localization studies. Preoperative localization studies are mandatory before reoperation of PHPT. Multiple localization studies are to date available and they can be divided into invasive and noninvasive techniques. Surgery should not be ruled out based on a negative preoperative imaging study. For such cases, bilateral neck exploration is performed as primary surgery.

Keywords

Hyperparathyroidism • Imaging • Parathyroid • Ultrasound, scintigraphy, PET

J. Schildt, MD
Department of Clinical Physiology
and Nuclear Medicine, University of Helsinki
and Helsinki University Hospital, Helsinki, Finland

V. Tunninen, MD
Department of Nuclear Medicine,
Satakunta Central Hospital, Pori, Finland

M. Seppänen, MD
Department of Clinical Physiology and Nuclear
Medicine, Turku PET Centre, University of Turku
and Turku University Hospital, Turku, Finland

C. Schalin-Jäntti, MD, PhD (✉)
Division of Endocrinology, Department of Medicine,
Abdominal Center, University of Helsinki
and Helsinki University Hospital,
340, Helsinki FI-00029, Finland
e-mail: camilla.schalin-jantti@hus.fi

L. Giovanella et al. (eds.), *Atlas of Head and Neck Endocrine Disorders: Special Focus on Imaging and Imaging-Guided Procedures*, DOI 10.1007/978-3-319-22276-9_14

14.1 Introduction

Primary hyperparathyroidism (PHPT) is the most common cause of hypercalcemia in the outpatient setting. PHPT is twice to three times more common among women compared to males [1]. PHPT is 80–85 % explained by a single parathyroid adenoma and by parathyroid hyperplasia in 15–20 % [1, 2]. Double adenomas are found in approximately 4 % of cases and parathyroid carcinoma in 1 % [1, 2]. PHPT may also be part of familial, genetic syndromes such as multiple endocrine neoplasia (MEN), hyperparathyroidism-jaw tumor (HPT-JT) syndrome, or familial isolated hyperparathyroidism due to *CDC73* gene or calcium-sensing receptor (*CaSR*) gene mutations [3, 4]. Recent data suggest that as many as 10 % of younger patients (<45 years) may harbor a germ-line mutation in one of the genes associated with familial forms of PHPT [5]. Parathyroidectomy in the setting of hereditary PHPT is challenging and usually requires bilateral neck exploration, as the patients often have multiglandular disease [6]. These patients are at higher risk of persistent and recurrent disease.

To date, PHPT is often mild and the patients may not present with classical symptoms of kidney stones and bone fractures [2, 7–9]. Currently, surgery is recommended for all symptomatic patients, for patients who demonstrate serum calcium concentrations 0.25 mmol/l above the upper reference limit, in patients with concomitant osteoporosis or vertebral fractures, and in patients with renal manifestations, such as impaired estimated glomerular filtration rate and kidney stones [7–9]. Surgery is also recommended for patients less than 50 years of age [7–9].

14.2 Preoperative Localization Studies

Ideally, preoperative imaging should accurately identify on which side of the neck the pathological parathyroid gland(s) resides, with no false-positive findings on the healthy side. It has been estimated that roughly 60–70 % of patients with PHPT are candidates for unilateral neck exploration. In patients scheduled for targeted surgery, preoperative imaging must unequivocally demonstrate single-gland disease [6]. Patients in whom preoperative imaging remains negative are more often characterized by mild single-gland disease, with only mild increases in serum calcium and PTH concentrations, and small tumor size [10]. Concomitant thyroid disease, such as goiter and thyroid nodules, reduces the true-positive results of both neck ultrasound and single-isotope sestamibi scintigraphy. Multiglandular disease, the rate of which has been estimated to be at least 15 %, is difficult to establish on preoperative imaging. A serious limitation of all preoperative imaging techniques is accurate localization of multiglandular disease [11]. The two main reasons for failed surgery in PHPT are undetected multiglandular disease and ectopically located parathyroid glands.

14.2.1 Neck Ultrasound

Most surgeons appreciate a preoperative neck ultrasound. It is of low expense, is noninvasive, and does not expose the patient to radiation. It is a very sensitive technique to evaluate the thyroid gland, both with regard to size in general and thyroid nodules (Fig. 14.1). It is limited in its ability to evaluate retroesophageal lesions and does not penetrate bony structures such as the sternum or the clavicles. Accordingly, accurate evaluation of possible ectopically located, mediastinal parathyroid glands is not possible. Although some studies comparing sensitivity and specificity of ultrasound and ^{99m}Tc-methoxyisobutylisonitrile (^{99m}Tc-sestamibi) for revealing hyperfunctioning parathyroid glands reported similar results, ultrasound is highly performer-dependent and is generally not

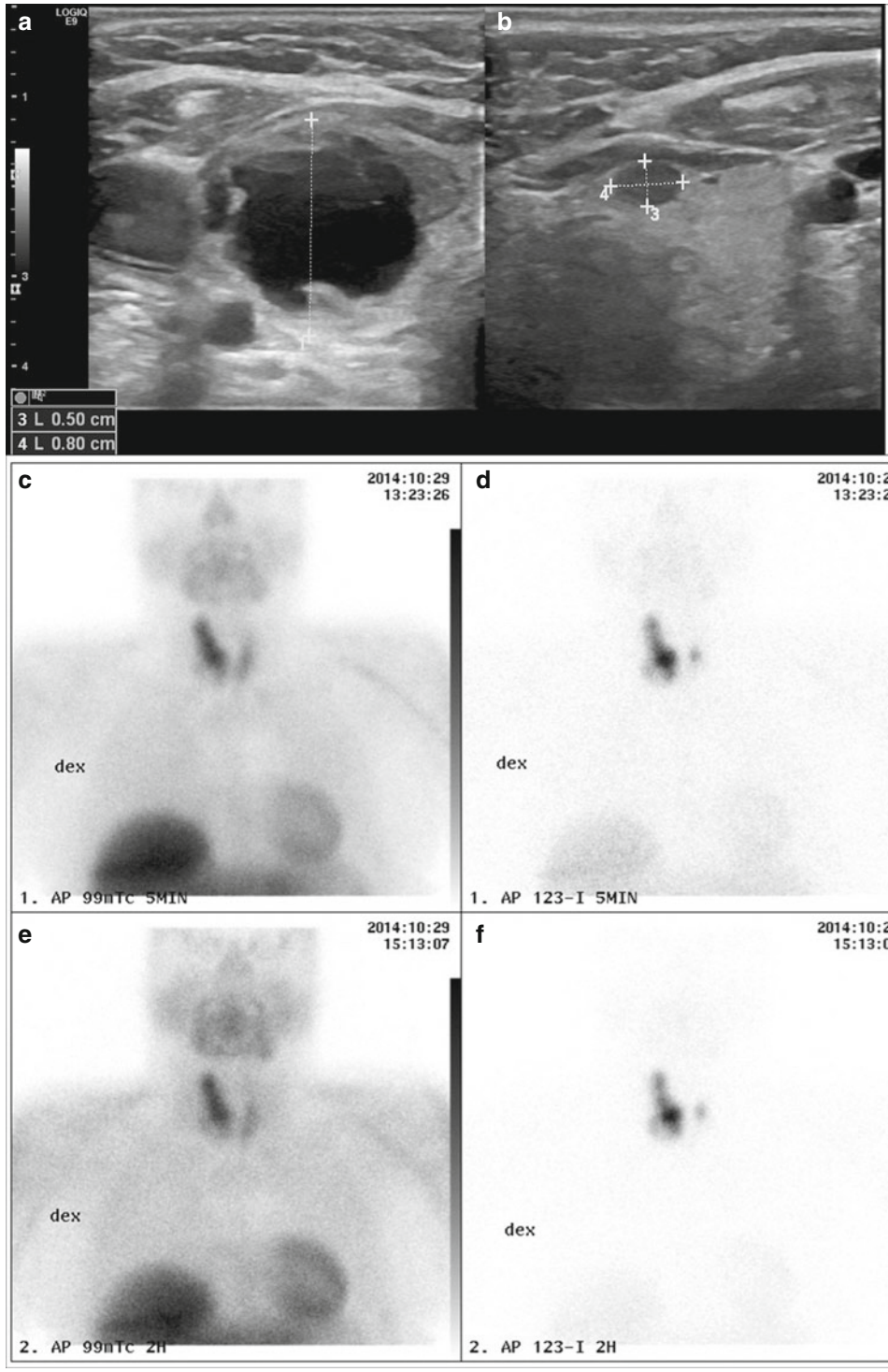

Fig. 14.1 A 54-year-old woman with type 2 diabetes was investigated because of kidney stones. Her serum ionized calcium was markedly increased, 1.74 mmol/l (reference range 1.16–1.30 mmol/l), and also her plasma PTH was markedly increased, 275 ng/l (reference range 15–65 ng/l). She was scheduled for surgery because of severe PHPT. Neck ultrasound demonstrated an enlarged right thyroid lobe with nodules compatible with goiter, the larger one measuring 2.5 cm (panels **a**, **b**). ^{123}**I**/^{99m}Tc-sestamibi scintigraphy (panels **c**–**f**) demonstrates an increased uptake in the left thyroid lobe both with ^{99m}Tc and ^{123}I at 5 min (**c**, **d**) and at 2 h (**e**, **f**), respectively. At surgery, a parathyroid adenoma was found within the left thyroid lobe, which was resected, and the patient was cured

recommended as the only preoperative investigation in PHPT [6, 12]. Figure 14.2 demonstrates the findings in a patient with PHPT for whom a parathyroid adenoma was visualized both with neck US and ^{123}I/^{99m}Tc-sestamibi scintigraphy.

14.2.2 Selective Venous Sampling

Selective venous sampling (SVS) was introduced for localization of hyperfunctioning parathyroid glands in 1969 by Reitz and colleagues [13]. Results from studies evaluating the accuracy of this invasive technique have not been consistent. The range of positive predictive results has varied from 39 to 93 % [12, 14]. Most studies have been retrospective and have not included direct comparison with other techniques. Some of the differences in outcome are explained by selection bias (selected patients only or up to 100 % of patients included having single adenoma disease with exclusion of multiglandular disease). Schalin-Jäntti and colleagues prospectively compared the performance of SVS, planar scintigraphy with ^{123}I/^{99m}Tc-sestamibi, ^{99m}Tc-sestamibi SPECT/CT, and ^{11}C-methionine PET/CT in PHPT patients scheduled for reoperation and found that SVS was the least accurate technique with a high proportion of false predictive findings [11].

14.2.3 Planar Scintigraphy and SPECT/CT in Combination with Single or Dual Isotopes

As introduced by Coakley et al. in 1989, ^{99m}Tc-sestamibi scintigraphy has gained great popularity. Worldwide, this is probably the imaging modality used most often before primary surgery of PHPT [15]. Uptake of ^{99m}Tc-sestamibi is, however, not tissue-specific but is sequestered within mitochondria both in the thyroid and parathyroid tissue, as well as in the salivary glands and normal cardiac cells [16]. Imaging using the single-tracer technique is based on the different washout kinetics for thyroid and parathyroid tissue. While maximum thyroid gland activity is reached within 5 min, parathyroid activity is sustained with delayed washout, which allows for parathyroid imaging two hours after the injection [16]. Thyroid nodules may have a prolonged washout and thus cause false-positive findings when using the single-tracer technique.

^{99m}Tc-sestamibi can also be used in combination with iodine-123 (^{123}I) or technetium-99 m pertechnetate (^{99m}TcO4^{-}), which are thyroid-specific isotopes. In this dual-isotope technique, the thyroid image is digitally subtracted from the ^{99m}Tc-sestamibi image and thus allows for the visualization of parathyroid tissue alone (Figs. 14.1 and 14.2). The EANM guidelines recommend the use of an additional thyroid-specific isotope over ^{99m}Tc-sestamibi imaging alone [17].

SPECT and SPECT/CT have gained much popularity for acquisition of abnormal parathyroid glands [18]. The combination of SPECT with CT allows for better anatomical identification of the abnormal gland. SPECT and SPECT/CT can also be performed either in combination with the single-isotope or dual-isotope method (Fig. 14.3). Using the single-isotope technique, Lavely and colleagues concluded that early SPECT/CT in combination with any delayed imaging performs better than planar scintigraphy or SPECT alone [19]. Tunninen et al. compared five parathyroid scintigraphic protocols in patients with primary or secondary hyperparathyroidism, including three scintigraphic protocols with dual-isotope (parallel-hole planar, pinhole planar, and SPECT/CT) and two with single-isotope (double-phase parallel-hole planar and SPECT/CT) and concluded that any dual-isotope protocol performs better than the single-isotope protocols [20].

A recent large retrospective study comparing the performance of dual- versus single-isotope ^{99m}Tc-sestamibi before primary surgery of PHPT demonstrated that dual-isotope ^{99m}Tc-sestamibi scintigraphy was significantly more accurate than ^{99m}Tc-sestamibi alone, with accuracies of 63.4 and 34.9 %, respectively [10]. Figure 14.2 demonstrates the ^{123}I/^{99m}Tc-sestamibi scintigraphy findings in a patient with PHPT; while ^{99m}Tc-sestamibi imaging at 5 min and 2 h remained negative, subtraction imaging revealed an abnormal uptake in the left inferior parathyroid gland, compatible with a parathyroid adenoma.

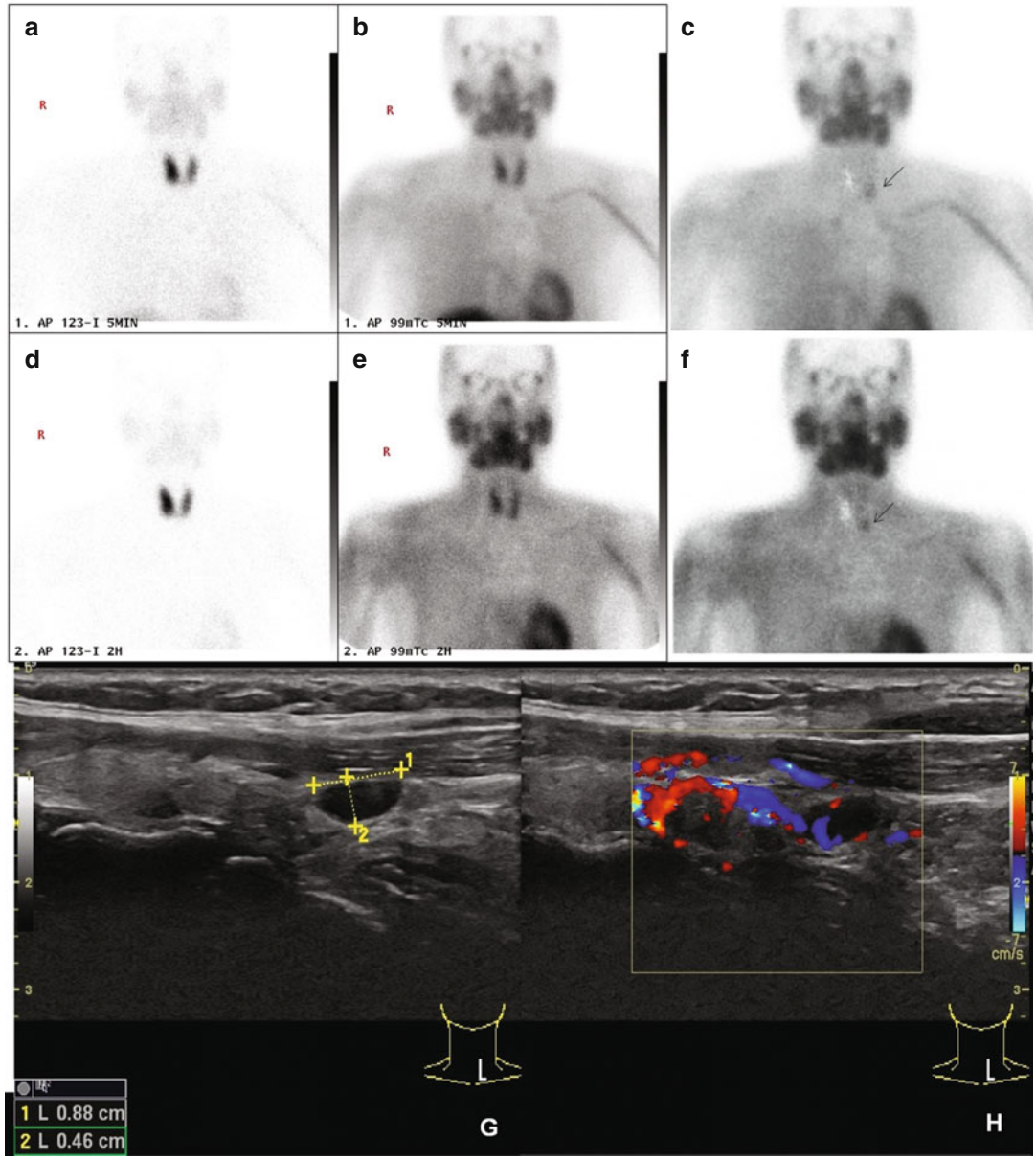

Fig. 14.2 A 56-year-old woman treated for breast cancer was screened for hypercalcemia. Her serum ionized calcium was increased, 1.42 mmol/l (reference range 1.16–1.30 mmol/l), and also her plasma PTH concentration was increased, 113 ng/l (reference range 15–65 ng/l). She was diagnosed with primary hyperparathyroidism. She underwent bone densitometry which revealed osteoporosis. She was scheduled for surgery and underwent ^{123}I/^{99m}Tc-sestamibi scintigraphy (**a**–**f**) and neck ultrasound (**g**, **h**). Planar scintigraphic images in anterior view demonstrate ^{99m}Tc and ^{123}I uptake at 5 min (**a**, **b**) and respective uptakes at 2 h (**e**, **d**) without parathyroid adenoma detection. The subtraction images at 5 min (**c**) and at 2 h (**f**) demonstrated abnormal uptake in the left inferior parathyroid gland (*arrow*). Neck ultrasound (**g**, **h**) showed a 5×9 mm tumor at the left inferior posterior thyroid lobe, which is compatible with a parathyroid adenoma

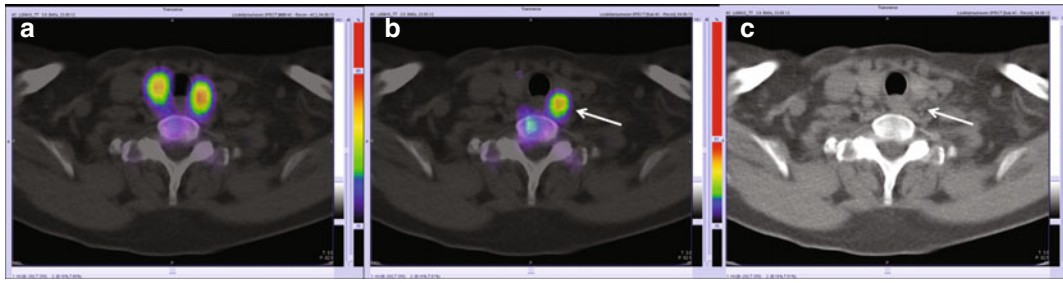

Fig. 14.3 This female patient with PHPT underwent dual-isotope SPECT/CT with ^{123}I and ^{99m}Tc 10 min after the ^{99m}Tc-sestamibi injection. The adenoma was not visible on transaxial fusion ^{99m}Tc-sestamibi imaging (**a**). Transaxial fusion subtraction imaging (**b**) revealed a parathyroid adenoma (*arrow*), which was also visible on low-dose CT imaging (**c**). At surgery, a parathyroid adenoma was found behind the left thyroid lobe. The patient was cured

14.2.4 PET/CT

^{11}C-methionine PET/CT has good specificity for hyperfunctioning parathyroid compared to surrounding head and neck tissue [21]. The use of ^{11}C-methionine PET has since been suggested for difficult cases of PHPT, with negative imaging results on conventional imaging [22–25]. ^{11}C-methionine PET is not available in all centers and the complicated labeling procedure may be regarded as a limitation. A prospective study comparing the accuracy of five different localization techniques (planar scintigraphy with ^{123}I/^{99m}Tc-sestamibi, $^{99mTc\text{-}sestamibi}$ SPECT/CT, SVS, and ^{11}C-methionine PET/CT) in complicated PHPT recommended planar scintigraphy with ^{123}I/^{99m}Tc-sestamibi as first-line imaging before reoperation and concluded that ^{11}C-methionine PET/CT provides additional information if ^{123}I/^{99m}Tc-sestamibi scintigraphy remains negative [11]. Figure 14.4 demonstrates a case in whom an ectopically located parathyroid adenoma was located with ^{11}C-methionine PET/CT before reoperation.

Preliminary findings show that in patients with hyperparathyroidism and with discordant or equivocal results on scintigraphy or on ultrasonography, hyperfunctioning parathyroid glands can be localized by radiolabeled choline PET/CT with good accuracy [26].

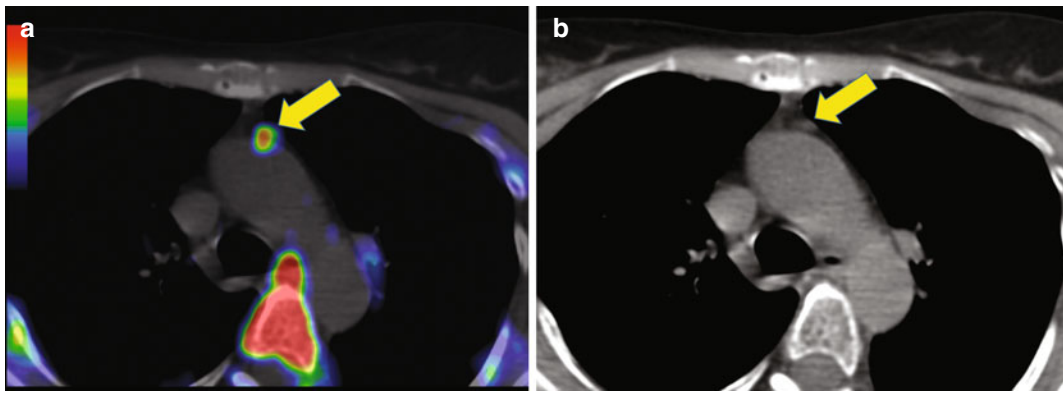

Fig. 14.4 A 52-year-old woman underwent bilateral neck exploration because of PHPT and osteoporosis. Conventional preoperative imaging (neck ultrasound, ^{123}I/^{99m}Tc-sestamibi scintigraphy) was negative. She was not cured by surgery and underwent selective venous sampling of plasma PTH and ^{11}C-methionine PET/CT before reoperation. Selective venous sampling was not helpful, but ^{11}C-methionine PET/CT revealed a focal uptake (**a**) corresponding to a 3 × 9 mm nodule located retrosternally in front of the aortic arch, 4 cm below the upper end of the sternum (**b**, *arrow*). The patient underwent sternotomy, an ectopically located parathyroid adenoma was resected, and she was cured after her second operation

References

1. Pallan S, Rahman MO, Khan AA (2012) Diagnosis and management of primary hyperparathyroidism. BMJ 344:e1013
2. Adami S, Marcocci C, Gatti D (2002) Epidemiology of primary hyperparathyroidism in Europe. J Bone Mineral Res 17(suppl 2):N18–23
3. Eastell R, Brandi ML, Costa AG et al (2014) Diagnosis of asymptomatic primary hyperparathyroidism: proceedings of the fourth International workshop. J Clin Endocrinol Metab 99:3570–3579
4. Korpi-Hyövälti E, Cranston T, Ryhänen E et al (2014) CDC73 intragenic deletion in familial primary hyperparathyroidism associated with parathyroid carcinoma. J Clin Endocrinol Metab 99:3044–3048
5. Lassen T, Friis-Hansen L, Rasmussen ÅK et al (2014) Primary hyperparathyroidism in young people. When should we perform genetic testing for multiple endokrine neoplasia 1 (MEN-1)? J Clin Endocrinol Metab 99:3983–3987
6. Udelsman R, Åkerström G, Biagini C et al (2014) The surgical management of asymptomatic primary hyperparathyroidism: proceedings of the fourth International workshop. J Clin Endocrinol Metab 99:3595–3606
7. Khan A, Bilezikian J (2000) Primary hyperparathyroidism: pathophysiology and impact on bone. CMAJ 163:184–187
8. Khan AA, Bilezikian JP, Potts JT Jr (2009) The diagnosis and management of asymptomatic primary hyperparathyroidism revisited. J Clin Endocrinol Metab 94:333–334
9. Bilezikian JP, Brandi ML, Eastell R et al (2014) Guidelines for the management of asymptomatic primary hyperparathyroidism: summary statement from the fourth international workshop. J Clin Endocrinol Metab 99:3561–3569
10. Ryhänen EM, Schildt J, Heiskanen I et al (2015) 99mTechnetium sestamibi-123Iodine scintigraphy is more accurate than 99mTechnetium sestamibi alone before surgery for primary hyperparathyroidism. Int J Mol Imaging 2015:391625
11. Schalin-Jäntti C, Ryhänen E, Heiskanen I et al (2013) Planar scintigraphy with 123I/99mTc-sestamibi, 99mTc-sestamibi SPECT/CT, 11C-methionine PET/CT, or selective venous sampling before reoperation of primary hyperparathyroidism? J Nucl Med 54:739–747
12. Cheung K, Wang TS, Farrokhyar F et al (2012) A meta-analysis of preoperative localization techniques for patients with primary hyperparathyroidism. Ann Surg Oncol 19:577–583
13. Reitz RE, Pollard JJ, Wang CA et al (1969) Localization of parathyroid adenomas by selective venous catheterization and radioimmunoassay. N Engl J Med 281:348–351
14. Granberg PO, Hamberger B, Johansson G et al (1986) Selective venous sampling for localization of hyperfunctioning parathyroid glands. Br J Surg 73:118–120
15. Coakley AJ, Kettle AG, Wells CP et al (1989) 99Tcm sestamibi – a new agent for parathyroid imaging. Nucl Med Commun 10:791–794
16. Greenspan BS, Dillehay G, Intenzo C et al (2012) SNM practice guideline for parathyroid scintigraphy. J Nucl Med Technol 40:111–118
17. Hindie E, Ugur Ö, Fuster D et al (2009) 2009 EANM parathyroid guidelines. Eur J Nucl Med Mol Imaging 36:1201–1216
18. Neumann DR, Esselstyn CB Jr, Go RT et al (1997) Comparison of double-phase 99mTc-sestamibi subtraction SPECT in hyperparathyroidism. AJR Am J Roentgenol 169:1671–1674
19. Lavely WC, Goetze S, Firedman KP et al (2007) Comparison of SPECT/CT, SPECT and planar imaging with single- and dual-phase 99mTc-sestamibi scintigraphy. J Nucl Med 48:1084–1089
20. Tunninen V, Varjo P, Schildt J et al (2013) Comparison of five parathyroid scintigraphic protocols. Int J Mol Imaging 2013:921260
21. Sundin A, Johansson C, Hellman P et al (1996) PET and parathyroid L-[carbon-11] methionine accumulation in hyperparathyroidism. J Nucl Med 37:1766–1770
22. Otto D, Boemer AR, Hofman M et al (2004) Preoperative localization of hyperfunctioning parathyroid tissue with 11C-methionine PET. Eur J Nucl Med Mol Imaging 31:1405–1412
23. Beggs AD, Hain SF (2005) Localization of parathyroid adenomas using 11C-methionine positron emission tomography. Nucl Med Commun 26:133–136
24. Tang BN, Moreno-Reyes R, Blocklet D et al (2008) Accurate pre-operative localization of pathological parathyroid glands using 11C-methionine PET/CT. Contrast Media Mol Imaging 3:157–163
25. Traub-Weidinger T, Mayerhoefer ME, Koperek O et al (2014) 11C-methionine PET/CT imaging of 99mTC-MIBI-SPECT/CT-negative patients with primary hyperparathyroidism and previous neck surgery. J Clin Endocrinol Metab 99:4199–4205
26. Michaud L, Burgess A, Huchet V et al (2014) Is 18F-fluorocholine-positron emission tomography/computerized tomography a new imaging tool for detecting hyperfunctioning parathyroid glands in primary or secondary hyperparathyroidism? J Clin Endocrinol Metab 99:4531–4536

Part IV

Other Endocrine Diseases of the Neck

Head and Neck Paragangliomas

15

Alexander Stephan Kroiss
and Irene Johanna Virgolini

Abstract

Head and neck paragangliomas (HNPGLs) are neuroendocrine tumors (NETs) usually characterized by benign features and slow progression. This chapter summarizes the main imaging methods used to evaluate HNPGL. In particular, the advantages of hybrid functional and morphological imaging, such as positron emission tomography/computed tomography (PET/CT), are described. About functional imaging methods, several PET radiopharmaceuticals could be used in this setting, evaluating different metabolic pathways or somatostatin receptor expression. Lastly, some example cases of HNPGL evaluated with different imaging methods are illustrated.

Keywords

Paraganglioma • Neuroendocrine • Functional imaging • PET/CT • Nuclear medicine • Somatostatin receptor • Glomus tumors

A.S. Kroiss, MD (✉) • I.J. Virgolini, MD
Department of Nuclear Medicine,
Medical University Innsbruck,
Anichstrasse 35, 6020 Innsbruck, Austria
e-mail: alexander.kroiss@i-med.ac.at

L. Giovanella et al. (eds.), *Atlas of Head and Neck Endocrine Disorders: Special Focus on Imaging and Imaging-Guided Procedures*, DOI 10.1007/978-3-319-22276-9_15

15.1 Introduction

Head and neck paragangliomas (HNPGLs) are neuroendocrine tumors (NETs) with the ability to bind somatostatin (SST). HNPGLs often are benign and progress slowly. The rate of metastatic spread is wide, ranging from less than 1 % to more than 60 %, depending on tumor location, size, and genetic background [1]. These tumors can be found anywhere from the neck to the pelvis associated with sympathetic or the parasympathetic nervous system [2]. Due to their sympathetic origin, most of the thoracic and abdominal extra-adrenal paragangliomas (PGLs) produce catecholamines and related substances, whereas HNPGLs – of parasympathetic origin – usually do not produce such substances [3].

15.2 Imaging Methods in HNPGL

Morphological imaging methods, for example, computed tomography (CT) or magnetic resonance imaging (MRI), provide excellent anatomic detail and high sensitivity [4, 5] but lack specificity as difficulties may occur when distinguishing between tumors derived from the sympathetic nervous system and other tumor entities [6]. In contrast to anatomic imaging, functional imaging provides high sensitivity and specificity, being able to distinguish between scars and tumor recurrence after previous surgery.

^{123}I-labeled metaiodobenzylguanidine (MIBG) and ^{111}In-pentetreotide-labeled somatostatin receptor (SSTR) imaging are functional imaging modalities, with moderate sensitivity in localizing metastatic and multifocal extra-adrenal PGL [7, 8]. However, both functional imaging modalities show limitations in localizing nonmetastatic extra-adrenal PGL due to limited resolution of planar scintigraphy and single-photon emission computed tomography (SPECT), respectively [1].

The introduction of hybrid imaging with integrated CT (e.g., SPECT/CT) enables exact anatomic correlation of functional pathologic lesions. However, lesions with a diameter below one centimeter can be missed by both planar scintigraphy and even SPECT/CT due to its limited resolution, respectively, as mentioned above.

The introduction of positron emission tomography (PET) and integrated computed tomography (PET/CT) into clinical practice, as well as the development of new PET radiopharmaceuticals, has produced promising results in the detection of these NETs [9, 10].

^{18}F-fluoro-L-dihydroxyphenylalanine (^{18}F-DOPA) has been proposed as a useful radiopharmaceutical for imaging catecholamine-secreting tumors [11], such as thoracic and abdominal PGL, because of the ability of these tumors to take up decarboxylate and store amino acids, such as DOPA, and their biogenic amines [12]. ^{18}F-DOPA shows high sensitivity and specificity for detecting nonmetastatic HNPGL [9, 13] (Fig. 15.1), but lower sensitivity for identifying metastases [7].

The introduction of SST analogues (DOTATOC, DOTATATE, DOTANOC) labeled with ^{68}gallium (^{68}Ga) as radiopharmaceuticals for PET has been used successfully for the diagnosis and therapy management of SST-expressing tumors, emphasizing the high sensitivity and specificity of NETs compared to SSTR scintigraphy and diagnostic CT [14].

A recent publication of our group compared both ^{68}Ga-DOTATOC PET and^{18}F-DOPA PET with diagnostic CT, observing a detection rate of 100 % for both functional imaging modalities in nonmetastatic glomus tumors [15]. However, in metastatic disease the per-lesion rate of ^{18}F-DOPA PET was lower compared to ^{68}Ga-DOTATOC PET (56 % versus 100 %, respectively), taking into account that foremost bone lesions, verified by both ^{68}Ga-DOTATOC PET and diagnostic CT, were ^{18}F-DOPA negative [15] (Figs. 15.2 and 15.3).

Recent publications and case reports confirmed the high detection rate of somatostatin receptor PET/CT in HNPGL, demonstrating the high diagnostic accuracy of ^{68}Ga-DOTANOC PET/CT compared to ^{131}I-MIBG scintigraphy and even to conventional imaging (CT or MRI), including distant metastases [16, 17]. This is in line with previous publication of our group, comparing ^{123}I-MIBG scintigraphy including SPECT/CT to ^{68}Ga-DOTATOC PET/CT in patients with glomus

tumors [18] (Figs. 15.4 and 15.5). Thereby, all head and neck manifestations were verified by both diagnostic CT and ^{68}Ga-DOTATOC PET compared to ^{123}I-MIBG SPECT/CT, which detected only one out of 17 positive ^{68}Ga-DOTATOC PET/CT lesions. Additionally, all distant metastases (e.g., the abdomen, bone) were verified by ^{68}Ga-DOTATOC PET/CT, providing the accurate tumor extent of patients with extra-adrenal PGL, compared to ^{123}I-MIBG scintigraphy, including SPECT/CT [18] (Figs. 15.4 and 15.5). To explain this on a molecular level, it has been suggested that extra-adrenal PGL could undergo dedifferentiation, leading to a loss of norepinephrine transporter or vesicular monoamine transporter (VMAT), which could then lead to false-negative ^{123}I-MIBG scintigraphy findings in metastatic disease [19]. In contrast to the excellence of ^{123}I-MIBG imaging in the detection of primary sympathetic PGL, its sensitivity is low in parasympathetic HNPGL [20]. Fottner et al. suggested that this could result from the under-expression of VMAT-1 in HNPGL [21]. Although ^{111}In-pentetreotide scintigraphy shows high sensitivity in HNPGL [8], as mentioned above, it is limited in detecting PGL lesions of sympathetic origin and – additionally – limited by its lower spatial resolution compared to PET [10].

The use of combined cross-sectional imaging (such as PET/CT or PET/MRI) increases diagnostic confidence and fully delineates the extent of tumor disease, from primary tumor to multifocal disease [15, 16, 18]. Unlike ^{18}F-DOPA, ^{68}Ga-labeled SST analogues give valuable information on tumor cell receptor status for planning peptide receptor radionuclide therapy, similar to ^{131}I-MIBG therapy, which is particularly useful in patients with surgically inoperable tumors or metastatic disease [15, 16, 18, 22].

To summarize, ^{68}Ga-labeled SST-analogue PET/CT offers high detection rate, both in metastatic and nonmetastatic glomus tumors due to high specific SST receptor subtype binding [23]. It has to be mentioned that prospective studies are warranted to confirm the high sensitivity and – in addition – to evaluate the specificity of ^{68}Ga-labeled SST analogues in patients with (metastatic) glomus tumors.

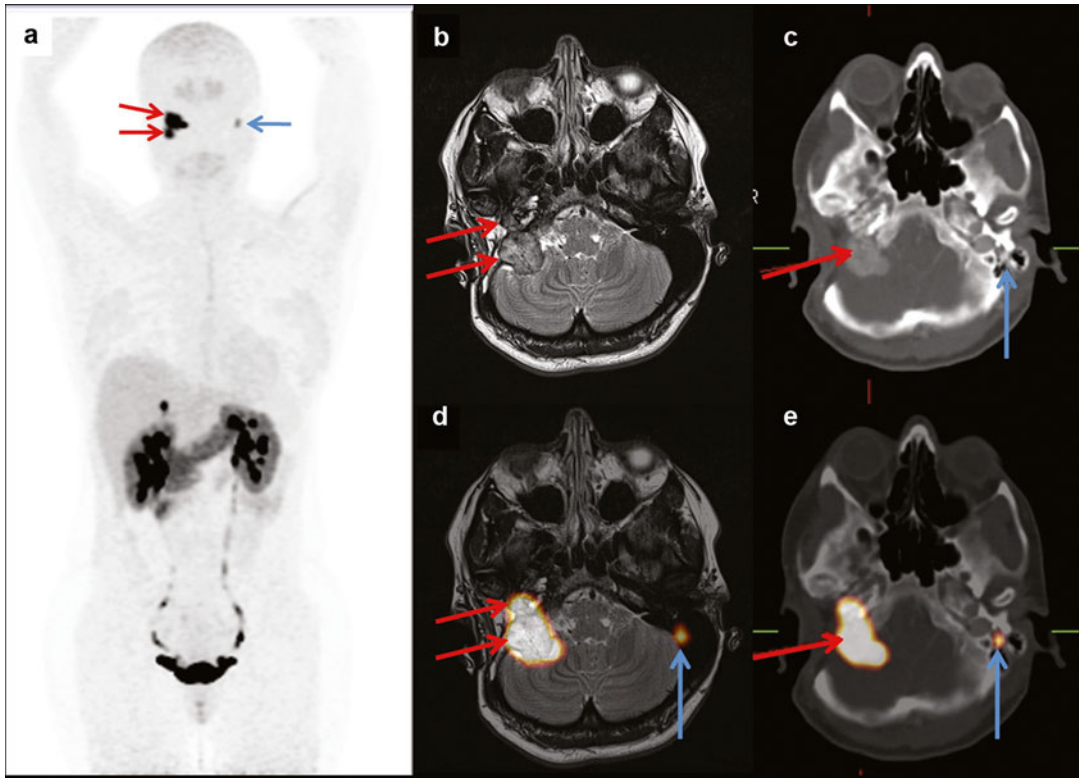

Fig. 15.1 Imaging in a 30-year-old female patient with multifocal head and neck paraganglioma. ^{18}F-DOPA PET maximum intensity projection (**a**), axial MRI (**b**), contrast-enhanced CT (**c**), and fused PET/MRI (**d**) and PET/CT images (**e**) showed multiple areas of increased radiopharmaceutical uptake corresponding to multiple paragangliomas of right (*red arrows*) and left (*blue arrows*) head and neck regions (Courtesy of Nuclear Medicine Department of the Oncology Institute of Southern Switzerland, Bellinzona and Lugano, Switzerland)

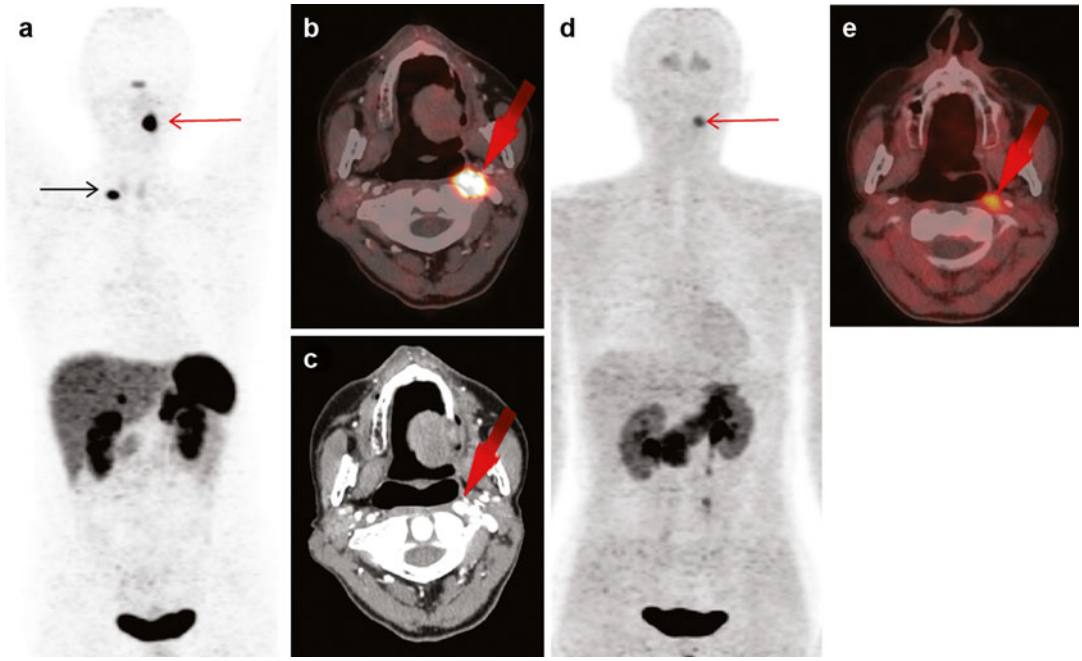

Fig. 15.2 Imaging in a 49-year-old woman with malignant head and neck paraganglioma. ^{68}Ga-DOTATOC-PET maximum intensity projection (MIP) image (**a**) and PET/CT transverse image (**b**) showed an area of intense focal ^{68}Ga-DOTATOC uptake (SUVmax 42.3) in the left head and neck region (*red arrow*). The diagnostic CT image (**c**) showed an area of strong contrast enhancement consistent with head and neck paraganglioma (red arrow). ^{18}F-DOPA PET MIP image (**d**) and PET/CT transverse image (**e**) were concordant (SUVmax 3.3). Another somatostatin receptor expressing lesion (**a**, *black arrow*) was identified as a small area of sclerosis in the transverse processes of the first thoracic vertebra (see Fig. 15.3)

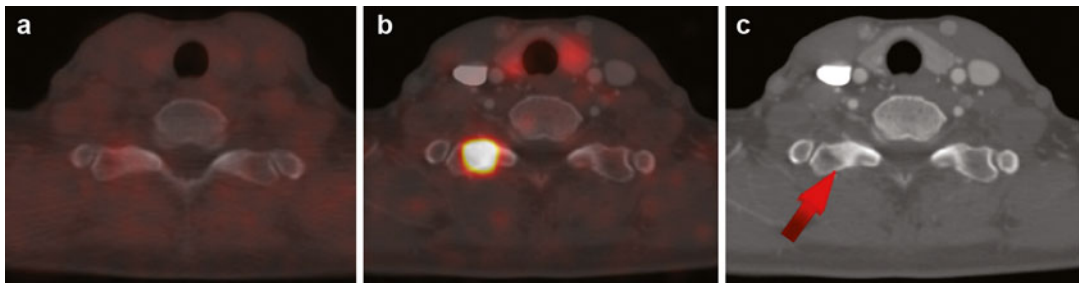

Fig. 15.3 Transverse thoracic images in the same patient as shown in Fig. 15.2^{18}F-DOPA PET/CT image (**a**) showed no abnormal uptake in the bone. ^{68}Ga-DOTATOC PET/CT image (**b**), in contrast, showed an area of intense focal uptake (SUVmax 19.8), corresponding to a small area of sclerosis at CT (**c**) in the right transverse process of the first thoracic vertebra (*arrow*), which was confirmed as osteoblastic metastasis. Considering both Figs. 15.2 and 15.3, ^{68}Ga-DOTATOC PET/CT fusion changed the tumor staging from primary tumor to metastatic disease in this patient

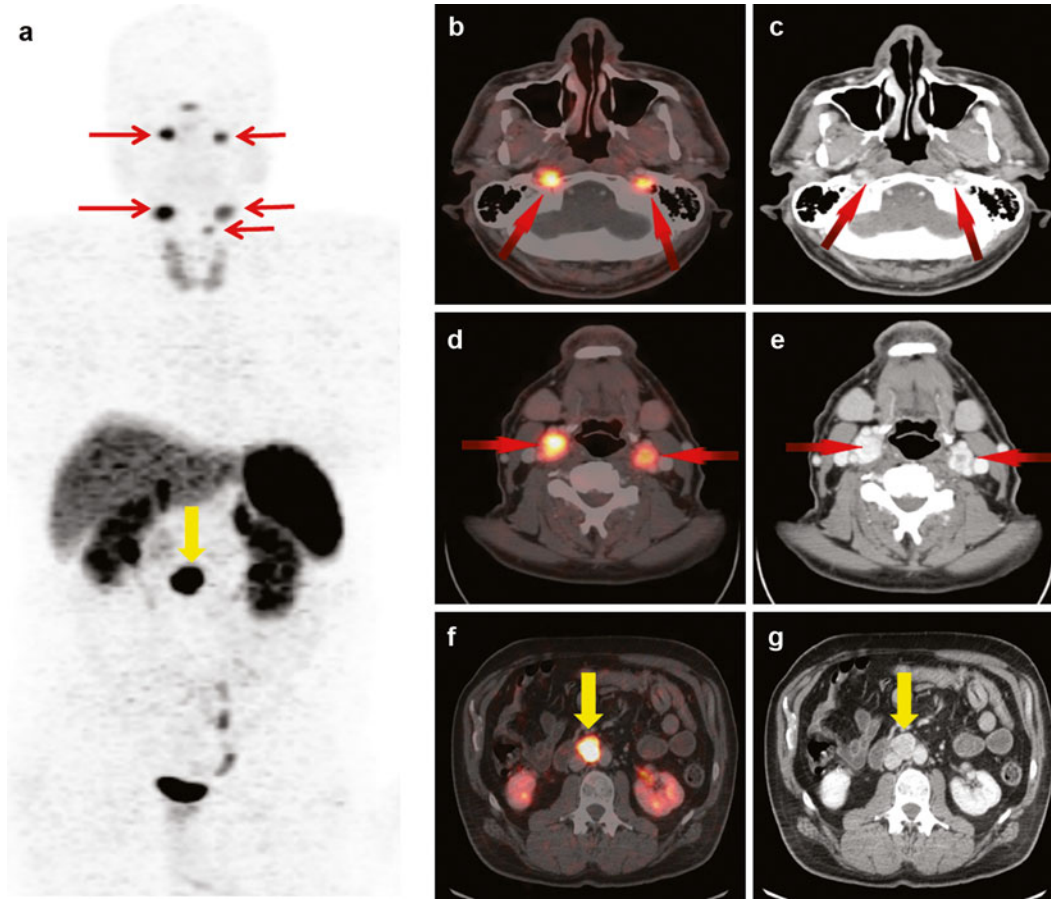

Fig. 15.4 Imaging in a 58-year-old man with multifocal extra-adrenal paraganglioma. ^{68}Ga-DOTATOC PET maximum intensity projection (MIP) image (**a**) and transverse PET/CT images (**b**, **d**) show some areas of intense focal ^{68}Ga-DOTATOC uptake in the head and neck region (*red arrows*). The diagnostic CT images (**c**, **e**) show strong contrast-enhanced lesions consistent with head and neck paragangliomas (*red arrows*). The intense focal uptake evident at ^{68}Ga-DOTATOC-PET in the abdomen (**a**, **f**, *yellow arrow*) is confirmed on diagnostic CT images (**g**, *yellow arrow*) as being an extra-adrenal paraganglioma

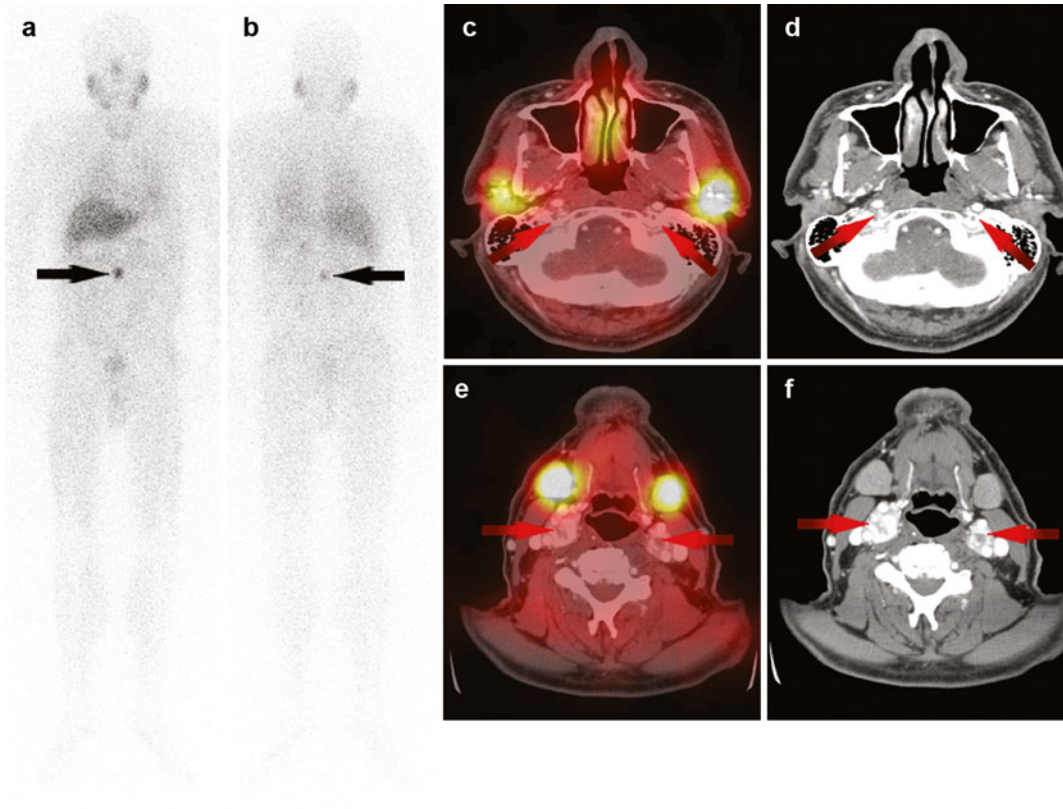

Fig. 15.5 Additional imaging in the patient seen in Fig. 15.4. ^{123}I-MIBG planar scintigraphy in anterior (**a**) and posterior (**b**) views shows a focal area of increased ^{123}I-MIBG uptake in the abdomen (*arrows*) confirmed by ^{68}Ga-DOTATOC PET/CT as being an extra-adrenal paraganglioma (see Fig. 15.4). After software-based image fusion of SPECT images with diagnostic CT images (**c**, **e**), symmetrical physiological ^{123}I-MIBG uptake was observed in the parotid (**c**) and submandibular (**e**) glands. All verified head and neck lesions evident at contrast-enhanced CT (**d**, **f**, *red arrows*) were ^{123}I-MIBG negative (**c**, **e**). Considering the findings showed in Figs. 15.4 and 15.5, ^{68}Ga-DOTATOC PET/CT changed the tumor staging from primary extra-adrenal paraganglioma to multifocal disease in this case

References

1. Taïeb D, Neumann H, Rubello D et al (2012) Modern nuclear imaging for paragangliomas: beyond SPECT. J Nucl Med 53:264–274
2. Martin TP, Irving RM, Maher ER (2007) The genetics of paragangliomas: a review. Clin Otolaryngol 32:7–11
3. Schwaber MK, Glasscock ME, Nissen AJ et al (1984) Diagnosis and management of catecholamine secreting glomus tumors. Laryngoscope 94:1008–1015
4. Van Gils AP, van Erkel AR, Falke TH et al (1994) Magnetic resonance imaging or metaiodobenzylguanidine scintigraphy for the demonstration of paragangliomas? Correlations and disparities. Eur J Nucl Med 21:239–253
5. Maurea S, Cuocolo A, Reynolds JC et al (1996) Diagnostic imaging in patients with paragangliomas. Computed tomography, magnetic resonance and MIBG scintigraphy comparison. Q J Nucl Med 40:365–371
6. Quint LE, Glazer GM, Francis IR et al (1987) Pheochromocytoma and paraganglioma: comparison of MR imaging with CT and I-131 MIBG scintigraphy. Radiology 165:89–93
7. Timmers HJ, Chen CC, Carrasquillo JA et al (2009) Comparison of 18F-fluoro-L-DOPA, 18F-fluorodeoxyglucose, and 18F-fluorodopamine PET and 123I-MIBG scintigraphy in the localization of pheochromocytoma and paraganglioma. J Clin Endocrinol Metab 94:4757–4767
8. Koopmans KP, Jager PL, Kema IP et al (2008) 111In-octreotide is superior to 123I-metaiodobenzylguanidine for scintigraphic detection of head and neck paragangliomas. J Nucl Med 49:1232–1237
9. Hoegerle S, Ghanem N, Altehoefer C et al (2003) 18F-DOPA positron emission tomography for the detection of glomus tumours. Eur J Nucl Med Mol Imaging 30:689–694
10. Rufini V, Treglia G, Castaldi P et al (2011) Comparison of 123I-MIBG SPECT-CT and 18F-DOPA PET-CT in the evaluation of patients with known or suspected recurrent paraganglioma. Nucl Med Commun 32:575–582
11. Brink I, Hoegerle S, Klisch J et al (2005) Imaging of pheochromocytoma and paraganglioma. Fam Cancer 4:61–68
12. Bergström M, Eriksson B, Oberg K et al (1996) In vivo demonstration of enzyme activity in endocrine pancreatic tumors: decarboxylation of carbon-11-DOPA to carbon-11-dopamine. J Nucl Med 37:32–37
13. Treglia G, Cocciolillo F, de Waure C et al (2012) Diagnostic performance of 18F-dihydroxyphenylalanine positron emission tomography in patients with paraganglioma: a meta-analysis. Eur J Nucl Med Mol Imaging 39:1144–1153
14. Gabriel M, Decristoforo C, Kendler D et al (2007) 68Ga-DOTA-Tyr3-octreotide PET in neuroendocrine tumors: comparison with somatostatin receptor scintigraphy and CT. J Nucl Med 48:508–518
15. Kroiss A, Putzer D, Frech A et al (2013) A retrospective comparison between 68Ga-DOTA-TOC PET/CT and 18F-DOPA PET/CT in patients with extra-adrenal paraganglioma. Eur J Nucl Med Mol Imaging 40:1800–1808
16. Sharma P, Thakar A, Suman KCS et al (2013) 68Ga-DOTANOC PET/CT for baseline evaluation of patients with head and neck paraganglioma. J Nucl Med 54:841–847
17. Treglia G, Cardillo G, Stefanelli A et al (2013) Multifocal extra-adrenal paraganglioma evaluated with different PET tracers: comparison between 18F-FDG, 18F-DOPA and 68Ga DOTANOC PET/CT. Clin Nucl Med 38:e458–e462
18. Kroiss A, Shulkin BL, Uprimny C et al (2015) (68)Ga-DOTATOC PET/CT provides accurate tumour extent in patients with extra adrenal paraganglioma compared to (123)I-MIBG SPECT/CT. Eur J Nucl Med Mol Imaging 42:33–41
19. Eisenhofer G (2001) The role of neuronal and extraneuronal plasma membrane transporters in the inactivation of peripheral catecholamines. Pharmacol Ther 91:35–62
20. King KS, Chen CC, Alexopoulos DK et al (2011) Functional imaging of SDHx-related head and neck paragangliomas: comparison of 18F-fluorodihydroxyphenylalanine, 18F-fluorodopamine, 18F-fluoro-2-deoxy-D-glucose PET, 123I-metaiodobenzylguanidine scintigraphy, and 111In-pentetreotide scintigraphy. J Clin Endocrinol Metab 96:2779–2785
21. Fottner C, Helisch A, Anlauf M et al (2010) 6-18F-fluoro-L-dihydroxyphenylalanine positron emission tomography is superior to 123I-metaiodobenzyl-guanidine scintigraphy in the detection of extraadrenal and hereditary pheochromocytomas and paragangliomas: correlation with vesicular monoamine transporter expression. J Clin Endocrinol Metab 95:2800–2810
22. Kroiss A, Putzer D, Uprimny C et al (2011) Functional imaging in phaeochromocytoma and neuroblastoma with 68Ga-DOTA-Tyr 3-octreotide positron emission tomography and 123I-metaiodobenzylguanidine. Eur J Nucl Med Mol Imaging 38:865–873
23. Blanchet EM, Martucci V, Pacak K (2012) Pheochromocytoma and paraganglioma: current functional and future molecular imaging. Front Oncol 1:58

Other Neuroendocrine Tumors of Head and Neck Region

16

Giorgio Treglia and Luca Giovanella

Abstract

The aim of this chapter is to introduce other neuroendocrine tumors (NETs) of the head and neck region beyond medullary thyroid carcinoma and paragangliomas. NETs of the head and neck are rare neoplasms and can be of epithelial or non-epithelial differentiation. Anatomical and functional imaging can be complementary for the diagnosis, staging, and monitoring of treatment response of these tumors. This chapter briefly describes the imaging methods used to evaluate these tumors and illustrates the imaging features of some NETs of the head and neck region.

Keywords

Neuroendocrine tumor • Neck • Small cell carcinoma • Carcinoid • PET • CT • MRI

G. Treglia, MD, MSc (✉)
Prof. Dr. med. L. Giovanella, MD, PhD
Department of Nuclear Medicine,
Thyroid and PET/CT Center,
Oncology Institute of Southern Switzerland,
Via Ospedale 12, CH-6500
Bellinzona and Lugano, Switzerland
e-mail: giorgio.treglia@eoc.ch;
luca.giovanella@eoc.ch

L. Giovanella et al. (eds.), *Atlas of Head and Neck Endocrine Disorders: Special Focus on Imaging and Imaging-Guided Procedures*, DOI 10.1007/978-3-319-22276-9_16

16.1 Introduction

Neuroendocrine tumors (NETs) of head and neck region are rare and heterogeneous neoplasms. Beyond medullary thyroid carcinoma and paragangliomas, other NETs may involve the head and neck region including typical and atypical carcinoids (well-differentiated NETs), large and small cell carcinomas (poorly differentiated NETs), olfactory neuroblastoma (arising from the neural crest), and Merkel cell carcinoma (a cutaneous neuroendocrine neoplasm with aggressive behavior).

Furthermore NETs arising from other anatomical regions may metastasize to the head and neck region [1].

16.2 Imaging for NETs of Head and Neck Region

Anatomical and functional imaging can be complementary for the diagnosis, staging, and monitoring of treatment response of these NETs.

About anatomical imaging, ultrasonography (US) has limited value in the detection of head and neck NETs beyond paragangliomas and medullary thyroid carcinoma. Computed tomography (CT) and magnetic resonance imaging (MRI) are the most used anatomical imaging methods in the evaluation of these neoplasms. They are useful to demonstrate the local extension of the disease and in detecting invasion of the adjacent structures or metastatic spread [1].

Several functional imaging methods including scintigraphic techniques using single-photon emitter radiopharmaceuticals or positron emission tomography (PET) using several positron emitter tracers may be used to evaluate NETs of head and neck regions. Functional imaging techniques may evaluate different cellular aspects in NETs including somatostatin receptor expression, glucose metabolism, or catecholamine synthesis and storage pathways [1].

The most useful functional imaging method in evaluating well-differentiated NETs (carcinoids) of head and neck region is somatostatin receptor imaging (including somatostatin receptor scintigraphy and somatostatin receptor PET), because these tumors usually overexpress somatostatin receptors on their cell surface [2, 3]. In more aggressive neuroendocrine tumors, such as small cell carcinomas and Merkel cell carcinomas, fluorine-18 fluorodeoxyglucose (^{18}F-FDG) PET is the functional imaging method of choice due to the high glucose metabolism of these neoplasms [4–7]. Radiolabeled catecholamine analogs or precursors may be useful in neural crest-derived NETs such as olfactory neuroblastoma.

Nevertheless, hybrid tomographic imaging methods (SPECT/CT, PET/CT, or PET/MRI) combining anatomical and functional information may provide higher accuracy in the detection of NETs of head and neck region compared to anatomical or functional methods alone (Figs. 16.1, 16.2, and 16.3) [2–7].

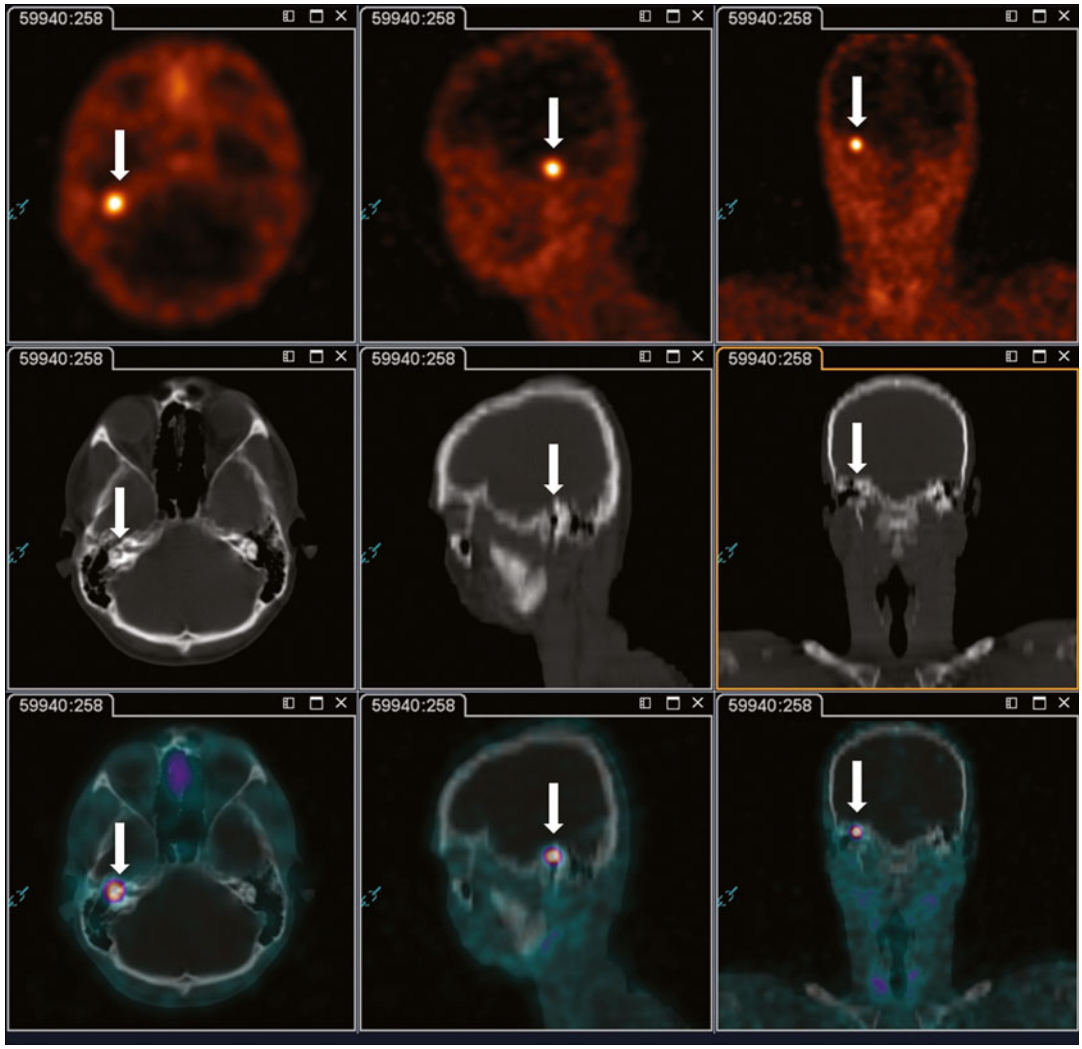

Fig. 16.1 Well-differentiated neuroendocrine tumor of the right middle ear detected by fused somatostatin receptor PET/CT. PET with somatostatin analogs labeled with gallium-68 (*upper row*) detected a focal area of increased radiopharmaceutical uptake (*arrows*) corresponding to a subcentimeter nodule in the right middle ear at CT (*mid row*) and fused PET/CT images (*lower row*)

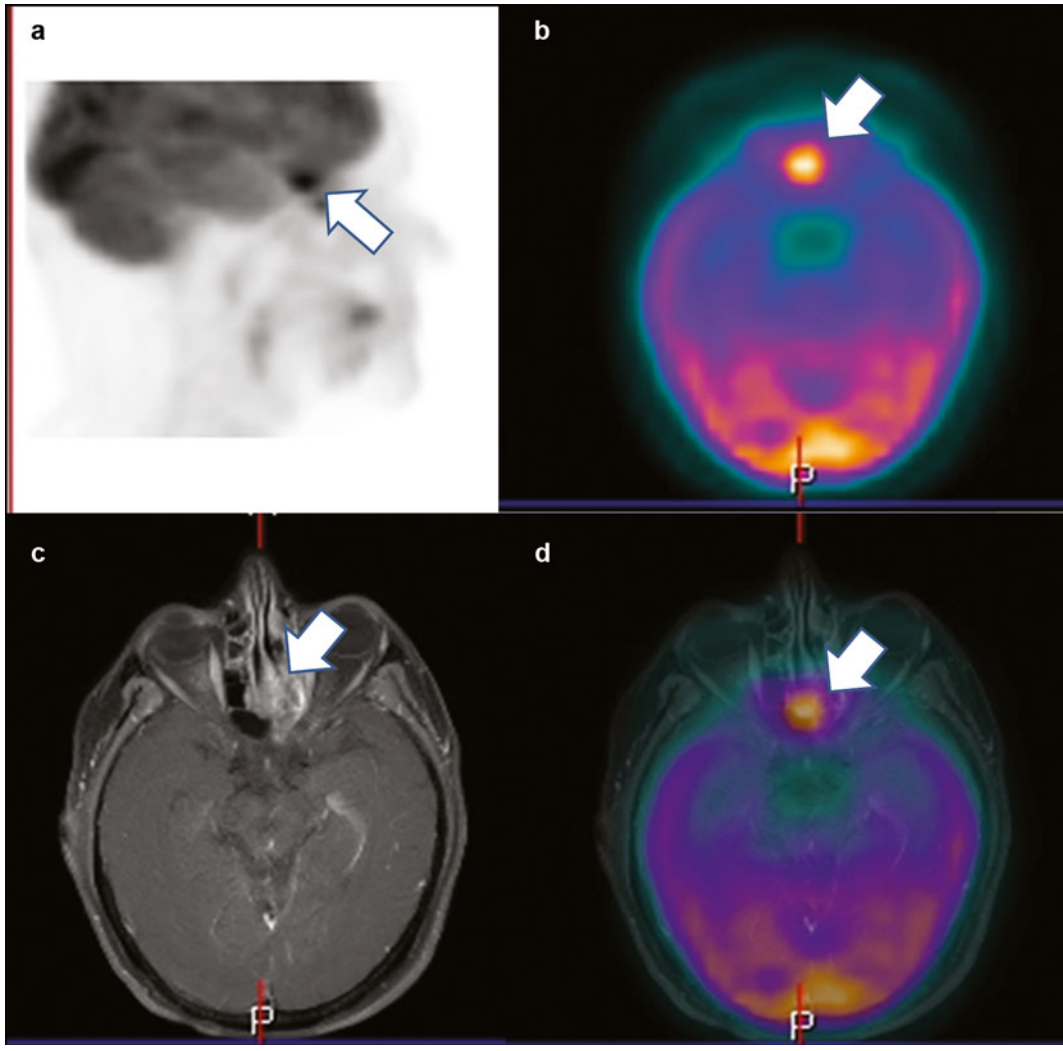

Fig. 16.2 Sinonasal small cell carcinoma of the left ethmoidal sinus (*arrows*) imaged by fluorine-18 fluorodeoxyglucose positron emission tomography (^{18}F-FDG PET) in sagittal (**a**) and axial projection (**b**), magnetic resonance imaging (MRI) in axial projection (**c**), and fused PET/MRI (**d**). This tumor was well-characterized by MRI which showed invasion of the adjacent structures. PET demonstrated increased glucose metabolism of this tumor without metastatic spread

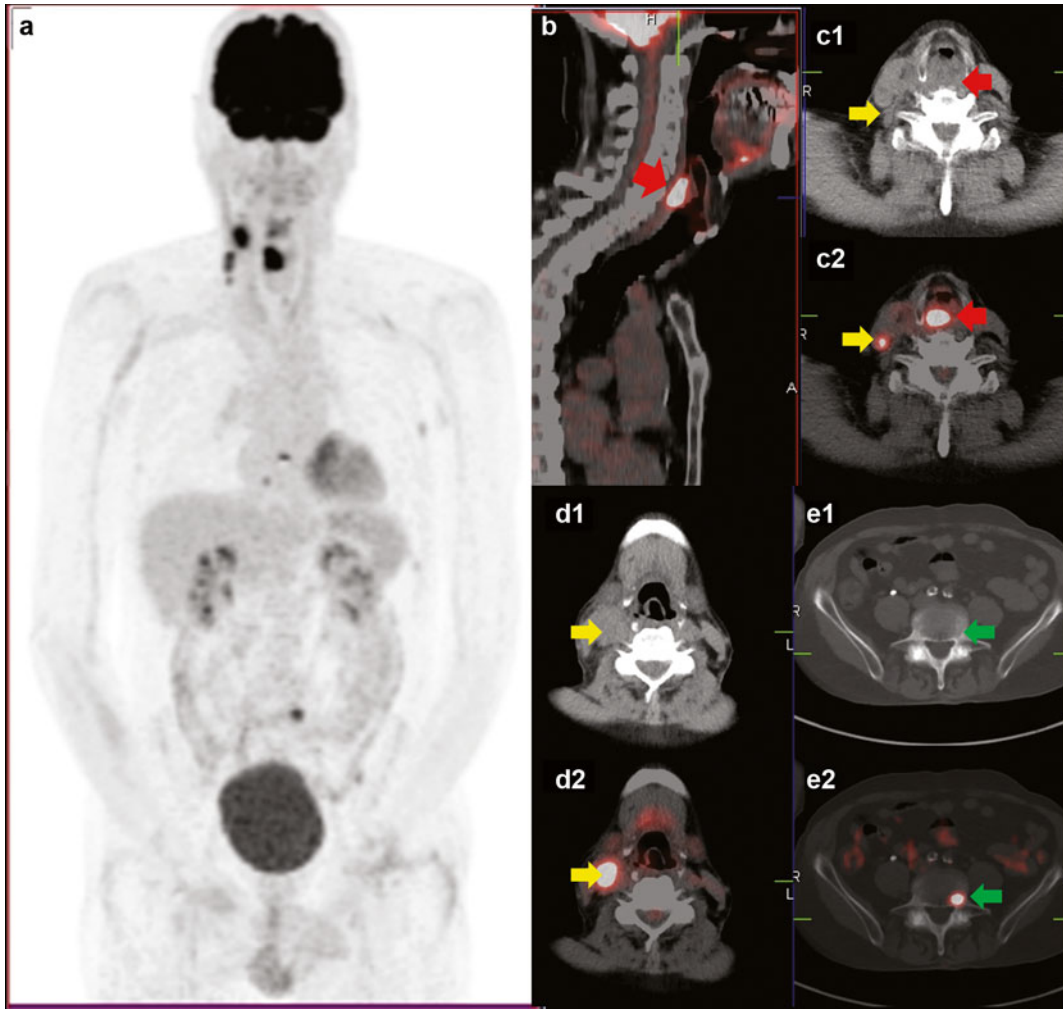

Fig. 16.3 Metastatic laryngeal small cell carcinoma imaged by fluorine-18 fluorodeoxyglucose positron emission tomography/computed tomography (^{18}F-FDG PET/CT). ^{18}F-FDG PET (**a**) showed an area of increased tracer uptake corresponding to a laryngeal tumor (*red arrow*) at CT (**c1**) and fused PET/CT images in sagittal (**b**) and axial projection (**c2**). Furthermore several right cervical lymph nodal metastases (*yellow arrows*) were detected by PET (**a**), CT (**c1**, **d1**), and fused PET/CT images (**c2**, **d2**). Interestingly, ^{18}F-FDG PET detected bone metastases (*green arrows*) without significant morphological abnormalities at co-registered CT (**e1**, **e2**)

References

1. Subedi N, Prestwich R, Chowdhury F et al (2013) Neuroendocrine tumours of the head and neck: anatomical, functional and molecular imaging and contemporary management. Cancer Imaging 13:407–422
2. Castaldi P, Rufini V, Treglia G et al (2008) Impact of 111In-DTPA-octreotide SPECT/CT fusion images in the management of neuroendocrine tumours. Radiol Med 113:1056–1067
3. Treglia G, Baldelli R, Cristalli G et al (2013) A rare case of neuroendocrine tumor of the middle ear detected by gallium-68-DOTANOC-PET/CT. J Clin Endocrinol Metab 98:1319–1320
4. Treglia G, Bongiovanni M, Paone G et al (2015) Metastatic small cell neuroendocrine carcinoma of the pyriform sinus evaluated by ^{18}F-FDG PET/CT. Rev Esp Med Nucl Imagen Mol 34:125–127
5. Treglia G, Bongiovanni M, Giovanella L (2014) Rare sinonasal small cell neuroendocrine carcinoma evaluated by F-18-FDG PET/MRI. Endocrine 47:654–655
6. Treglia G, Salvatori M, Giovanella L (2014) Small cell carcinoma of the thyroid gland with a solid brain metastasis detected by F-18-FDG PET/CT. Endocrine 46:682–683
7. Treglia G, Kakhki VR, Giovanella L et al (2013) Diagnostic performance of fluorine-18-fluorodeoxyglucose positron emission tomography in patients with Merkel cell carcinoma: a systematic review and meta-analysis. Am J Clin Dermatol 14:437–447